AD-A085 924 DAVID W TAYLOR NAVAL SHIP RESEARCH AND DEVELOPMENT CE--ETC F/G 13/10
SIMULATION ANALYSIS OF AUTOMATIC AND QUICKENED MANUAL CONTROL O--ETC(U)
JUN 80 S H BROWN, J G DIMMICK

UNCLASSIFIED DTNSRDC-80/007 NL

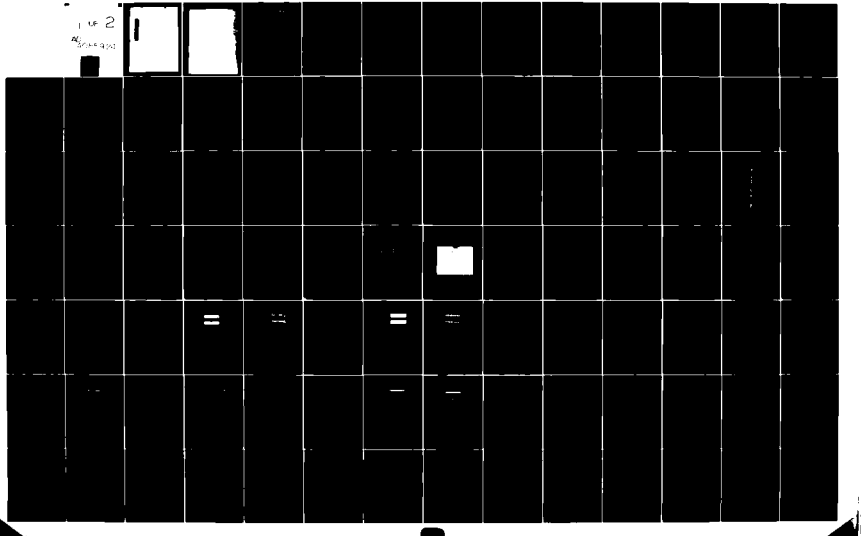

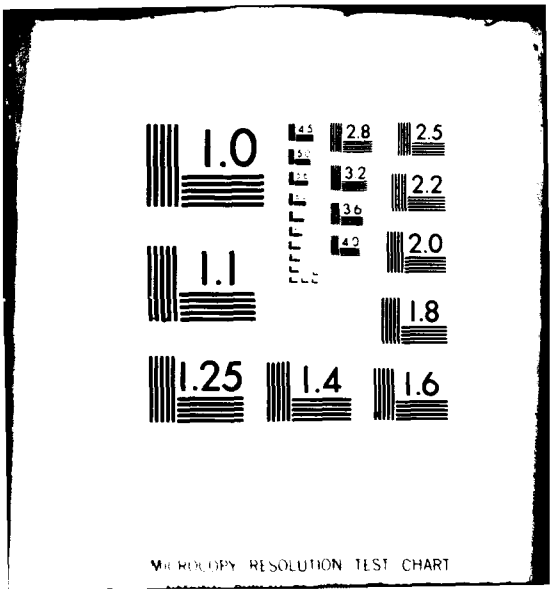
1.0
1.1
1.25
1.4
1.6
1.8
2.0
2.2
2.5
2.8
3.2
3.6
4.0
MICROCOPY RESOLUTION TEST CHART

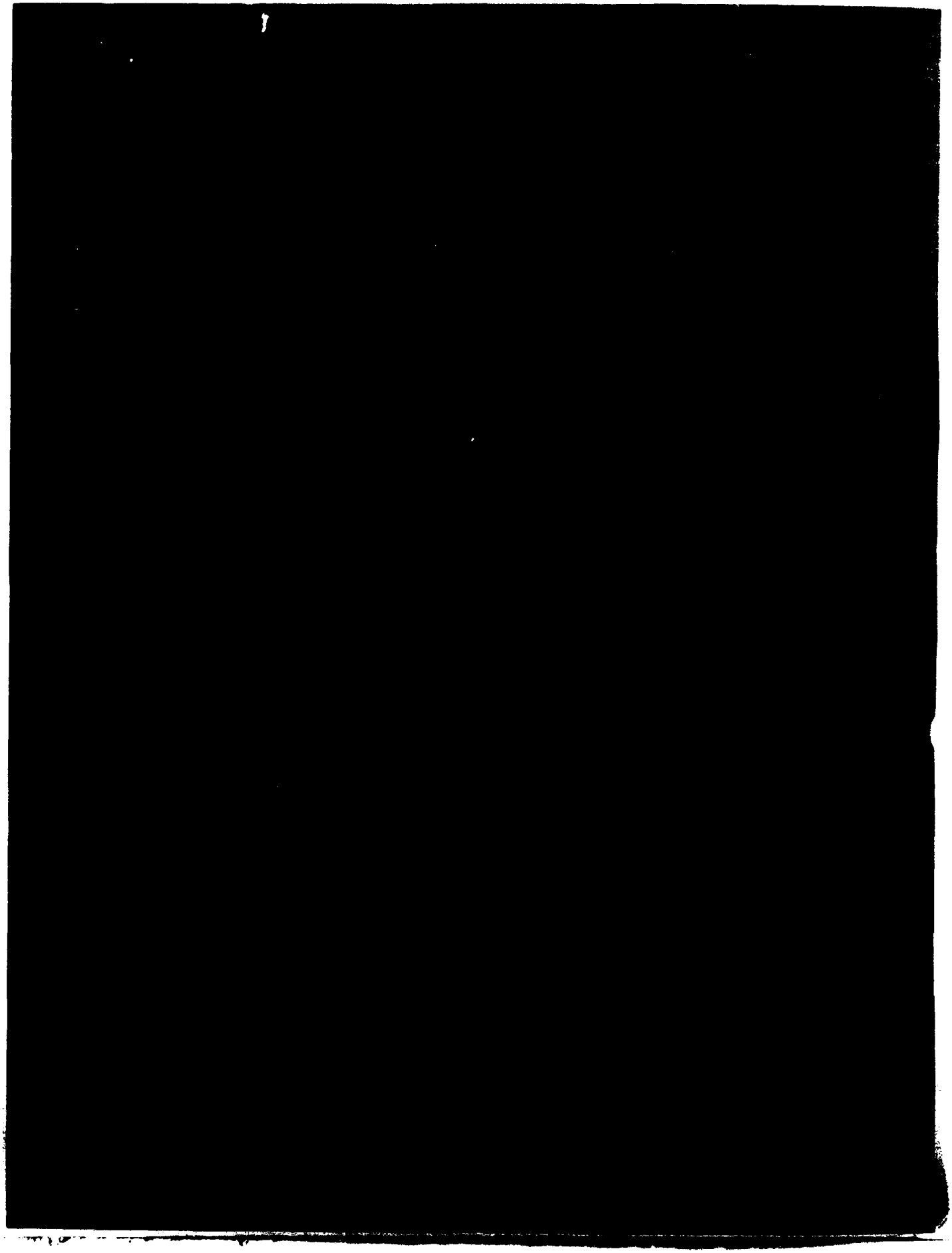

UNCLASSIFIED

SECURITY CLASSIFICATION OF THIS PAGE (When Data Entered)

LEVEL II

12

REPORT DOCUMENTATION PAGE

READ INSTRUCTIONS BEFORE COMPLETING FORM

1. REPORT NUMBER: DTNSRDC-80/007	2. GOVT ACCESSION NO.: AD-A085 924
3. RECIPIENT'S CATALOG NUMBER:	
4. TITLE (and Subtitle): SIMULATION ANALYSIS OF AUTOMATIC AND QUICKENED MANUAL CONTROL DURING UNDERWAY REPLENISHMENT	5. TYPE OF REPORT & PERIOD COVERED: Research and Development
	6. PERFORMING ORG. REPORT NUMBER:
7. AUTHOR(s): Samuel H. Brown and Joseph G. Dimmick	8. CONTRACT OR GRANT NUMBER(s):
9. PERFORMING ORGANIZATION NAME AND ADDRESS: David W. Taylor Naval Ship R&D Center, Bethesda, MD 20084	10. PROGRAM ELEMENT, PROJECT, TASK AREA & WORK UNIT NUMBERS: Program Element 62543N; Task Area SF43433302; Work Unit 2730-100
11. CONTROLLING OFFICE NAME AND ADDRESS: Naval Sea Systems Command (SEA 05R), Washington, DC 20362	12. REPORT DATE: June 1980
	13. NUMBER OF PAGES: 139
14. MONITORING AGENCY NAME & ADDRESS (if different from Controlling Office)	15. SECURITY CLASS. (of this report): UNCLASSIFIED
	15a. DECLASSIFICATION/DOWNGRADING SCHEDULE

16. DISTRIBUTION STATEMENT (of this Report)

APPROVED FOR PUBLIC RELEASE; DISTRIBUTION UNLIMITED

17. DISTRIBUTION STATEMENT (of the abstract entered in Block 20, if different from Report)

DTIC ELECTE JUN 25 1980 S D E

18. SUPPLEMENTARY NOTES

19. KEY WORDS (Continue on reverse side if necessary and identify by block number)

Underway Replenishment
Mariner
Sea State
Interaction Forces Between Ships

20. ABSTRACT (Continue on reverse side if necessary and identify by block number)

This final report summarizes the final results and conclusions of a program to define and analyze the control parameters affecting the dynamic interactions between two ships during Underway Replenishment (UNREP) and to make recommendations for a prototype ship separation monitoring system. Results of hybrid computer simulations of UNREP by two identical, Mariner class ships, including consideration of nonlinear maneuvering

(Continued on reverse side)

DD FORM 1 JAN 73 1473 EDITION OF 1 NOV 65 IS OBSOLETE
S/N 0102-LF-014-6601

UNCLASSIFIED
SECURITY CLASSIFICATION OF THIS PAGE (When Data Entered)

(Block 20 continued)

equations, regular waves, severe first- and second-order irregular-wave excitations, time-sampled separation measurements, and low-pass filters, are presented. Contrary to earlier assumptions, first-order irregular-wave excitations were found to dominate the UNREP control problem. Use of either automatic or quickened manual control was found to be feasible, but work is needed to define the capabilities and limitations of quickening in this application. Recommendations for development of a prototype ship separation sensing system are presented.

TABLE OF CONTENTS

LIST OF FIGURES

Page

Page

Page

LIST OF TABLES

NOMENCLATURE

A	Longitudinal separation distance measured between centers of mass of the two ships
B	Lateral separation distance between the two ships (side-to-side distance)
a_T	Gain constant in integral feedback loop
$F^{(n)}$	Term n in functional series
g	Gravitational constant
$H(\omega)$	First-order (linear) transfer function
$H(\omega_1,\omega_2)$	Second-order transfer function
h	Wave height (crest to trough) for regular wave
h_n	nth-order impulse response function
$\dot{Im}$	Imaginary part
I_z	Moment of inertia about z-axis
K	Kernal of integral equation
$\underline{K_L}$	Feedback gain vector for leading ship
$\underline{K_T}$	Feedback gain vector for tracking ship
L	Ship length between perpendiculars
m	Mass of ship
n	Instantaneous propeller revolutions per minute
n_1	Initial propeller revolutions per minute (ahead straight-line motion)
Δn	$n - n_1$ (n - propeller revolutions per minute)
N	Yawing moment about z-axis
r	Angular velocity of yaw ($r = \dot{\psi}$)

$S_X(\omega)$	Pierson-Moskowitz Spectrum
$t, \Delta t$	Time and time interval, respectively
u, v	Velocity components of the origin of the body axes (longitudinal and transverse components, respectively, corresponding to surge and sway velocity components)
u_1	Initial equilibrium velocity component (ahead straight-line motion at constant speed with rudder at amidships)
Δu	$u - u_1$
$\dot{u}, \dot{v}$	Acceleration components of the origin of the body axes (longitudinal and transverse components, respectively)
$\vec{V}$	Velocity vector of the origin of the body axes
x, y, z	Coordinate axes fixed in ship. Origin of axes system need not be at the center of gravity of the ship (positive direction forward, starboard, and downward, respectively)
x_o, y_o, z_o	Coordinate system fixed with respect to the surface of the earth
$\bar{x}_o, \bar{y}_o, \bar{z}_o$	Coordinates of the center of mass of the ship relative to the coordinate system fixed with respect to the surface of the earth
$X(t)$	Free-surface elevation
X, Y	Hydrodynamic force components on ship body (longitudinal and lateral components, respectively)
ζ	Wave amplitude for regular wave
δ	Angular displacement of the rudder
$\varepsilon(\omega)$	Random phase angle
λ	Wave length of regular wave
ρ	Water mass density
$\phi(\omega)$	Phase of first-order system
$\phi(\omega_1, \omega_2)$	Phase of second-order system

$'$	Represents nondimensional value when used as superscript on symbol
ψ	Angle of yaw
χ	Ship-to-wave heading angle
ω	Radian frequency

LIST OF ABBREVIATIONS

deg	Degrees
deg/s	Degrees per second
ft	Feet
ft/s	Feet per second
lb	Pound
lb-ft	Pound-feet
m	Meters
m/s	Meters per second
N	Newtons
Nm	Newton-meters
rad	Radians
rad/s	Radians per second
s	Second
UNREP	Underway replenishment

Conversion Units
1 foot = 0.3048 meters
360 deg = 2π radians
1 pound = 4.448 Newtons

EXECUTIVE SUMMARY

INTRODUCTION

The overall objectives of the Underway Replenishment (UNREP) Simulation Program are to define and analyze the control parameters affecting the complex dynamic interactions between two ships maneuvering in close proximity during underway replenishment and to make recommendations concerning the selection of a prototype sensing and display system for ship separation monitoring during UNREP. The objective of this report is to summarize the final results, conclusions, and recommendations of the program.

The maneuvering control problem for UNREP was studied by developing and exercising a hybrid computer simulation. Two identical Mariner-class merchant ships were modeled in the investigation, because sufficient hydrodynamic interaction data for naval surface ships were not available in time for an in-depth study. However, limited investigations of an AO 177 and a destroyer study ship were conducted in the final stages of the program.

Early work included the beginning development of the hybrid computer underway replenishment maneuvering model and simulation of UNREP in calm and regular seas using manual control of both the rudder angles and the propeller shaft speeds. An automatic controller was later incorporated into the simulation to avoid subjective results due to the skill factors of the operators. After linear, irregular sea effects in the sway and yaw degrees of freedom were added to the simulation, the requisite control parameters for both manual and automatic control were determined to be heading, heading rate, longitudinal and lateral separation, lateral separation rate, propeller shaft speed, and rudder angle. Some nonlinear excitations approximating an irregular, moderate sea state (4 or 5 on the Beaufort Scale), as defined by the Pierson-Moskowitz spectrum were then added to the model. The provisional results then indicated that sensor noise and measurement errors of approximately 3 to 5 percent in the maneuvering control variables should be acceptable under the conditions of the simulation.

This final report presents conclusions and recommendations based on the results of simulations conducted to analyze the following additional factors:

- Nonlinear maneuvering equations
- Regular wave excitations
- First-order irregular wave excitations
- Second-order irregular wave excitations
- First- and second-order irregular wave excitations
- Quickened manual control versus automatic control
- Severe sea states
- Time-sampled separation measurements
- Low-pass filters on the rudder control input.

CONCLUSIONS

Simulations were conducted to analyze factors not considered in earlier work and to attempt to confirm some provisional assumptions and results. In general, previous results were found to be valid, but the current work contradicts some earlier assumptions and points out the need for some additional work in the areas of displays, human factors engineering, and automatic controls.

It has been assumed throughout the previous work that the drifting type of second-order irregular sea state excitations were more important than the higher-frequency, first-order irregular sea state excitations. The current work, which includes detailed studies of first-order irregular sea state excitations for the first time, indicates that the opposite is true--first-order irregular sea state excitations dominate the UNREP steering control problem. This new finding is based on analysis of results of simulations conducted with first- and second-order irregular effects considered separately and in combination. Those results with both effects in combination are very similar to results with first-order effects only, but are not similar to results with second-order effects only. Simulations with first-order, irregular excitations singly or in combination result in significantly higher amplitudes, frequencies, and rates of lateral separation, headings, and rudder excursions than simulations with second-order, irregular excitations only.

In simulations with second-order irregular excitations only, the calm water hydrodynamic interaction forces and moments dominate control of lateral separation, even in severe sea states of 16-foot significant wave heights. Lateral separation excursions with severe, second-order excitations are the same as lateral separation excursions with no sea state excitation. Second-order effects of severe, irregular seas slightly increase rudder activity and heading excursions with respect to the calm sea (no excitation) condition, but have no significant effect on lateral separation control.

Assuming that a reasonable criterion for satisfactory lateral separation control is to maintain separation within 20 feet of the set point ($80 \leq B \leq 120$ feet), unsatisfactory lateral separation control occurred under several conditions. With regular wave excitations, lateral separation control was unsatisfactory with: (a) automatic control, 10-foot waves and the encounter frequency which maximizes sway force; and (b) quickened manual control, 5-foot waves and the encounter frequency which maximizes yaw moment. With severe, irregular wave excitations, and automatic control, lateral separation control was unsatisfactory with lateral separation measurements occurring at intervals in excess of 1.0 second and with a low-pass filter at the input to the rudder control system of the simulation tracking ship.

Previous results, which were based on lower-frequency, second-order, irregular excitations only, indicated that lateral separation measurement intervals of as long as 30 seconds could be tolerated, but with first-order excitations included, it is now clear that the measurement interval should be no longer than 1.0 second. This finding is consistent with the conclusion that first-order excitations dominate the UNREP steering control problem in realistic sea conditions.

Under some conditions, the quality of control, as described by lateral separation, rudder and heading excursion amplitudes, frequencies and rates, is as good with quickened manual steering as it is with automatic steering, but this is not always the case. One case of unsatisfactory lateral separation control was with quickened manual steering. With all conditions identical except for automatic steering, lateral

separation excursions were reduced by 27 feet and were within the criterion of $80 \leq B \leq 120$ feet. However, since the simulations were not designed to give statistically valid comparisons of automatic and quickened manual steering, it is reasonable to conclude that quickened manual steering control shows promise of being as satisfactory as automatic control, and that some additional human factors engineering experiments are needed to define its advantages and disadvantages more accurately.

The unsatisfactory lateral separation control which resulted from putting a low-pass filter on the input to the rudder control system of the simulated tracking ship is entirely consistent with the conclusions that the higher-frequency, first-order irregular excitations dominate the UNREP steering control problem. With the low-pass filter installed, the rudder, and consequently the ship, were unable to respond to the first-order excitations as well as they did without the filter.

It is likely that better results could be obtained with a better designed automatic controller. Improving the automatic controller, possibly by adding adaptive capabilities, should also improve the quality of quickened manual control.

To summarize, the major conclusions of this final report are:

- First-order excitations of irregular seas dominate the UNREP steering control problem.
- Lateral separation measurement intervals should not exceed 1.0 second.
- Quickened manual steering shows promise for UNREP, but requires further study and human factors engineering experiments.
- The automatic controller used in the simulation could be significantly improved by a re-design based on modern control theory techniques. The preliminary results from the simulation of an AO 177 and a destroyer study ship corroborate the conclusions drawn for the Mariner ships.

RECOMMENDATIONS

Since completion of the present simulation work provides a good definition of the parameters which must be measured and controlled to improve lateral separation control during UNREP, the next objective should be to design and evaluate the required sensing systems, specifically for

longitudinal and lateral separation and separation rate. If the sensing system chosen makes measurements at discrete time intervals, the intervals should be 1.0 second or less.

If the sensing system development is successful, it should be integrated with an automatic or quickened manual controller to provide the best performance. Both the automatic and quickened manual controller designs described in this report are practical, but must be modified to suit the maneuvering characteristics of any Navy ship in which they may be installed.

Additional human factors engineering experiments should be conducted to define the capabilities of quickened manual control and to identify specific areas for improvements.

The methodology available as a result of the present work is valuable for simulation and analysis of interaction effects among different ship types. All future work using this or similar methodologies should include first-order irregular sea state excitations. Before additional ships or combinations of ships can be simulated, hydrodynamic data must be made available.

Finally, it must be strongly cautioned that although results for different ships are expected to be qualitatively similar, the quantitative results must not be applied to different ships or to the same ships at different speeds or other conditions. In particular, safe speeds, separation distance, and sea conditions for the ships simulated in the present work should not be assumed to apply equally to other ships. Because the simulations were applicable only for UNREP operations in open seas, the results are not valid for shallow water, nor for ships moving in close proximity to vertical obstructions such as channel banks. The effects of ship size, speed, maneuverability, reserve power, and rudder turning moments, as well as sea state effects, water depth, channel width, and UNREP rig forces and moments are all large and must be considered on a case-by-case basis in determining safe speeds and lateral separations for overtaking, passing, or UNREP.

ABSTRACT

This final report summarizes the final results and conclusions of a program to define and analyze the control parameters affecting the dynamic interactions between two ships during Underway Replenishment (UNREP) and to make recommendations for a prototype ship separation monitoring system. Results of hybrid computer simulations of UNREP by two identical, Mariner class ships, including consideration of nonlinear maneuvering equations, regular waves, severe first- and second-order irregular-wave excitations, time-sampled separation measurements, and low-pass filters are presented. Contrary to earlier assumptions, first-order irregular-wave excitations were found to dominate the UNREP control problem. Use of either automatic or quickened manual control was found to be feasible, but work is needed to define the capabilities and limitations of quickening in this application. Recommendations for development of a prototype ship separation sensing system are presented.

ADMINISTRATIVE INFORMATION

This work was funded by NAVSEA under Element 62543N, Task Area SF43433302, Work Unit 2730-100, Task 19296.

INTRODUCTION

OBJECTIVE

The overall objectives of the underway replenishment (UNREP) simulation program are to define and analyze the control parameters affecting the complex dynamic interactions between two ships maneuvering in close proximity during underway replenishment[1-5*] and to make recommendations concerning the selection of a prototype sensing and display system for ship separation monitoring during UNREP. The objective of this report is to summarize the final results, conclusions, and recommendations of the program.

---

*A complete listing of references is given on page 117.

APPROACH AND PROGRESS

The maneuvering control problem for UNREP was studied by developing and exercising a hybrid computer simulation. Two identical Mariner-class merchant ships were modeled in the investigation, because sufficient hydrodynamic interaction data for naval surface ships were not available in time for an in-depth study. However, limited investigations of an AO 177 and a destroyer study ship were conducted in the final stages of the program.

Early work included the beginning development of the hybrid computer underway replenishment maneuvering model[6] and simulation of UNREP in calm and regular seas[7] using manual control of both the rudder angles and the propeller shaft speeds. An automatic controller was later incorporated[8] into the simulation to avoid subjective results due to the skill factors of the operators. After linear, irregular sea effects[8] in the sway and yaw degrees of freedom were added to the simulation, the requisite control parameters for both manual and automatic control were determined to be heading, heading rate, longitudinal and lateral separation, lateral separation rate, propeller shaft speed, and rudder angle. Some nonlinear excitations approximating an irregular, moderate sea state (4 or 5 on the Beaufort Scale),[9,10] as defined by the Pierson-Moskowitz spectrum[11] were then added to the model. The provisional results then indicated that sensor noise and measurement errors of approximately 3 to 5 percent in the maneuvering control variables should be acceptable under the conditions of the simulation.[9,10,12]

This final report presents conclusions and recommendations based on the results of simulations conducted to analyze the following additional factors:

- Nonlinear maneuvering equations
- Regular wave excitations
- First-order irregular wave excitations
- Second-order irregular wave excitations[9,10]
- First- and second-order irregular wave excitations
- Quickened manual control versus automatic control[12-18]
- Severe sea states[19]

- Time-sampled separation measurements
- Low-pass filters on the rudder control input

Nonlinear maneuvering equations for each Mariner study ship were used for the first time as the basis of the UNREP control mathematical model to increase the accuracy and faithfulness of the simulation, which previously had included only linear maneuvering equations. All of the Mariner-class UNREP simulation results reported herein reflect the inclusion of nonlinear maneuvering equations.

The effects of four distinct types of wave excitations simulating sea states ranging from calm to severe were analyzed separately and in combination to determine the contribution of each to the overall UNREP control problem. Calm seas (no excitation) were simulated to determine the effect of adding the nonlinear maneuvering equations to the mathematical model. Moderate and severe regular wave excitations were simulated because, although rare in nature, regular waves concentrate energy in a single frequency and thus represent a worst-case control problem. First- and second-order irregular wave excitations were simulated separately to analyze the effects of each; and in combination to provide the most realistic simulation of natural sea conditions.

Severe sea states (6 to 7 on the Beaufort Scale and 10-foot regular waves) were simulated to examine the capability of the simulated automatic controls even though it was recognized that UNREP operations would be conducted under those conditions only in an emergency.

UNREP simulation results with quickened manual control[14,17] were compared to those with fully automatic control, because some form of quickened manual control[12,13] has the potential for combining the superior course-keeping capabilities of the automatic controller with the adaptability and judgment of the human operator.

Discrete, time-sampled ship separation measurements rather than continuous measurements were used in some UNREP simulations because several candidate ship separation sensing systems provide discrete, rather than continuous, measurements. Three different sampling intervals were simulated to estimate the tolerable interval between discrete measurements of separation.

Because it was observed that the automatic controller was responding to high-frequency excitations, even though the simulated ships could not respond at that frequency, a low-pass filter was added to the simulation between the automatic controller output and the rudder control system input in an attempt to analyze the effects of reducing high-frequency rudder oscillations.

The results and the conclusions contained in this report characterize some of the physical and human factors that bear on the problem of maneuvering in close proximity to other ships and provide new insight as to the essential details of UNREP maneuvering.

BACKGROUND

The ability to replenish ships at sea,[12] far from ports of supply, is a major factor in maintaining naval forces on station or moving them swiftly over long distances. The skills acquired and kept sharpened through frequent use by generations of Navy men have formed the keystone of the seamanship traditions of the U.S. Navy for several decades. Thousands of underway replenishments have been conducted routinely on the oceans of the world, despite foul weather, poor visibility, equipment failure, and enemy action. This tremendous achievement has not been without cost; there have been occasional collisions, damage, injuries, and even deaths. To a certain extent, this is inevitably part of the price of readiness. Steering, propulsion, or other failures at critical times can create chain reactions that none of our shiphandling skills can stop. Human errors of inexperience, momentary poor judgment, and fatigue will always be present. Replenishment ships have grown in size and speed, making the short separation distances more hazardous. Ships are larger, faster, and often less maneuverable than they were even a decade ago. These factors reduce our maneuvering options.

A study of Navy Safety Center records revealed 20 UNREP collisions during the period January 1969 to July 1973. Some collisions had more than one important cause factor. In 12 of those collisions, equipment failure was not a factor. Of those 12, ten occurred during the approach phase. Unfortunately, no data were available on the hundreds of UNREPs

conducted successfully in a professional and seamanlike manner during that same period. It should be no surprise to experienced ship handlers that, of the accidents which could be attributed to poor shiphandling, the majority occurred during the approach phase.

In the reports, the phrase, "failure to maintain adequate separation," was found frequently. It applies to the events preceding the actual collision. The hydrodynamic interaction forces and moments acting on the ships reverse themselves twice during the approach, alongside, and breakaway phases. The leading ship during a typical UNREP sets a predetermined straight-line course, while the passing ship tracks the leading ship and maintains lateral separation. There is an indistinctly defined point of no return in lateral separation, beyond which collision is inevitable. The hydrodynamic interaction forces and moments are roughly a function of the square of ship speed. The margin for error decreases much faster than is apparent from the distance line or stadimeter. At some point, the interaction forces and moments between the two hulls will be greater than can be overcome by steering and propulsion. From that point, collision is inevitable. In engineering terms, this is an unstable system. The instabilities must be countered by continuous adjustment of the helm which controls the rudders. This aspect of UNREP was approached as a control engineering problem. The work in the multifaceted research and development program presented here concentrated on one aspect - steering to maintain adequate separation.

UNREP COMPUTER FACILITY

The UNREP computer simulation was done using the Machinery Systems Simulation Facility at the David W. Taylor Naval Ship Research and Development Center (DTNSRDC)/Annapolis. This facility includes a hybrid computer system consisting of a PDP-15 unichannel digital computer interfaced to a fully expanded EAI 680 (Electronic Associates, Inc.) analog computer through an EAI 693 hybrid interface unit. The PDP-15 has 40,000 words of core memory, a RAMTEK raster scan color graphics display, 3 RK-05 cartridge disk drives, and an LPS-11 interface system. An eight-channel, strip-chart recorder is available for the EAI 680. Also included in the facility is

an AN/UYK-20 militarized minicomputer system, which is interfaced to the PDP-15.

Since the UNREP computer simulation was to allow for man-in-the-loop operation, it was required to run in real time. This requirement was met by existing analog computing capability. The need for flexible graphics display and control of the simulation as well as memory functions necessary for implementation of irregular sea states required a digital computer. The use of a hybrid system makes both analog and digital capabilities available. In a hybrid system, the digital computer is also used heavily to set up and check out the analog computer program.

UNREP MANEUVERING CONTROL SIMULATION MATHEMATICAL MODEL

BACKGROUND

The general flow diagram for the UNREP maneuvering control simulation is shown in Figure 1. The simulation mathematical model is discussed in this section of the report of the following three subsections:

- UNREP Maneuvering Mathematical Model
- Computer Generation of Excitations
- The Automatic Controllers.

The first subsection discusses mathematical modeling of the maneuvering dynamics of both the leading and tracking ships, using the nonlinear maneuvering equations and the hydrodynamic interaction forces between the ship hulls.[23] Other relevant ship data are also described. The second subsection discusses the computer generation of the sea state excitations acting on each ship's hull. The third subsection discusses the mathematical model of the automatic controller on each ship.[8,9] The mathematical symbols are defined in the Nomenclature section of the report.

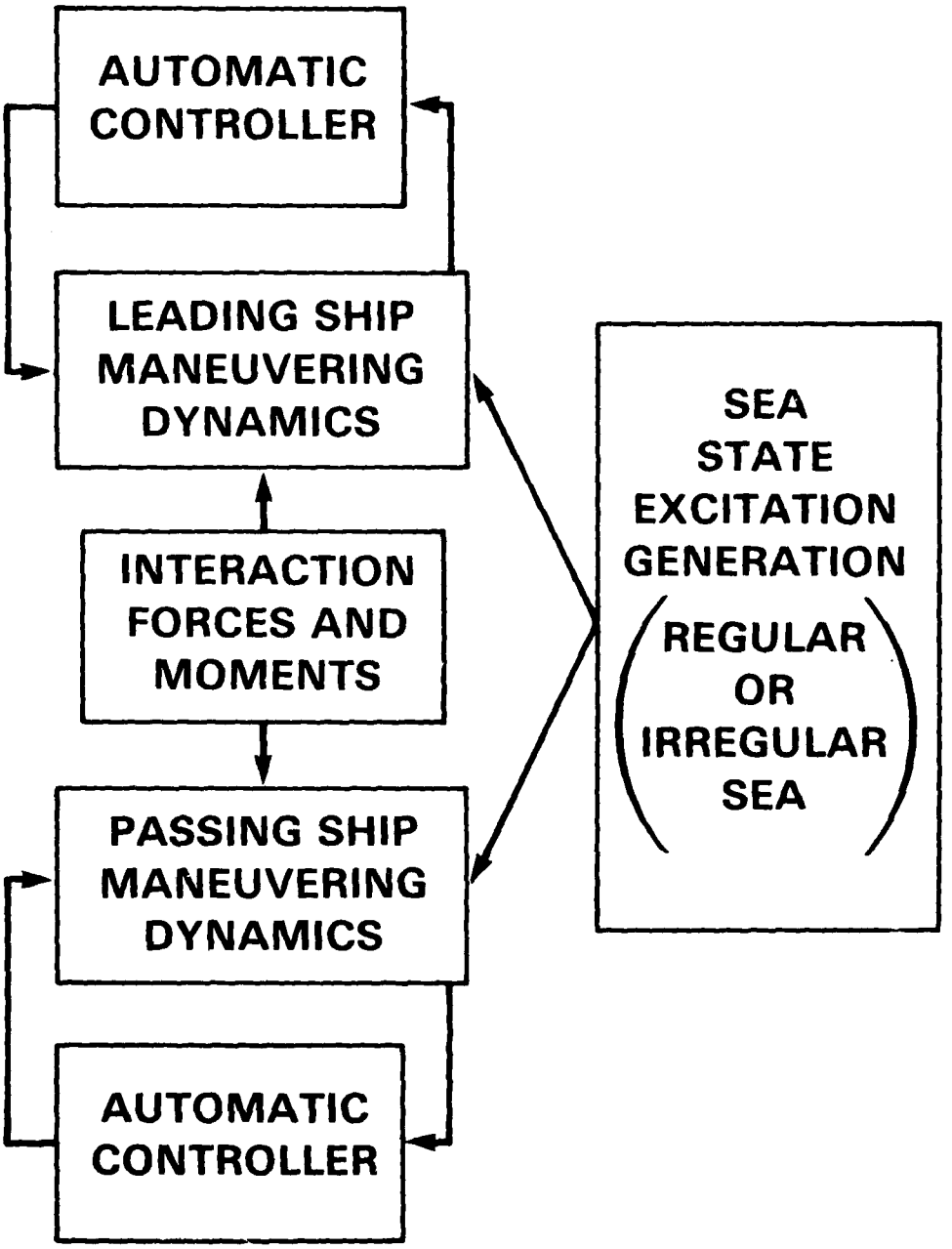

Figure 1 - General Diagram of Underway Replenishment Maneuvering Control Simulation

UNREP MANEUVERING MATHEMATICAL MODEL

General Discussion

The UNREP hydrodynamic mathematical maneuvering model developed for this study incorporates approximate linear and nonlinear sea state excitations and the hydrodynamic interaction forces and moments acting on both the leading and tracking ships (Figure 2), which are traveling at approximately 15 knots. The UNREP control simulation has the capability of manually or automatically controlling either the leading or tracking ship's rudder and propeller shaft speed; but automatic control and quickened manual control of only the rudder are considered in this work. The basic Mariner study ship characteristics are presented in Table 1. The direction of the oblique sea acting on the study ship hull has a ship-to-wave angle of 150 deg (Figure 3).

TABLE 1 - CHARACTERISTICS OF MARINER STUDY SHIP

Length between Perpendiculars	527.8 ft	160.9 m
Beam	76.0 ft	23.2 m
Draft	29.75 ft	9.07 m
Displacement	16,800 tons	16.9×10^6 kg
Block Coefficient, C_b	0.6	0.6
Note: The ship's coordinates are assumed to be at the ship's center of gravity (i.e., x_G, $y_G \approx 0$).		

Basic Mathematical Model

The ship-hydrodynamic, maneuvering mathematical model for each of the two identical Mariner study ships used in this work consists of a set of nonlinear equations in the horizontal plane (i.e., surge, sway, and

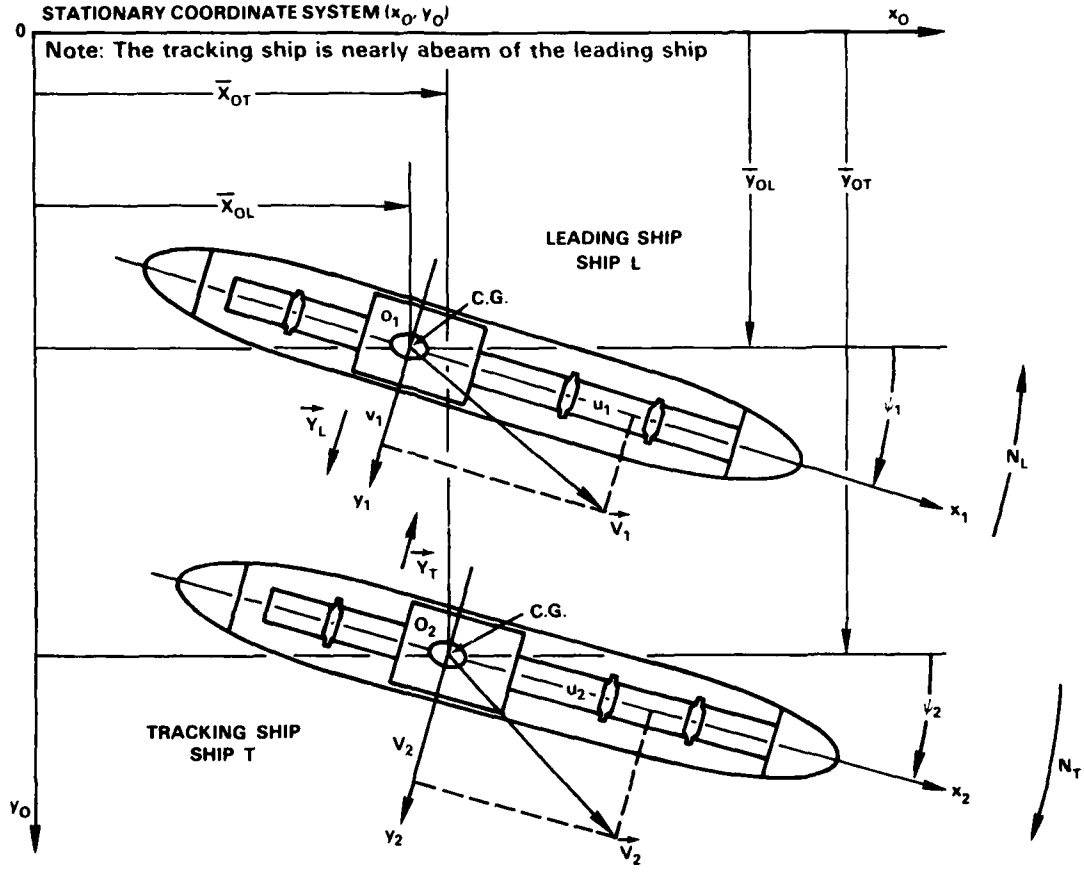

NOTE:
(x_o, y_o) Represents space axis.
(x, y) Represents moving axis fixed in ship.
(N, ψ) Moments and Angular Displacements are positive in the clockwise direction.
(Y, u, v,) Forces and velocity components are positive along the forward directions of the arrows along the axis (x, y) fixed on ship
(Detailed definitions of symbols are presented in the nomenclature sections of this report).

Figure 2 - Orientation of the Leading and Tracking Ships during Underway Replenishment

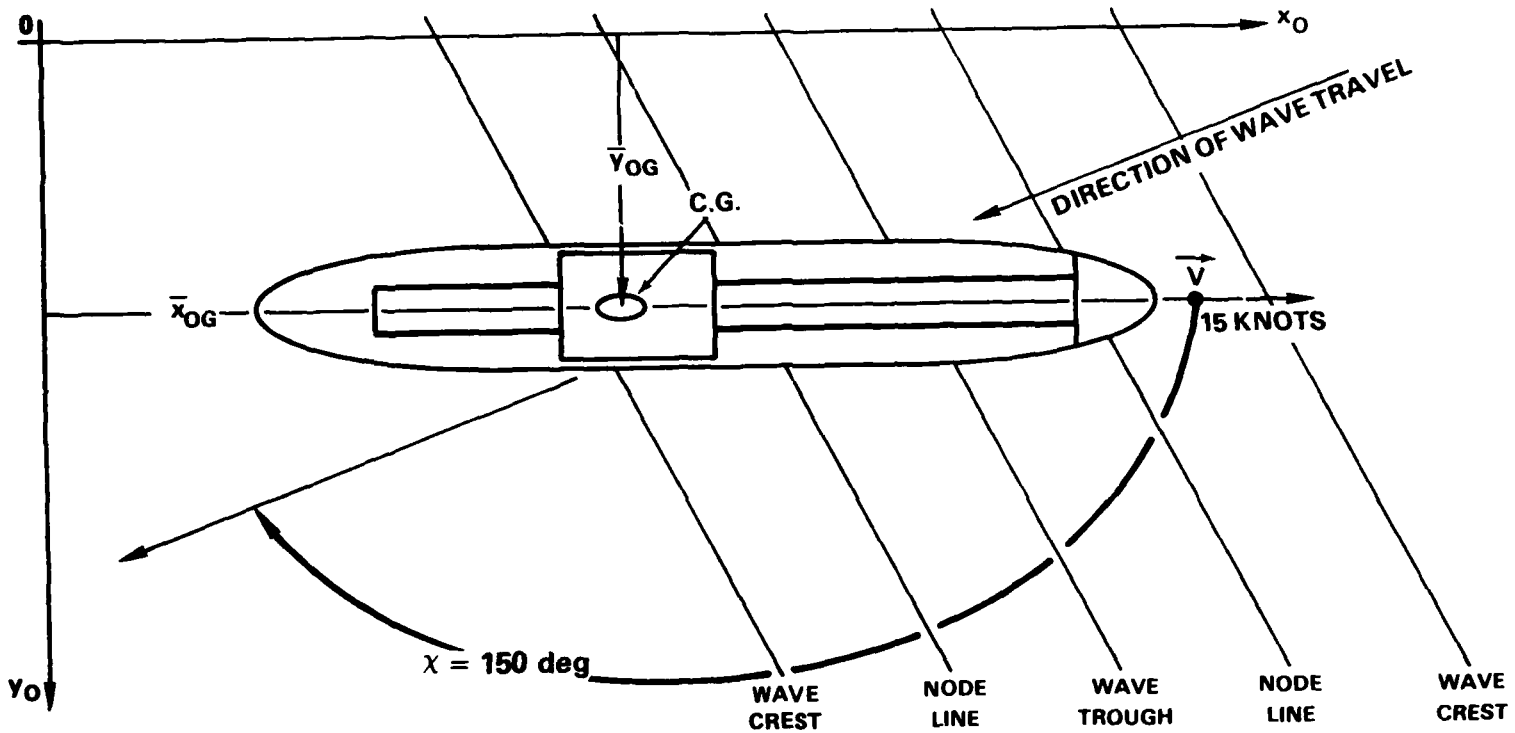

$(\bar{x}_O, \bar{y}_O)$ REPRESENTS SPACE AXIS

(x_{OG}, y_{OG}) REPRESENTS COORDINATES FROM SPACE AXIS TO CENTER OF GRAVITY OF SHIP

$\vec{V}$ = SHIP VELOCITY VECTOR EQUALS 15 KNOTS

* NOTE: SHIP-TO-WAVE ANGLE χ FOR THE IRREGULAR SEAS WAS ALSO 150 deg.

Figure 3 - Orientation of Ship and Regular Waves

yaw). The nonlinear hydrodynamic interaction forces and moments[20] acting between the ship hulls, and the linear and nonlinear effects of the oblique seaway (30 deg off the port bow; Figure 3) are added to the maneuvering equations as additional forces and moments. The sea state simulation is discussed in the following subsection. The effects of the hydrodynamic forces and moments on the ship's hull during UNREP control simulations in both oblique regular or irregular waves were studied. The detailed mathematical model including nonlinear maneuvering equations, hydrodynamic maneuvering coefficients, and other relevant ship data are presented in Appendix A. The steady-state ship interaction curves used in the maneuvering equations are for two Mariner ships traveling at 15 knots on parallel paths. Figures A.1 and A.2 in Appendix A show curves of the hydrodynamic sway forces and yaw moments acting between the two mariners. During UNREP control simulations, the effects of the yawing action of either ship on the interaction forces and moments are assumed negligible since the interaction curves are measured when the ships are on parallel paths. Because transients, in general, are relatively small for the UNREP control simulations, only the steady-state interaction forces and moments are considered.

The lag time and "dead band" in the rudder dynamics[9] when a helm angle is commanded are important aspects of the maneuvering control problem. The rate of change of the rudder angle was assumed to be inversely proportional to the error signal, subject to a maximum rate of 3.5 deg/s. The rudder "dead band" was set at ± 0.5 deg. An analog diagram of the rudder dynamics is presented in Appendix A. Appendix A includes a figure showing the response of the rudder system to step commands. A discussion of the coordinate system for the ship maneuvering problem is also presented in Appendix A.

The UNREP hydrodynamic mathematical maneuvering model has the following assumptions:

- Only oblique irregular and regular seas are simulated. Ship control is assumed to be more difficult for this sea condition than in the head-sea condition where the latter is generally the sea condition for UNREP operations.
- Under the simulation conditions, it is assumed that the ship-to-wave angle (Figure 2) does not change significantly.

- Propeller loading and power plant loading are not considered here because these effects manifest themselves in longitudinal control which is not of primary concern in this study.
- It is assumed that the leading and tracking ships are subjected to the same irregular wave system at any specified instant of time.

COMPUTER GENERATION OF SEA-STATE EXCITATIONS

Regular-Wave Simulation

The first-order sway force and first-order yaw moment induced on the Mariner study ship in oblique regular waves (ship-to-wave angle equals 150 deg) at 15 knots were calculated by a computer program using a strip theory developed by Salvesen, Tuck, and Faltinson.[21] The computer runs were made by the Ship Performance Department of DTNSRDC. The calculated, nondimensional, first-order sway force and nondimensional first-order yaw moment versus regular-wave encounter frequency obtained from these runs are presented in Table 2 and graphed in Figure 4. These data were used in the UNREP maneuvering control simulation runs on regular waves. The computer results are presented later in the report.

First-Order Irregular-Wave Excitations

The first-order sea-state excitations in irregular waves induced on the Mariner study ship hull in an oblique seaway were calculated on the computer. The mathematical equations used to generate the first-order irregular-wave excitations are presented in Appendix B and were presented in detail by Neal.[25] The Pierson-Moskowitz energy density spectrum is needed as a computer input to characterize the sea state. In this work, the Pierson-Moskowitz spectrum[12] was calculated for a significant wave height of 16 ft for a fully developed, wind-driven sea at the ship-wave frequency of encounter. Linear transfer functions of sway force and yaw moment also needed as computer input were obtained from the regular wave data (Table 2).

TABLE 2 - NONDIMENSIONAL FIRST-ORDER SWAY FORCE AND YAW MOMENT IN REGULAR WAVES
(Ship-to-Wave Angle χ Equals 150 deg (See Figure 3))
(Ship Speed = 15 Knots)

ω_e (rad/s)	$F(\omega_e)$ = Sway Force/ ($Mg\zeta/L$)	Sway Force Phase Angle (deg)	$Y(\omega_e)$ = Yaw Moment/ ($Mg\zeta$)	Yaw Moment Phase Angle (deg)
0.293	1.3191	274	0.07246	169
0.361	1.9473	277	0.03741	138
0.433	2.5082	277	0.08306	32
0.509	2.9529	280	0.22726	19
0.588	3.2653	287	0.42925	22
0.679	3.3462	290	0.67170	23
0.756	3.0542	293	0.89061	23
0.845	2.3640	294	0.99661	26
0.938	1.5397	292	1.0366	27
1.034	0.66240	281	0.94590	24
1.133	0.21465	163	0.73952	19
1.236	0.73203	122	0.47369	10
1.342	1.0330	110	0.19894	339
1.452	1.0222	101	0.17588	242
1.565	0.68012	87	0.31972	211
1.682	0.27829	40	0.34974	197
1.801	0.37778	313	0.25216	185
1.925	0.55739	290	0.07516	146
2.052	0.46259	280	0.15072	24

Symbols
M = Displaced mass
g = Acceleration of gravity
ζ = Wave amplitude
L = Length between perpendiculars

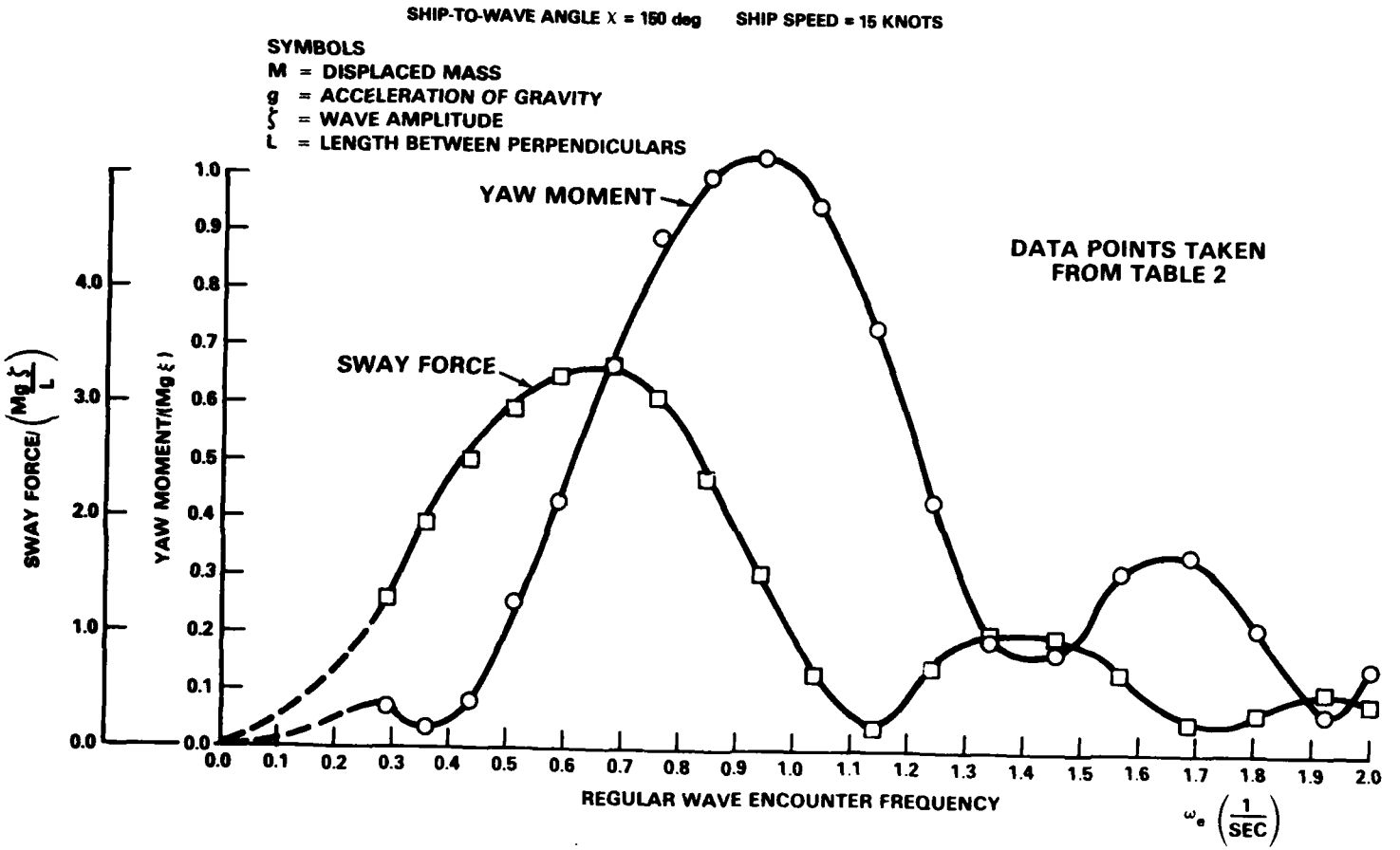

Figure 4 - Nondimensional Sway Force and Yaw Moment versus Regular Wave Encounter Frequency

The linear transfer function $H(\omega_e)$ is defined as

$$H(\omega_e) = \frac{X(\omega_e)}{\zeta(\omega_e)}$$

where $X(\omega_e)$ = sway force or yaw moment at a particular wave encounter frequency

$\zeta(\omega_e)$ = wave amplitude at the same wave encounter frequency.

$H_s(\omega_e)$ can be obtained from the nondimensional sway forces $F(\omega_e)$ in Table 2 as follows:

$$H_s(\omega_e) = F(\omega_e) \times \frac{Mg}{L}$$

and similarly for the nondimensional yaw moment $Y(\omega_e)$:

$$H_y(\omega_e) = Y(\omega_e) \times Mg$$

Figure 5 shows the first-order sway force excitations versus time acting on the Mariner study ship hull in an oblique, irregular wave (ship to wave angle equals 150 deg) with a significant wave height of 16 ft. Figure 6 shows the analogous first-order yaw moment excitation versus time acting on the ship hull. These data, derived from the mathematical equations described in Appendix B, were used in the UNREP maneuvering simulation runs in irregular waves.

Second-Order Irregular-Wave Excitations

Digital computer programs developed by Neal[25] were used to generate the second-order, slowly varying, irregular-sea-state excitations acting on the Mariner study ship hull. The mathematical equations[26-35] used to generate these second-order irregular-wave excitations are presented in Appendix B. The oblique, irregular seaway in the UNREP maneuvering control

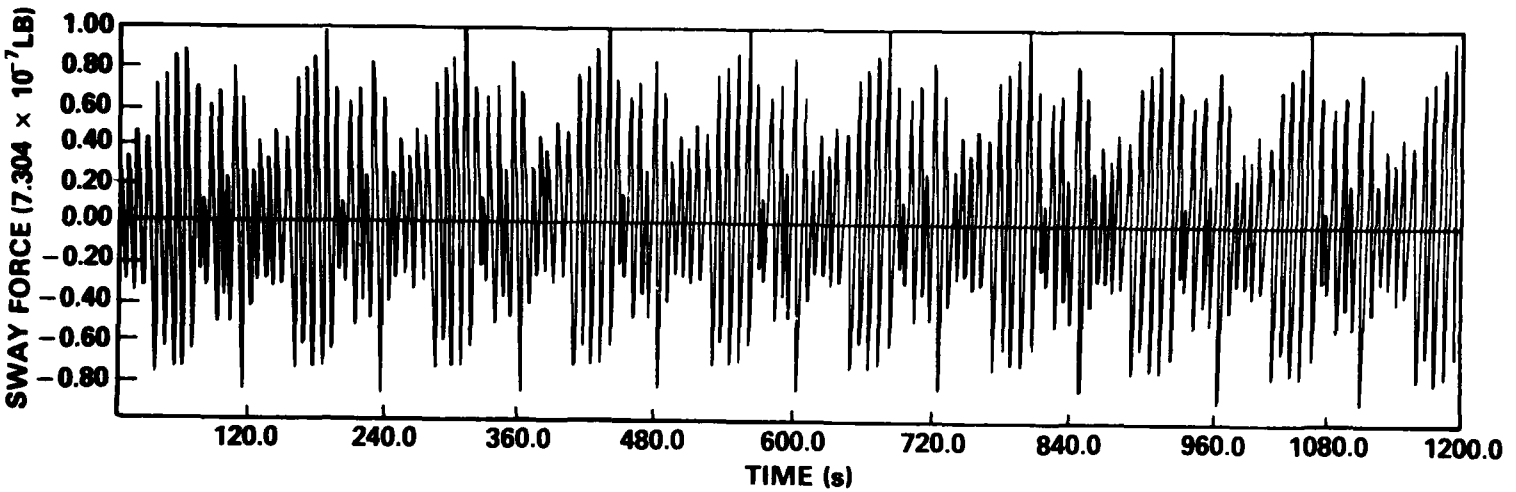

Figure 5 - Sway Force Excitation Acting on Mariner Hull in Irregular Waves versus Time

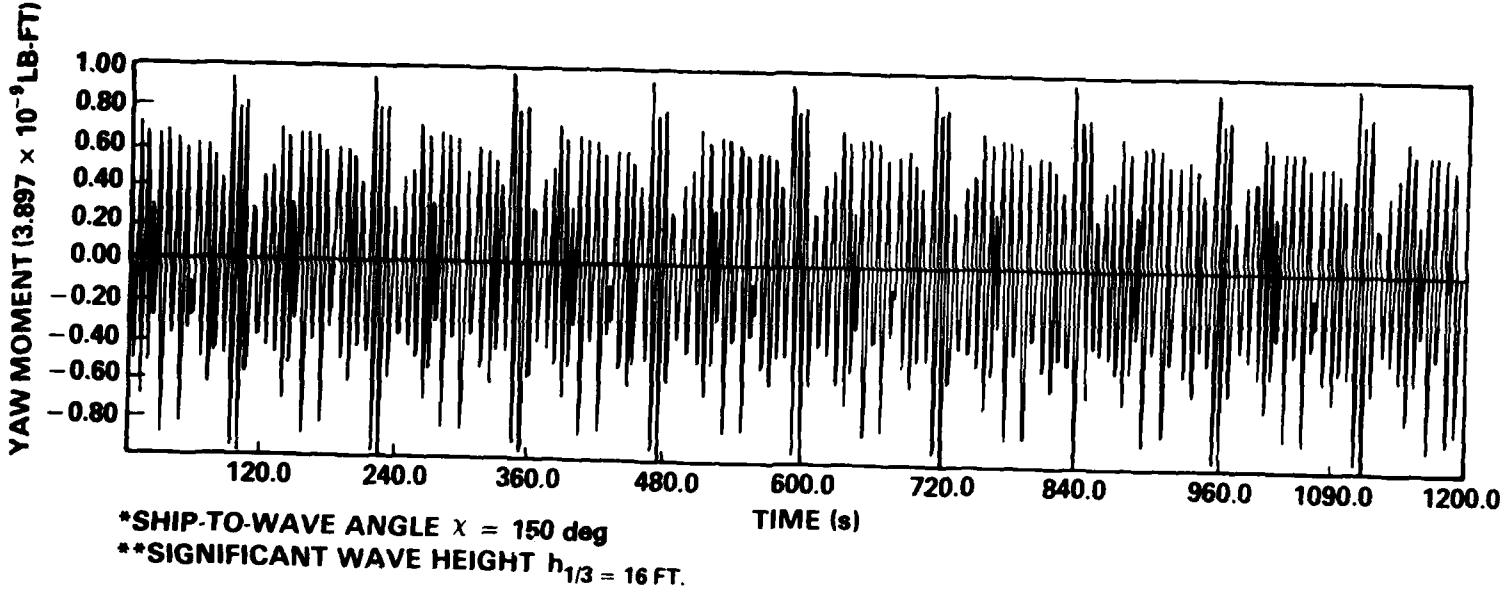

Figure 6 - Yaw Moment Excitation Acting on Mariner Hull in Irregular Waves versus Time

simulation is assumed to be unidirectional and long-crested. The computer input required to generate the time series consists of the Pierson-Moskowitz wave energy spectrum and the Newman approximation to the transfer function associated with the slowly varying sway force (and moment).[34] The seaway is statistically represented in this work by a Pierson-Moskowitz wave energy spectrum representing a sea state 4 on the Beaufort scale.[9,10] The sea state, wave height time series corresponding to the Pierson-Moskowitz spectrum is shown in Figure 7.

The digital computer-generated,[25] nonlinear, hydrodynamic sway force versus time, and the nonlinear, yaw moment versus time acting on the Mariner study ship at 15 knots in a 150-deg, low, irregular sea (significant wave height of 4 ft)[9,10] are presented in Figures 8 and 9, respectively. The slowly varying sway force and moment time series for 8- and 16-ft significant wave heights were approximated by multiplying the above time series amplitudes by factors of 4 and 16, respectively. These data were used in the UNREP maneuvering control runs in irregular waves presented later in the report.

THE AUTOMATIC CONTROLLERS

The automatic feedback control algorithms required for the UNREP control simulation work were initially developed in the earlier work by Alvestad.[8] During UNREP operations at sea, the leading ship is charged with maintaining a constant heading while the tracking ship is responsible for maintaining a constant separation distance. In the hybrid computer simulation, the control algorithms for the two ships were adjusted to reflect their different maneuvering control functions.[8-10] The basic flow diagram for the automatic control for a single ship is shown in Figure 10. Both the leading and tracking ships have automatic controllers which act independently of each other. The details of the mathematical modeling of the automatic controller on each ship are described in Appendix C.

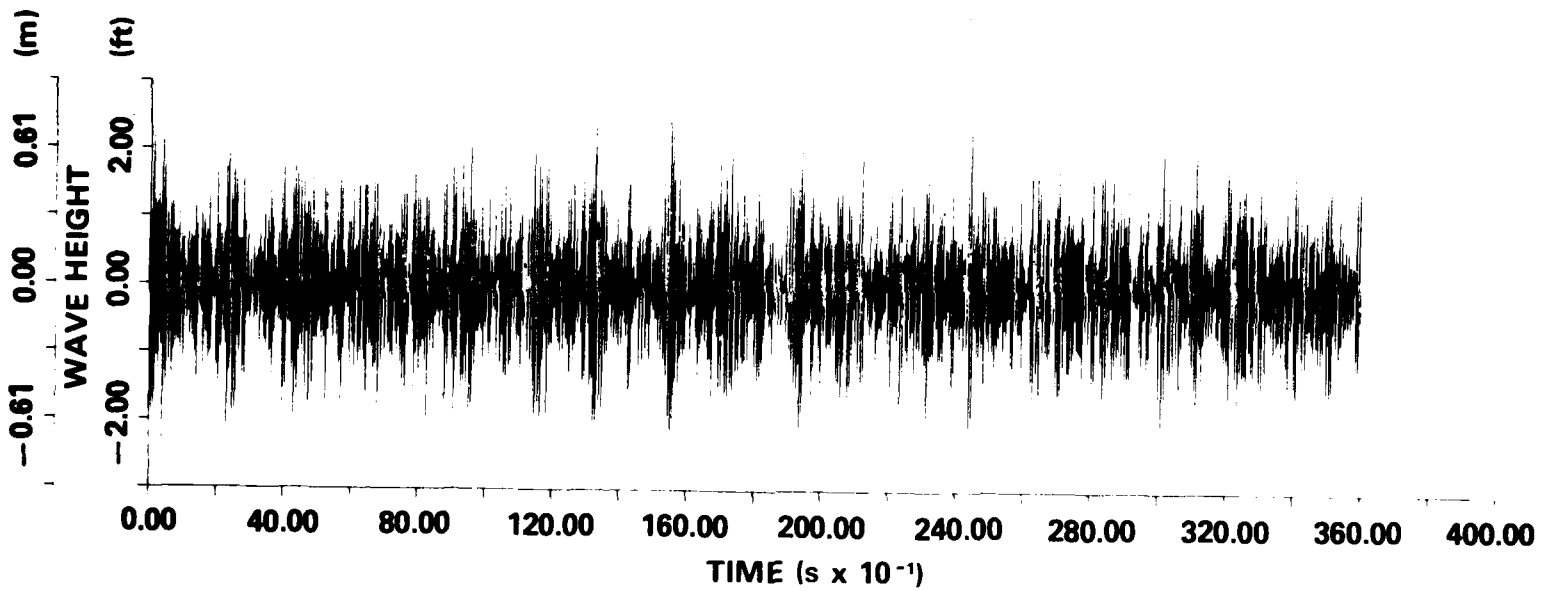

***State 4 sea on Beaufort scale (approximately significant wave height of 4 ft)**

Figure 7 - Stationary Seaway Represented by Wave Height Time Series[10]

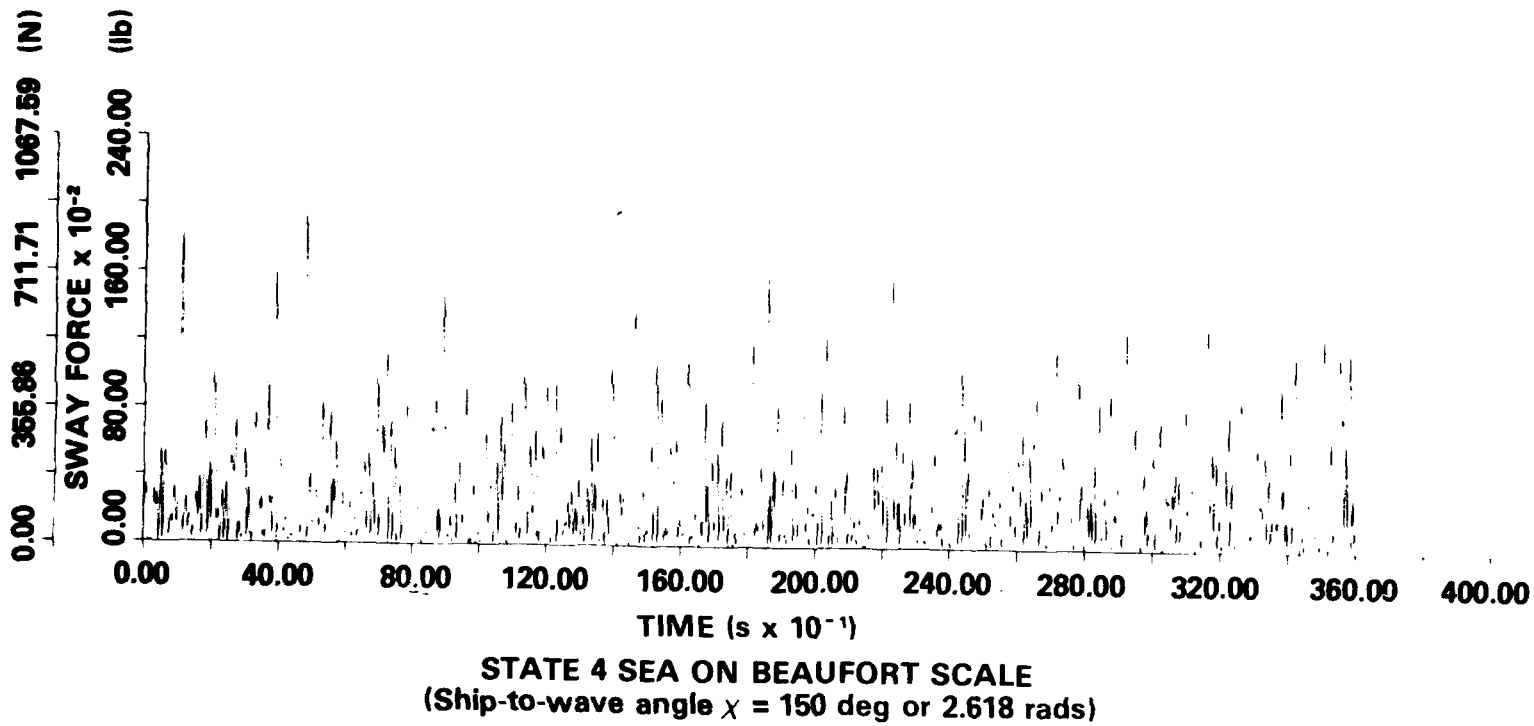

Figure 8 - Slowly Varying, Second-Order, Hydrodynamic Sway Force[10] versus Time for Mariner Study Ship at 15 Knots in Oblique, Irregular Waves (χ = 150 Degrees)

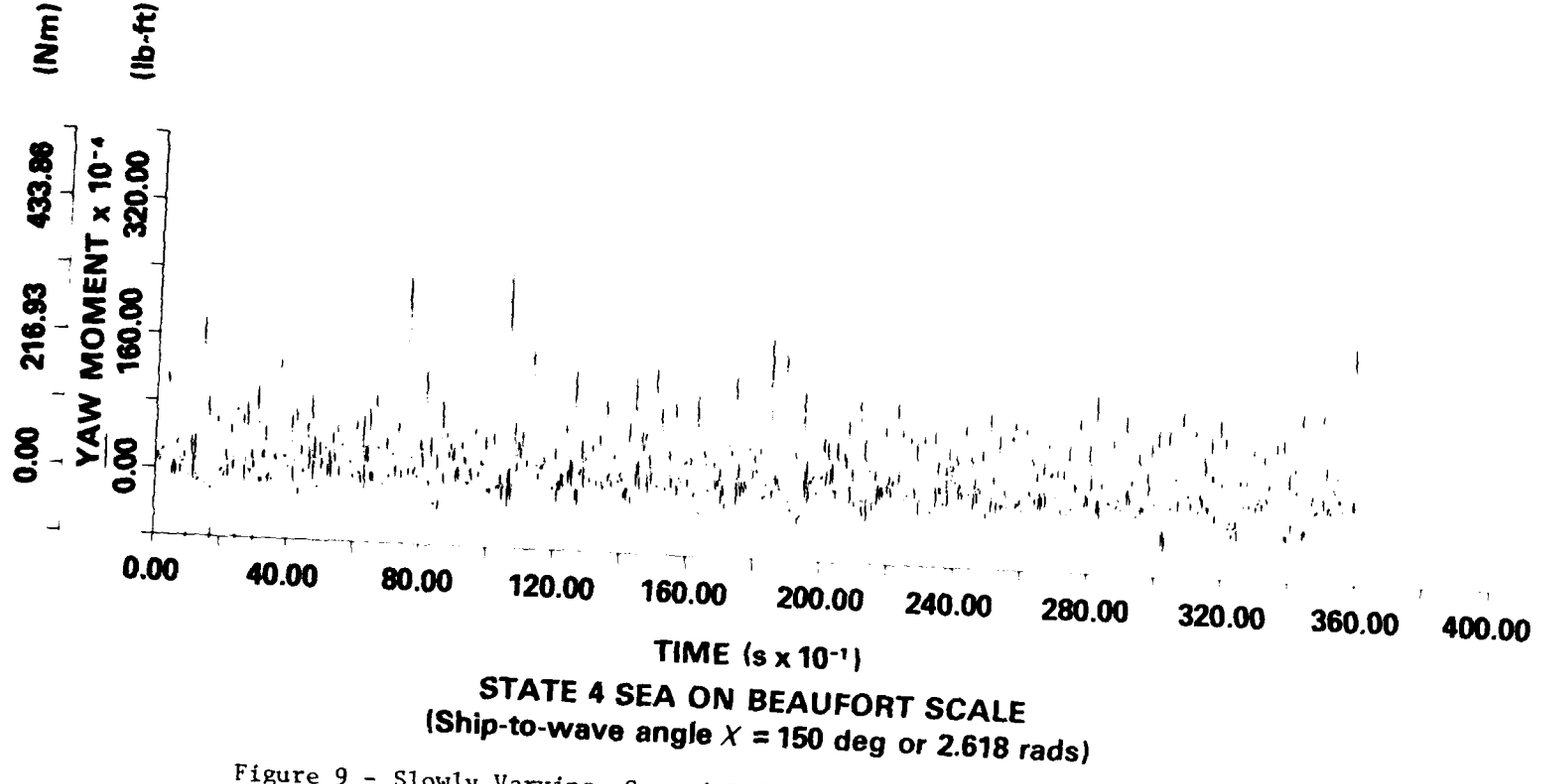

Figure 9 - Slowly Varying, Second-Order, Hydrodynamic Sway Force[10] versus Time for Mariner Study Ship at 15 Knots in Oblique, Irregular Waves (χ = 150 Degrees)

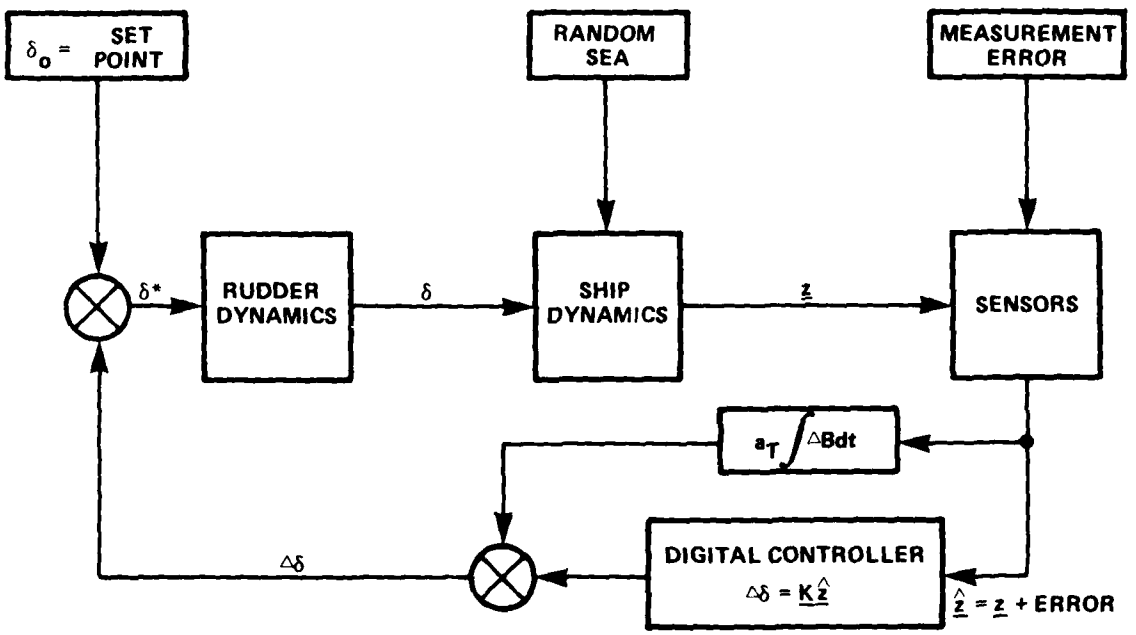

Figure 10 - Automatic Controller Flow Diagram[12] for Single Ship
(The leading ship's automatic controller acts independently
of the automatic controller on the tracking ship.)

The automatic controller is based on simple, classical control considerations and has some limitations. The high-frequency disturbances caused by the high-frequency part of the irregular sea acting on the ships' hulls during UNREP (which cannot be compensated for by the rudder) should be filtered out (i.e., adaptive wave motion filtering). Some runs were made by incorporating an electronic, low-pass filter into the automatic controller configuration to remove some of the high-frequency noise. The filter was placed on the commanded rudder signal, which decreased the high-frequency oscillations of the rudder on each ship and resulted in reduced lateral control. A sample run is reported in the UNREP Simulation Results Section.

AUTOMATIC CONTROL AND QUICKENED MANUAL CONTROL

Based on results of earlier work on this project, it was concluded that the requisite control variables for adequate control of the tracking ship during UNREP are ship speed, heading, heading rate, lateral separation, and lateral separation rate. It was also found that sensor noise and measurement errors in the range of 3 to 5 percent in a Beaufort sea state 4 or 5 (containing only sway force and yaw moment nonlinear excitations) allowed maintenance of a safe lateral separation (100 ft).[9] It remained to be determined how to use those variables in the ship control problem. There are two possibilities--fully automatic control or some form of quickened manual control.

The earlier results[9,10] showed that, under the conditions of the simulation, an automatic controller is capable of controlling the ship to maintain adequate lateral separation. A block diagram of the automatic controller used in that work is shown in Figure 10. More details of this work are in Appendix C. Without the lateral separation inputs, the automatic controller is representative of an ordinary autopilot. The automatic controller model also provides a good mathematical description of the total UNREP ship control equations which must be solved continuously in real time by a man, a machine, or some combination of both. Totally replacing the automatic controller with a man means that, although he does not consciously think in the usual mathematical terms, he must solve the same

ship control equations continuously. This is the case during current UNREP maneuvers in which the man is required to act as a differentiator and to estimate both the errors and error rates of at least two variables in a system that responds slowly.

In closed-loop, man-machine applications where it is not feasible to replace the person with a fully automatic controller, it is good human engineering practice to ensure that the transfer function mathematically representing the control actions of the operator is as simple as possible.[12-14] Current UNREP practice has the opposite effect. A measure of the complexity of the human tasks may be found in the fact that UNREP steering control responsibilities are shared by two very busy people--the conning officer and the helmsman.[1,2]

It is anticipated that shipboard personnel[12,14] will be extremely reluctant to accept fully automatic control of steering during UNREP. Autopilots generally capable of maintaining a heading with the required precision are not normally used during UNREP. One reason for this is safety. Without the incorporation of failure detection schemes and/or redundancy, autopilot failure modes could result in such large rudder angles that collision becomes inevitable before corrective action can be begun.

"Quickening" is a process for simplifying the task of the human operator.[12,14] It combines the superior course-keeping capabilities of the autopilot with the adaptability and judgment of the human operator. It allows him to make use of the computational capabilities of the autopilot while remaining in a position to begin manual corrective actions from a condition which is very nearly correct. A quickened display directly shows the operator what control action is required, while permitting him to retain the same degree of physical control he would have without the quickened display.

Although quickened displays are not in general use aboard ship, one was recently developed and patented[17] in a configuration suitable for ship steering control. Moreover, its design allows it to be integrated with the UNREP automatic controller developed for the sensitivity analyses.[8,9] The resulting configuration is shown in Figure 11. Note that,

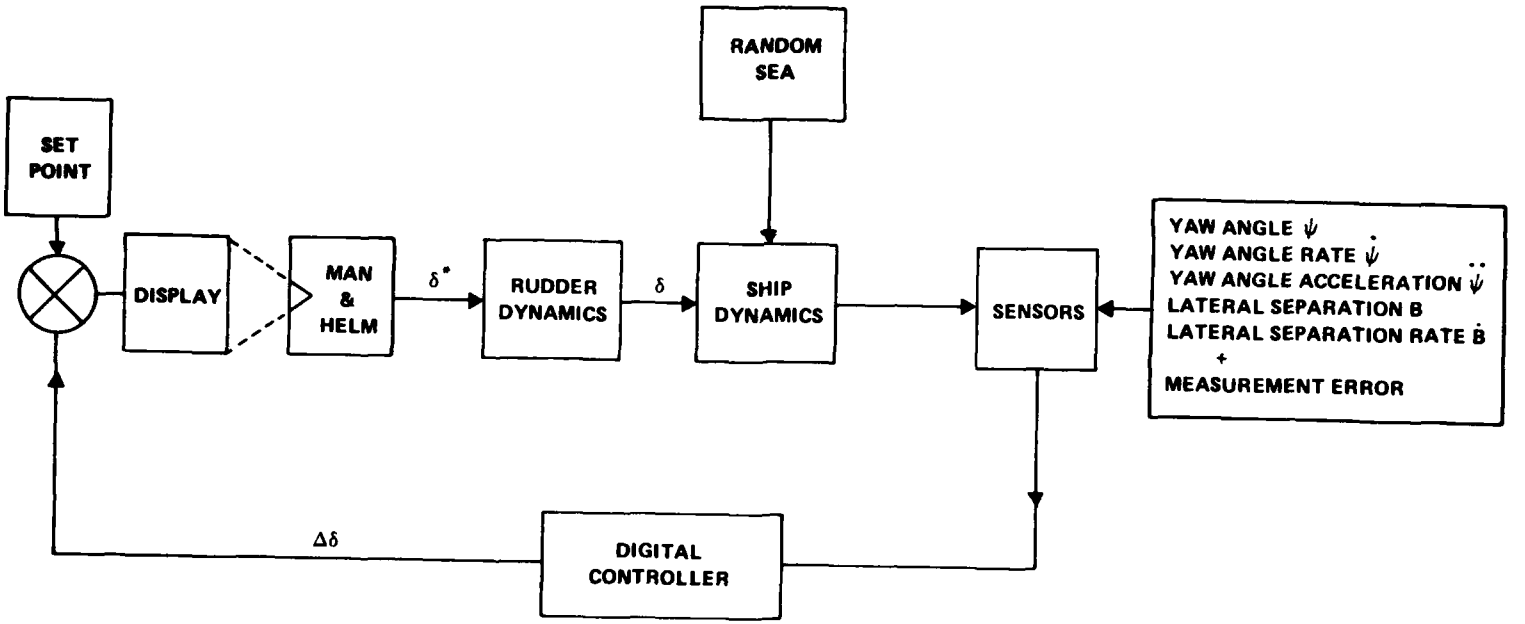

Figure 11 - Simulated Quickened Display Block Diagram[12] (Passing Ship)

although the computational capabilities of the automatic controller are retained, a human operator is available for timely intervention in case of a digital controller malfunction.

The quickened display, shown in Figure 12, uses a double-pointer dial with a digital vernier. One pointer is driven by the digital controller output that would, in a fully automatic configuration, control the rudder. The other pointer is driven by the helm wheel, which is used by the helmsman to control the rudder manually. To match the accuracy, efficiency, and speed of response of the automatic controller, the helmsman has only to move his wheel to keep the pointers matched. In this work, the quickened control was effected by a human operator controlling a potentiometer while observing the display.

To evaluate the feasibility of using the automatic controller while retaining a significant degree of human intervention capability, the quickened steering display was produced on a digital television (Figure 13) and added to the fully automatic controller (Figure 11). Data were then collected using both the automatic and quickened manual steering modes to evaluate the ability of a human operator, aided by the quickened display, to match the performance of the fully automatic controller.

INSTRUMENTATION FOR SEPARATION MEASUREMENT

The instrumentation in the block diagram for the quickened display (Figure 12) must be determined. Most of the sensors[11] that are required are currently available and meet the estimated accuracy requirement. The log, gyro, helm-angle transmitter, and rudder angle transmitter are instruments available on virtually all ships. Production of the range and bearing sensors is currently feasible in industry and these sensors are becoming available as commercial instruments.

Ideally, the candidate range finder would have continuous outputs. However, the type of range finder available may only make discrete measurements. Therefore, UNREP control simulations were performed using automatic control in a high sea state to determine how long the automatic controller on the tracking ship could wait for updated separation and separation rate information (see UNREP Simulation Results Section).

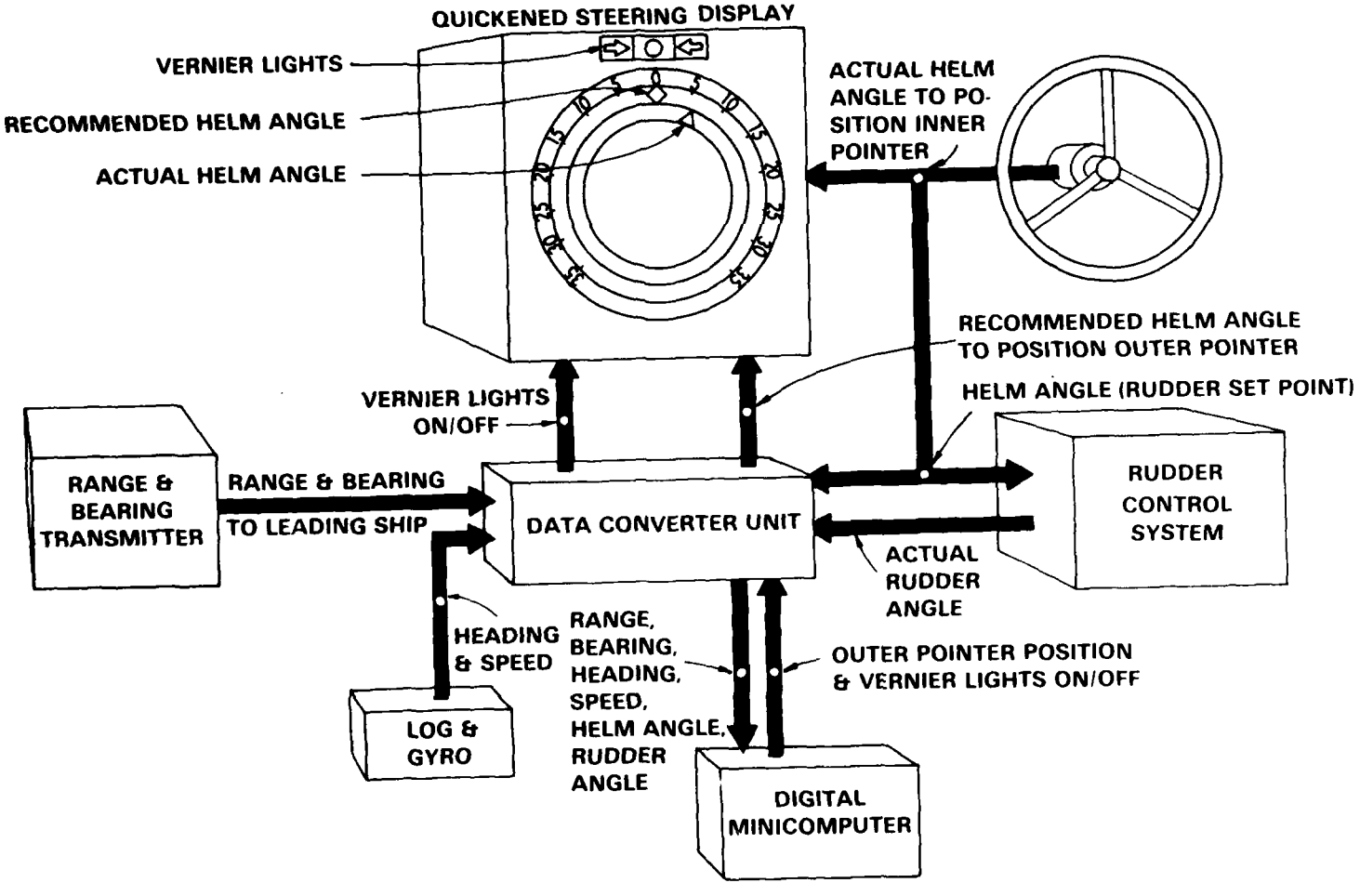

Figure 12 - Quickened Display Pictorial Diagram[12]

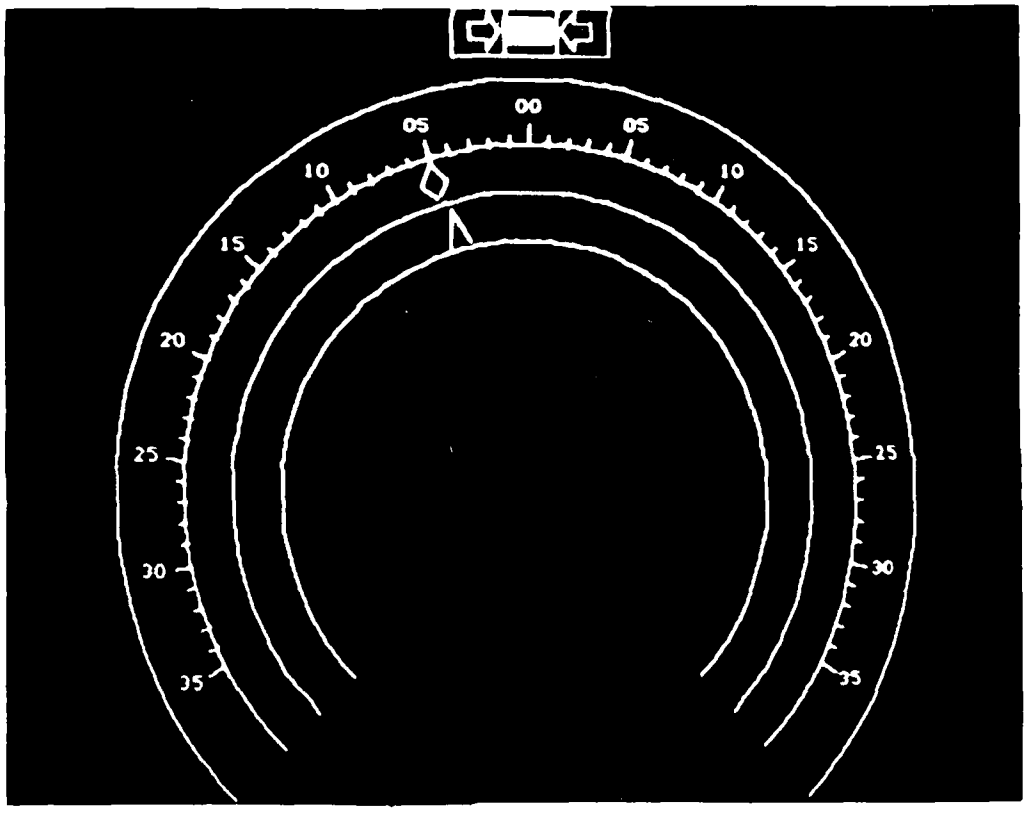

Figure 13 - Quickened Display Television Screen Used during Simulation

GPO 865 152

Infrared lasers, ultrasonic transponders, optical range finders, and radar are currently being considered for application as range and bearing sensors for UNREP.[12] The candidate instrument must measure lateral separation distance and rate. The final sensor should be chosen from the candidates by considering cost, accuracy, and results from full-scale sea trials. Earlier simulation control results in moderate seas (using only nonlinear sea state excitations) indicated that 3 percent accuracy[8,9] over a range of 100 to 2000 ft is sufficient. The sensor should be passive, automatic, and update the output at least every second. It should be remembered that the requirements for accuracy and update are based on simulation control studies only. Full-scale sea trials or model tests using automatic control are required to completely validate these results.

An infrared laser range finder[12] emits radiation in a frequency band where large amounts of radiation are present. Thus, the infrared laser frequency can be selected to be absorbed by the atmosphere, while maintaining a signal of sufficient strength to measure the range over the 2000 ft, as required. This type of instrument is currently used by the Army and is commercially available. These instruments also have the option of voice communication over several channels. However, infrared laser range finders are not available in a design configuration that will work aboard ship. Radar range finders are good candidates because they have already been developed except for roll, pitch, and yaw compensation. However, radar systems may not be able to meet covert operation requirements. An excellent candidate is an optical range finder because it is inexpensive, passive, and sufficient time is probably available between output updates for calculation and adjustment. Roll, pitch, and yaw compensation would have to be designed into an optical system. An airborne ultrasonic transponder is a system that is in the development stage. It emits highly dispersive radiation which makes it essentially undetectable from enemy craft.

Roll, pitch, and yaw produce alignment and motion-induced errors in all candidate systems. This problem must be solved in the potential sensors before any would be feasible for shipboard application. At the Center, experiments are being planned for the laboratory and at sea during UNREP to evaluate the candidate range and bearing sensors.

UNREP SIMULATION RESULTS

The strip-chart recordings in this section show the results of hybrid computer UNREP simulations conducted to analyze the effects of factors which were not considered in earlier work. Simulation conditions pertaining to each figure are tabulated in Table 3. All simulations were conducted at a ship-to-wave angle of 150 deg, as shown in Figure 3. The eight channels of each strip-chart recording show the following parameters:

Channel 1 - deflection of the rudder of the leading ship, (δ_L).

Channel 2 - deflection of the rudder of the tracking ship, (δ_T).

Channel 3 - longitudinal separation distance measured between centers of mass of the leading and tracking ship, (A).

Channel 4 - lateral separation distance between two ships (side-to-side distance measured between the two ships), (B).

Channel 5 - yaw angle of the leading ship, (ψ_L).

Channel 6 - yaw angle of the tracking ship, (ψ_T).

Channel 7 - sway force excitation induced by sea state on ship hull, ($Y_s(\chi)$).

Channel 8 - yaw moment excitation induced by sea state on ship hull, ($N_s(\chi)$).

The channel assignments for Figure 14 are the same as those above, except that channels 7 and 8 are assigned as follows:

Channel 7 - cross-track location of the center of mass of the leading ship relative to the coordinate system fixed with respect to the surface of the earth, (y_L).

Channel 8 - cross-track location of the center of mass of the tracking ship relative to the coordinate system fixed with respect to the surface of the earth, (y_T).

TABLE 3 - SIMULATED SEA STATE CONDITIONS

Simulation Conditions

Figure	Calm Seas	Regular Seas	First-Order Only	Second-Order Only	First- & Second-Order	Severe Sea State	Automatic Control	Quickened Manual Control	Sampled Measurements	Rudder Input Low-Pass Filter	Navy Ships	Pierson-Moskowitz Spectrum	Newman Approximation
14	X						X						
15		X					X						
16		X						X					
17		X				X	X						
18		X					X						
19		X						X					
20		X				X	X						
21			X			X	X					X	
22			X			X		X				X	
23				X			X					X	X
24				X			X					X	X
25				X		X		X				X	X
26				X		X	X					X	X
27					X	X	X					X	X
28					X	X		X				X	X
29					X	X	X		X			X	X
30					X	X	X		X			X	X
31					X	X	X		X			X	X
32					X	X	X			X		X	X
33					X	X	X					X	X
E.1	X						X				X		
E.2		X					X				X		

Sea State Definitions

Sea State	Excitations on Ship Hull	Simulation Methodology
Calm Sea	No sea state excitations	--
First-Order Irregular Sea	Large low- and high-frequency excitations; with high-frequency excitations a major control problem	Linear Superposition Theory
Second-Order Irregular Sea	Small, low-frequency excitations; no major control problem	Nonlinear Theory, using Weiner Volterra Series (see Neal)[25]
Regular Waves (sinusoidal waves)	Large, low- or high-frequency excitations; with the frequency of the waves concentrated around one frequency	Strip Theory (see Salvesen et al.)[21]

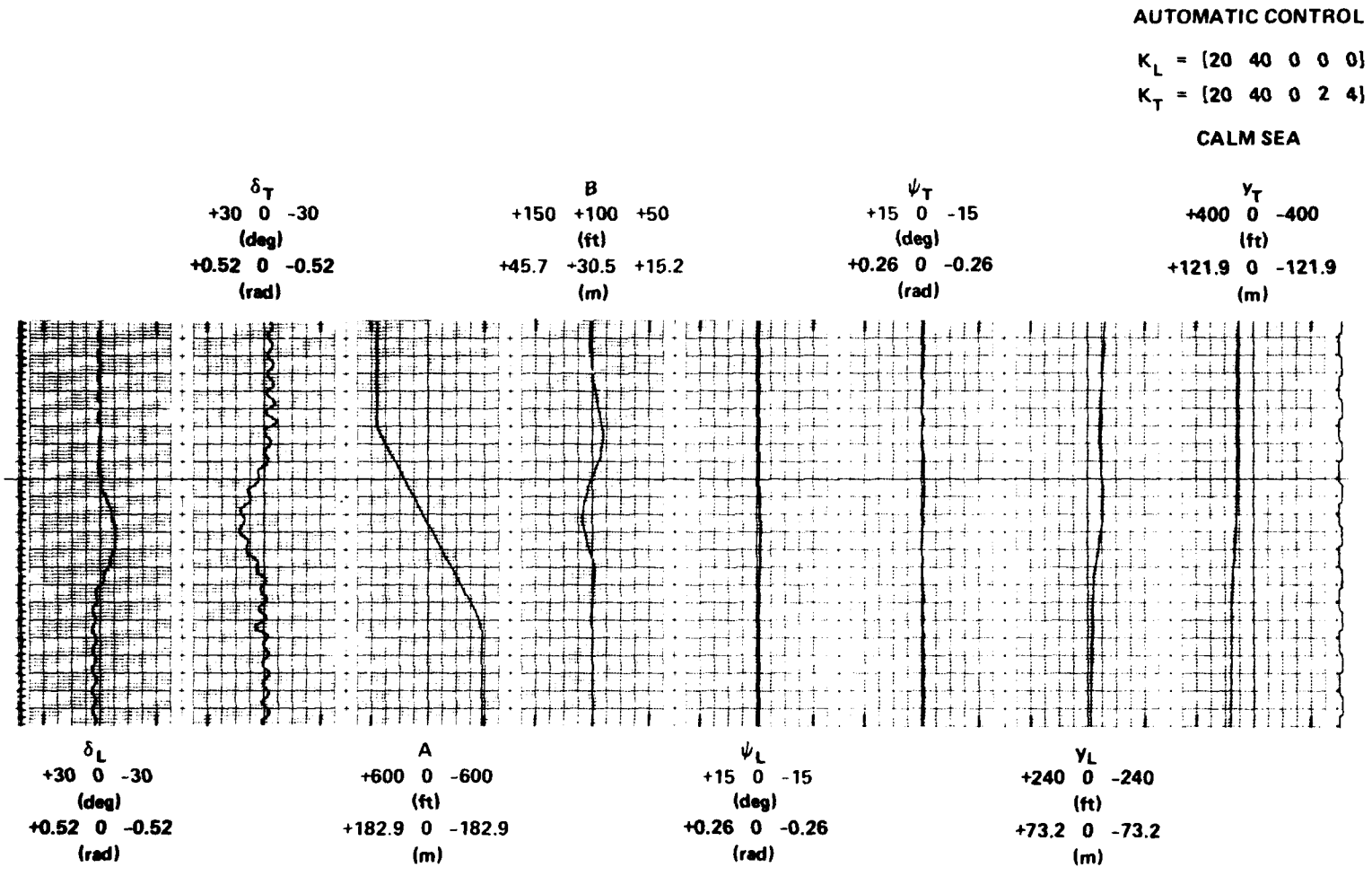

Figure 14 - Underway Replenishment Control Passing Maneuver in Calm Water (Automatic Control)

In all figures, subscripts L and T on the symbols in the figures refer to the leading and tracking ship, respectively. The gains on the controller of each ship are shown at the top of each figure.

Speeds of both Mariner study ships are approximately 15 knots in all UNREP control simulation maneuvers. Hydrodynamic interaction experimental data (taken from Calvano)[23] limit the side-to-side separation to a distance of 50 to 150 ft (15.2 to 47.72 m). The rudder commands on each ship are limited to ±30 deg in the simulation. Each ship has a separate automatic controller. When the quickened manual control mode is used, the automatic controller on the passing ship is replaced by a quickened manual controller (Figures 10 and 11). On the tracking ship, the controller's function is to maintain the lateral separation distance at the desired value (100 ft). The leading ship's controller function is to maintain a predetermined straight-line course. The controllers on each ship are not directly coupled.[8-10] The passing maneuver is the only maneuver simulated since it is more difficult to control than a stationkeeping maneuver.

In Appendix D, curves and tables of the hydrodynamic interaction forces and moments between the AO 177 and a destroyer study ship are presented. In Appendix E, preliminary simulation results are presented for the AO 177 class and a destroyer study ship.

NONLINEAR MANEUVERING EQUATION RESULTS

The ability of the automatic controllers to maintain adequate lateral separation after the addition of nonlinear maneuvering equations to the UNREP maneuvering mathematical model is illustrated by the results shown in Figure 14. It also shows the behavior of the simulated ships and automatic controllers in the absence of wave excitations. The continuous, small, rudder oscillations that occur on each ship, even though the water is calm, illustrate the fact that the ships are in unstable equilibrium and require continuous adjustments to the rudders to maintain lateral separation between 90 and 110 ft.

REGULAR-WAVE EXCITATION RESULTS

Moderate and severe regular-wave excitations were simulated at three different frequencies of encounter; one frequency which maximizes sway force, one frequency which maximizes yaw moment, and one frequency at which both sway force and yaw moment are greatly reduced but not simultaneously minimized.

Results of UNREP control simulations conducted with 5-ft and 10-ft amplitude regular waves at a frequency of encounter of 0.679 rad/s, which corresponds to 793-ft wave length, are shown in Figures 15 through 17. Sway-force excitations are maximized (see Figure 4) at this frequency. Figures 15 and 16 show the results for moderate (5-ft) amplitude waves with automatic and quickened manual control, respectively. With automatic control, lateral separation varies smoothly from 90 ft to 115 ft. Rudder movements and heading changes for both the leading and tracking ships are small and of approximately equal amplitude, frequency, and phase.

With quickened manual control of the tracking ship, as illustrated by Figure 16, lateral separation varies over a slightly wider range (85 ft to 120 ft) and the amplitudes of both rudder movements and heading changes on the tracking ship are greater than with automatic control.

Figure 17 shows the result of increasing the regular wave amplitude to 10 ft and changing the coefficients of the automatic controller of the tracking ship slightly. Lateral separation and tracking ship heading both vary much more than with 5-ft waves. The fact that there is little more amplitude of rudder motion to correct the large error in separation distance than there is to correct the small errors observed from Figure 15 suggests that the automatic controller is not sufficiently responsive to changes in lateral separation under these conditions.

Figures 18 and 19 show the results of UNREP control simulations conducted with 5-ft amplitude regular waves encountered at a frequency of 0.938 rad/s, which maximizes yaw moment due to regular wave excitations at the 150-deg angle of encounter. This frequency corresponds to 473-ft wave length. With automatic control on both ships, as shown in Figure 18, rudder and heading excursions of both ships are small and match the frequency of the wave excitations. Lateral separation varies smoothly from

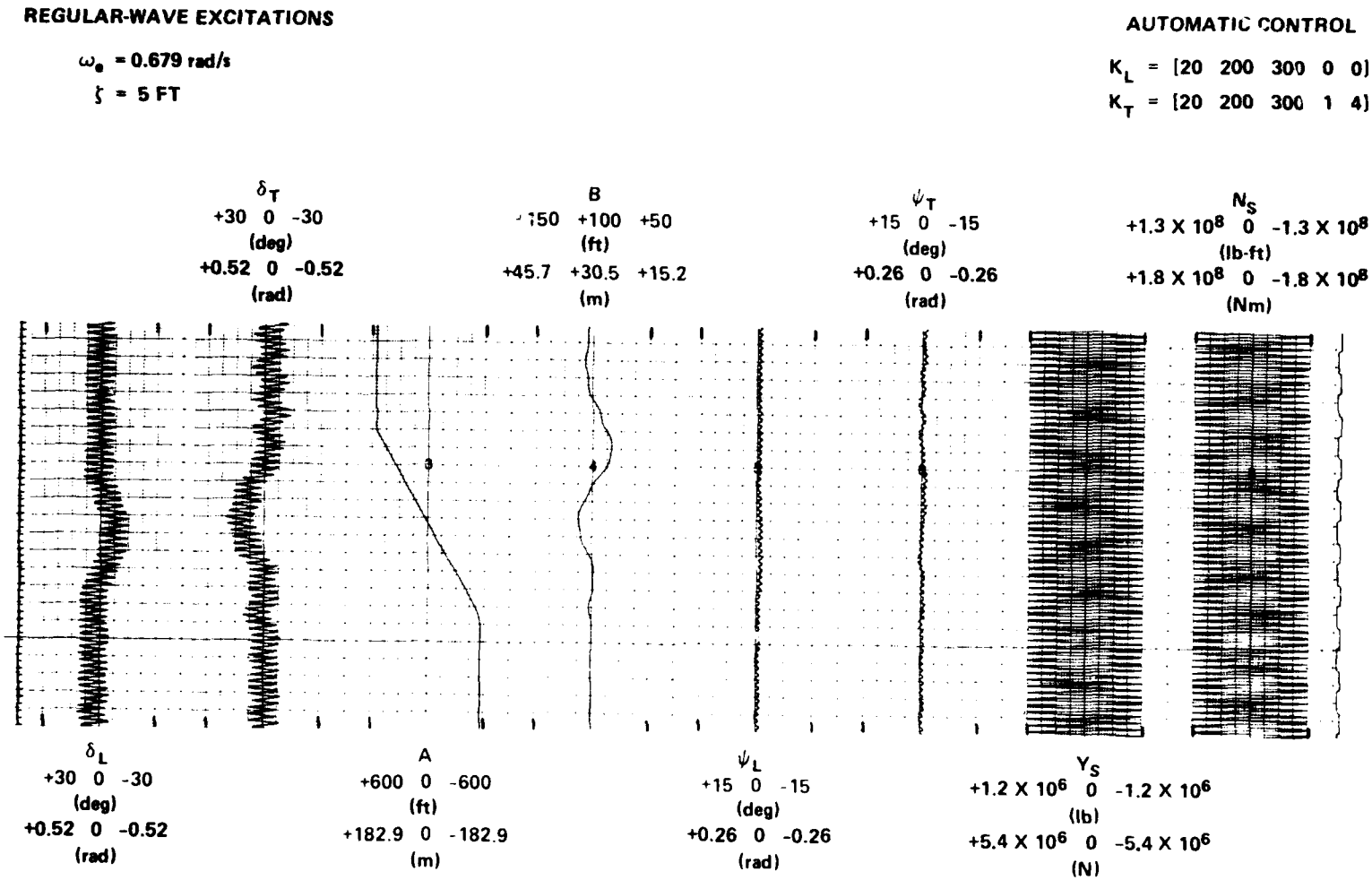

Figure 15 - Underway Replenishment Control Passing Maneuver in Regular Waves (Automatic Control)

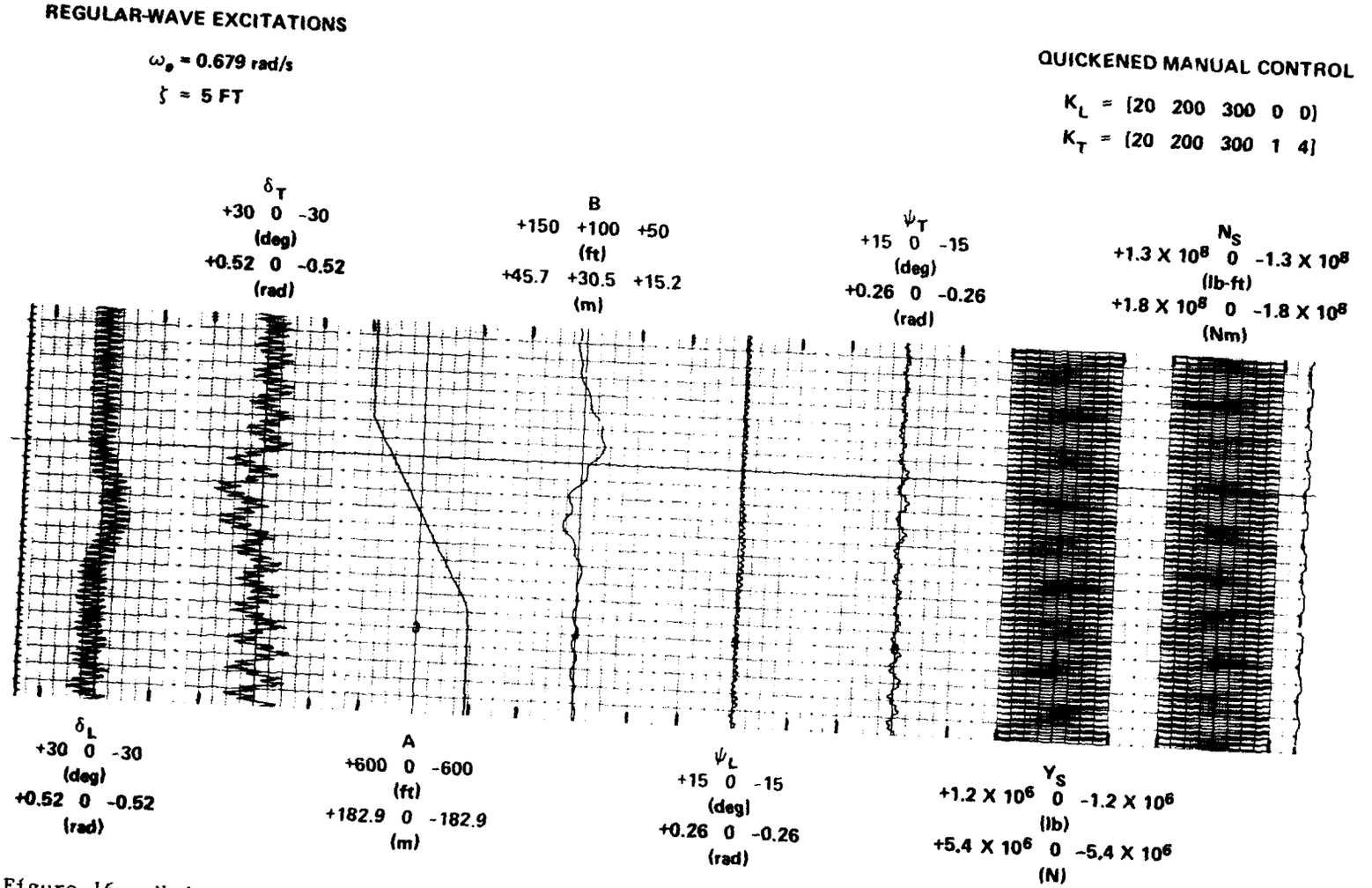

Figure 16 - Underway Replenishment Control Passing Maneuver in Regular Waves (Quickened Manual Control)

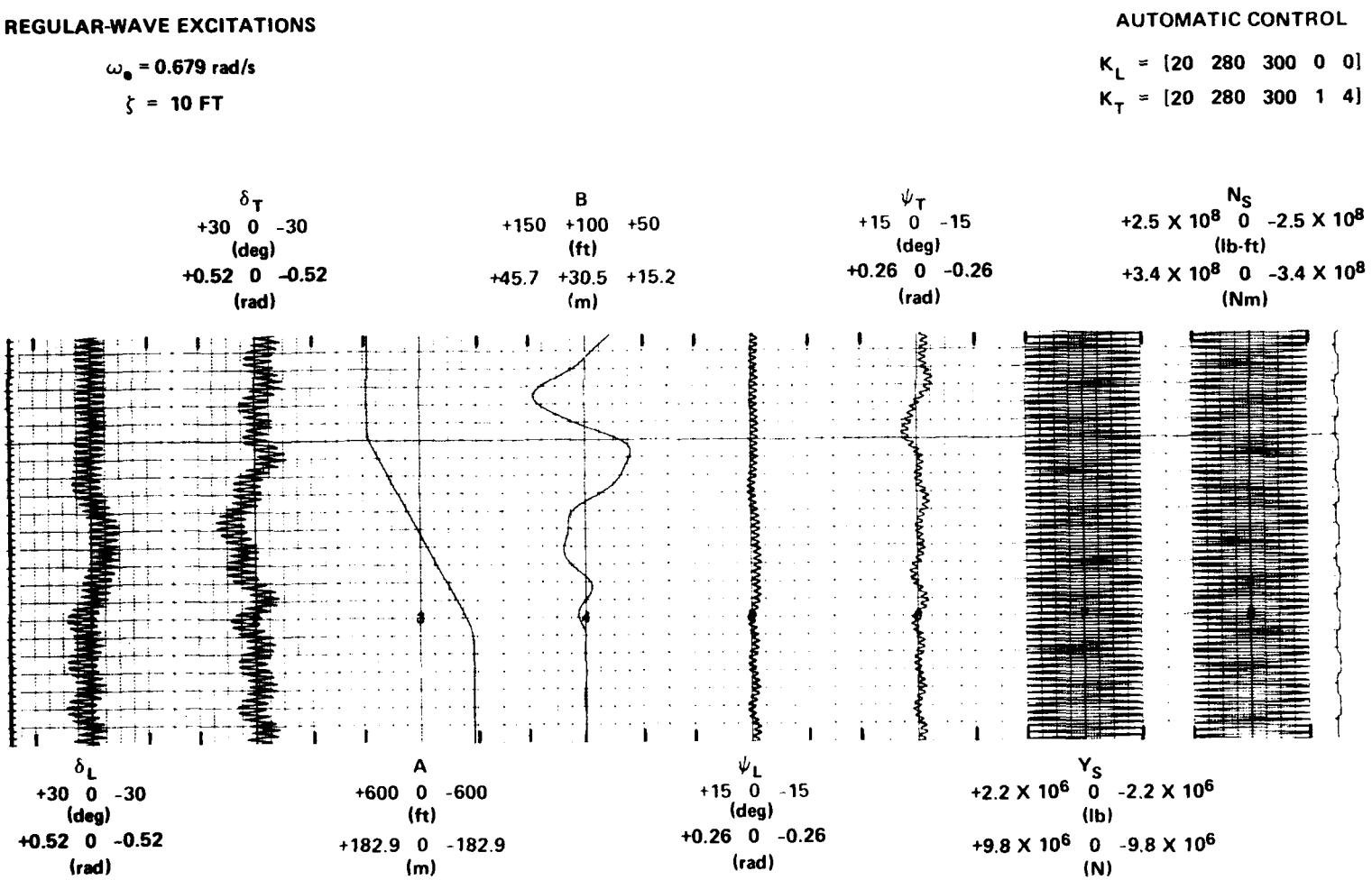

Figure 17 - Underway Replenishment Control Passing Maneuver in High Regular Waves (Automatic Control)

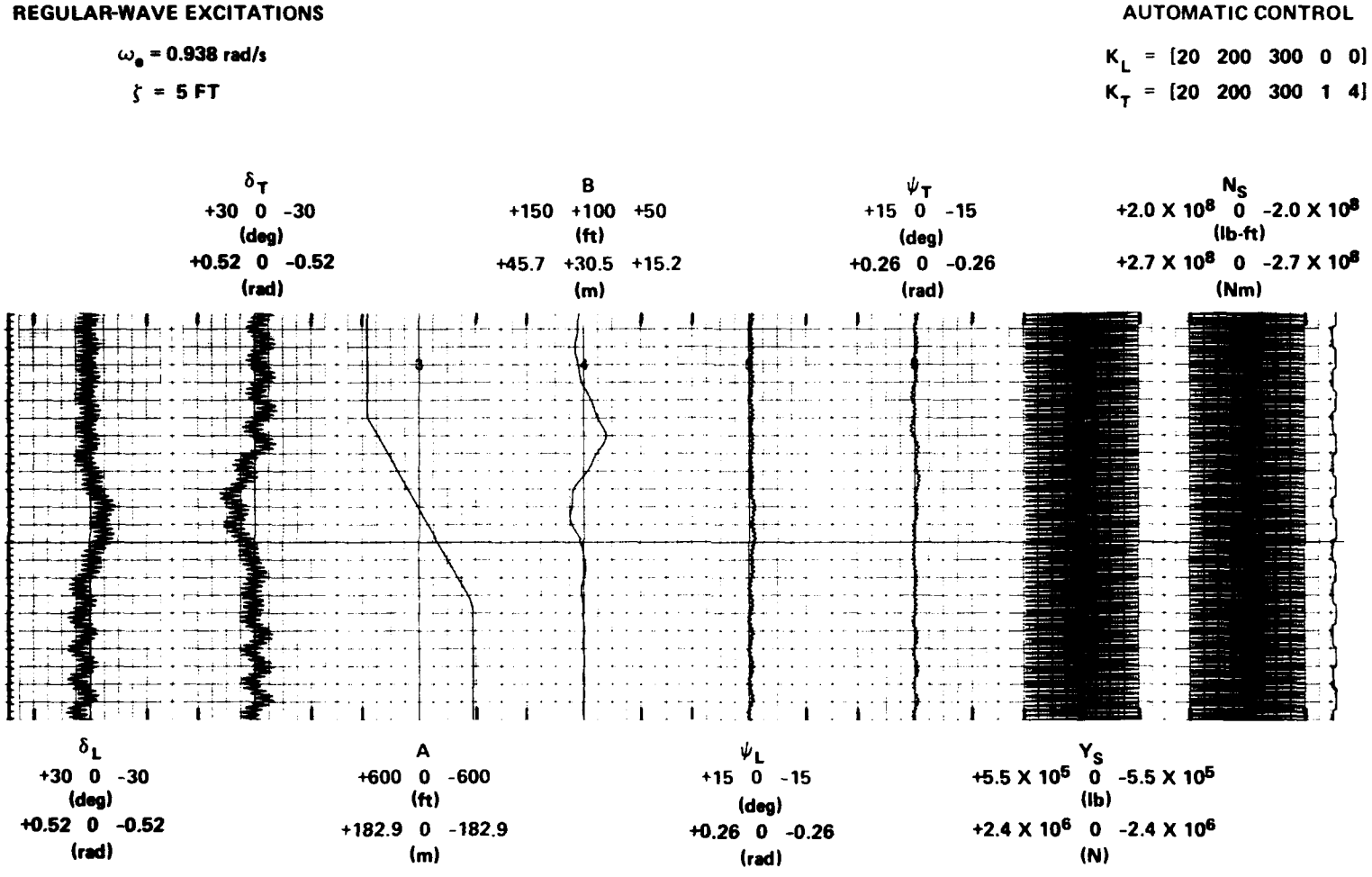

Figure 18 - Underway Replenishment Control Passing Maneuver in Medium Frequency Regular Waves (Automatic Control)

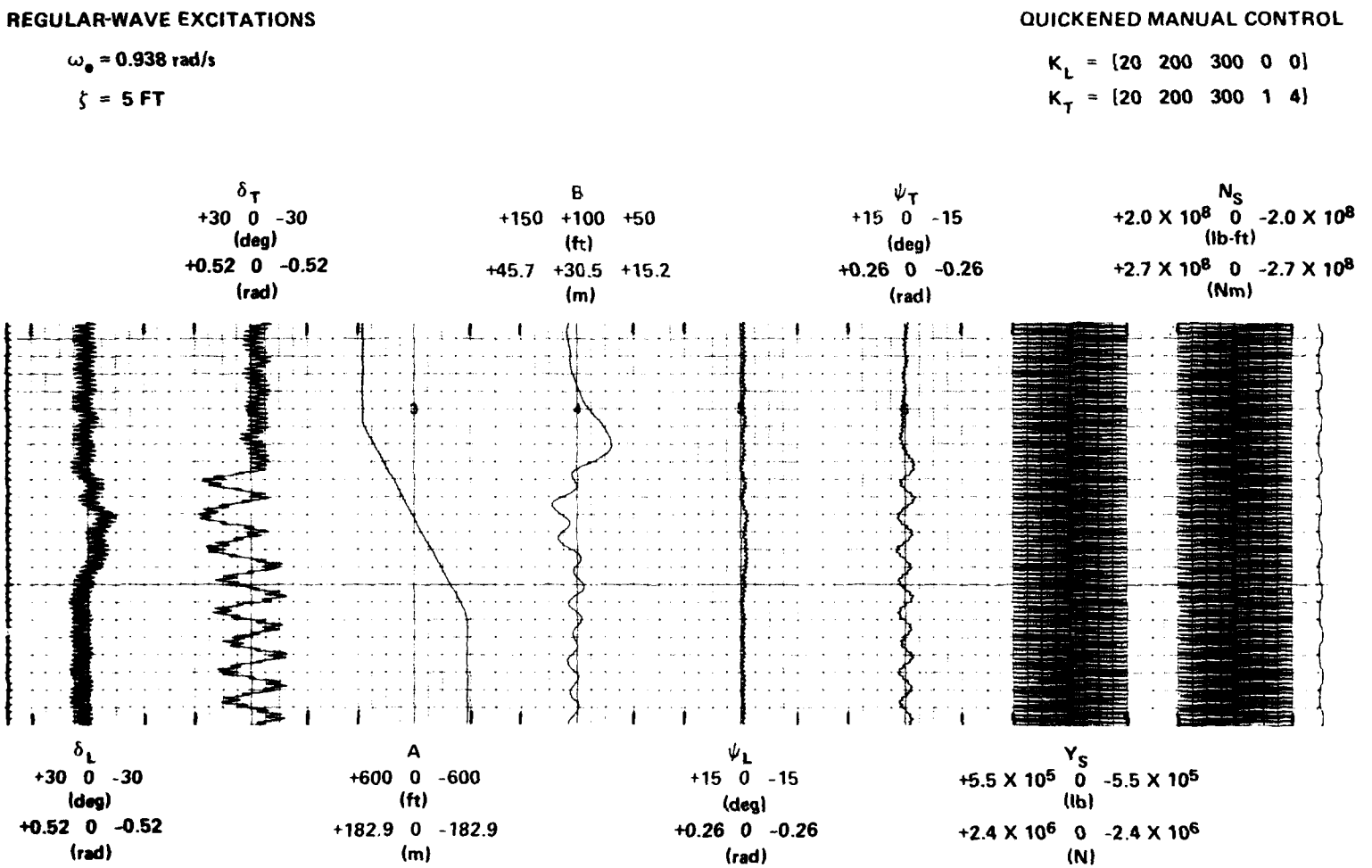

Figure 19 - Underway Replenishment Control Passing Maneuver in Medium Frequency Regular Waves (Quickened Manual Control)

88 to 120 ft. With quickened manual control of the tracking ship under the same conditions (Figure 19), lateral separation varies continuously with lower frequency than the excitation frequency. Heading and rudder angles vary at approximately the same frequency as the lateral separation frequency. Rudder angle, heading, and lateral separation excursions are of much greater amplitude than with automatic control. Lateral separation ranges from 75 to 130 ft, or almost twice the variation under automatic control.

UNREP control simulation results with regular waves at a high frequency of encounter are illustrated by Figure 20. It can be seen that although the wave amplitudes are high (10 ft), lateral separation is maintained smoothly between 92 and 108 ft. Rudder excursions on both ships are small and of approximately the same frequency as the wave excitations.

FIRST-ORDER IRREGULAR-WAVE EXCITATION RESULTS

The effects of severe, first-order, irregular-wave excitations are illustrated by Figures 21 and 22. The irregular waves had a significant wave height of 16 ft, and were characterized by the Pierson-Moskowitz spectrum. Lateral separation control was maintained easily by both the automatic and quickened manual control systems; although large, rapid rudder excursions were required in both cases. The automatic controller maintained lateral separation between 90 and 110 ft, while the quickened manual controller allowed it to vary between 80 and 120 ft. Another difference was that lateral separation and tracking ship rudder and heading excursions were larger with quickened manual control than with automatic control.

SECOND-ORDER IRREGULAR-WAVE EXCITATION RESULTS

The effects of second-order irregular-wave excitations were analyzed separately from the effects of first-order irregular-wave excitation to estimate the contributions of each to the UNREP control problem. Automatic control simulation results with 4-ft and 8-ft significant height waves are shown in Figures 23 and 24, respectively. Simulation results

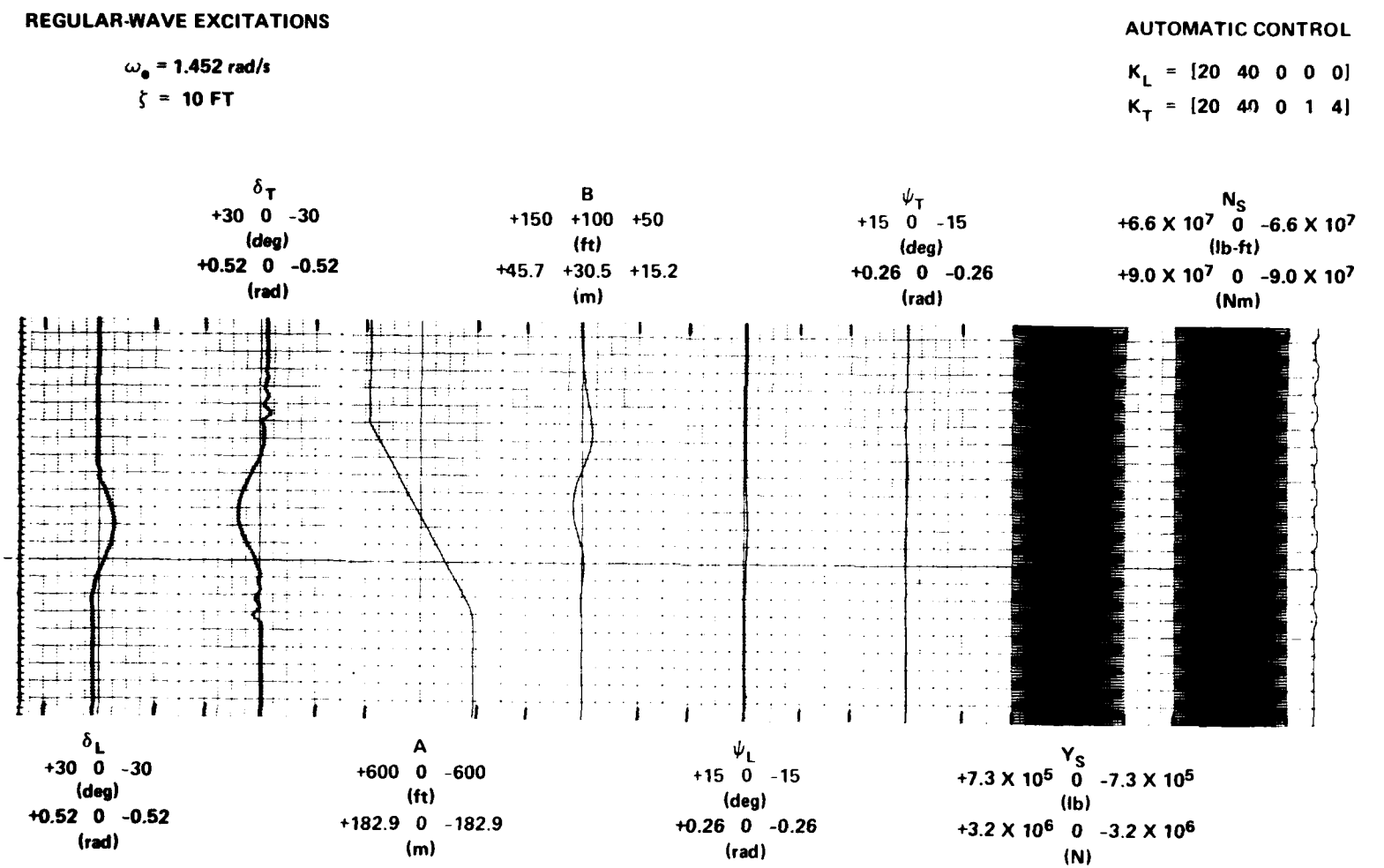

Figure 20 - Underway Replenishment Control Passing Maneuver in High Frequency Regular Waves (Automatic Control)

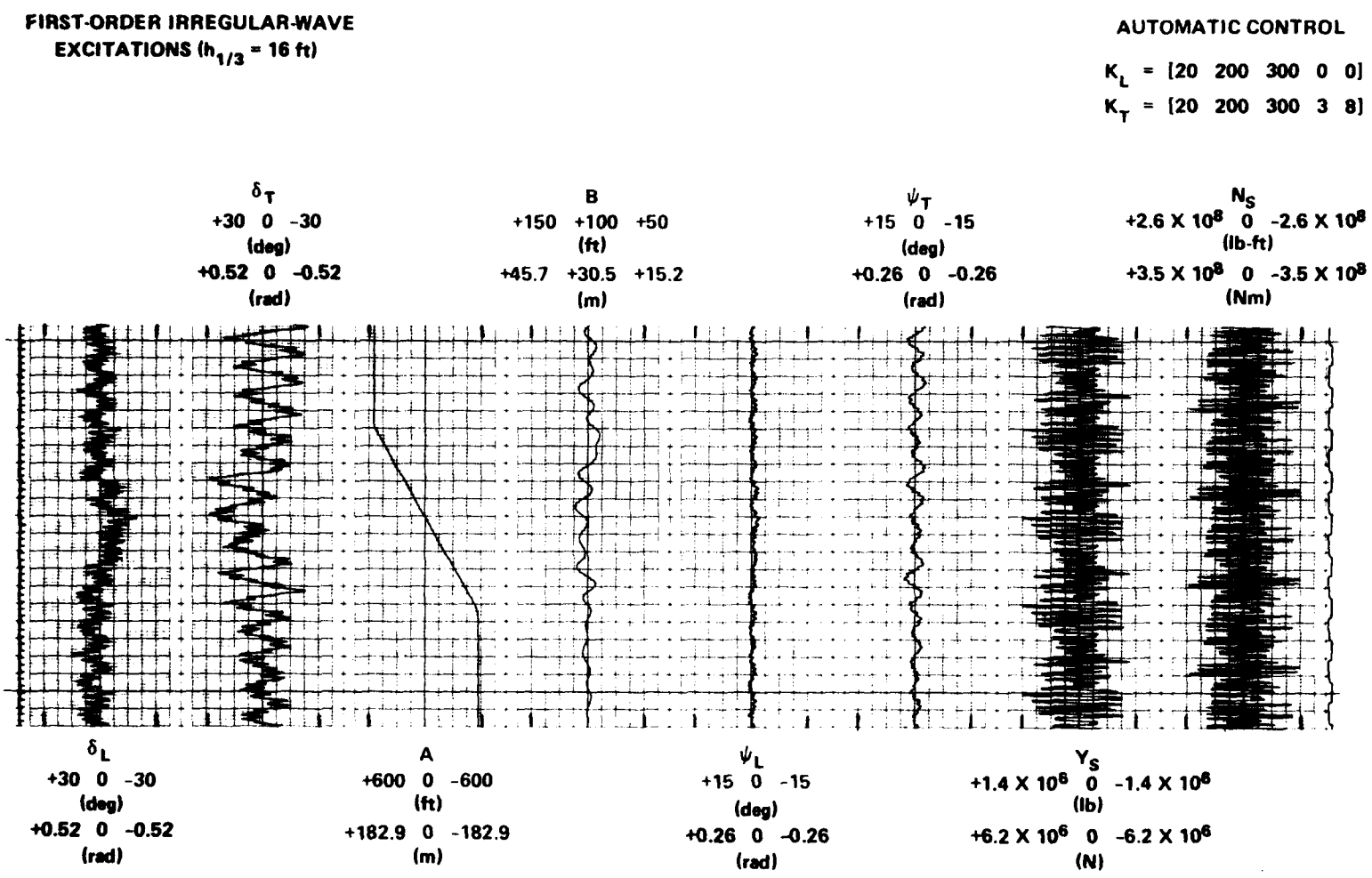

Figure 21 - Underway Replenishment Control Passing Maneuver in First-Order Irregular Waves (Automatic Control)

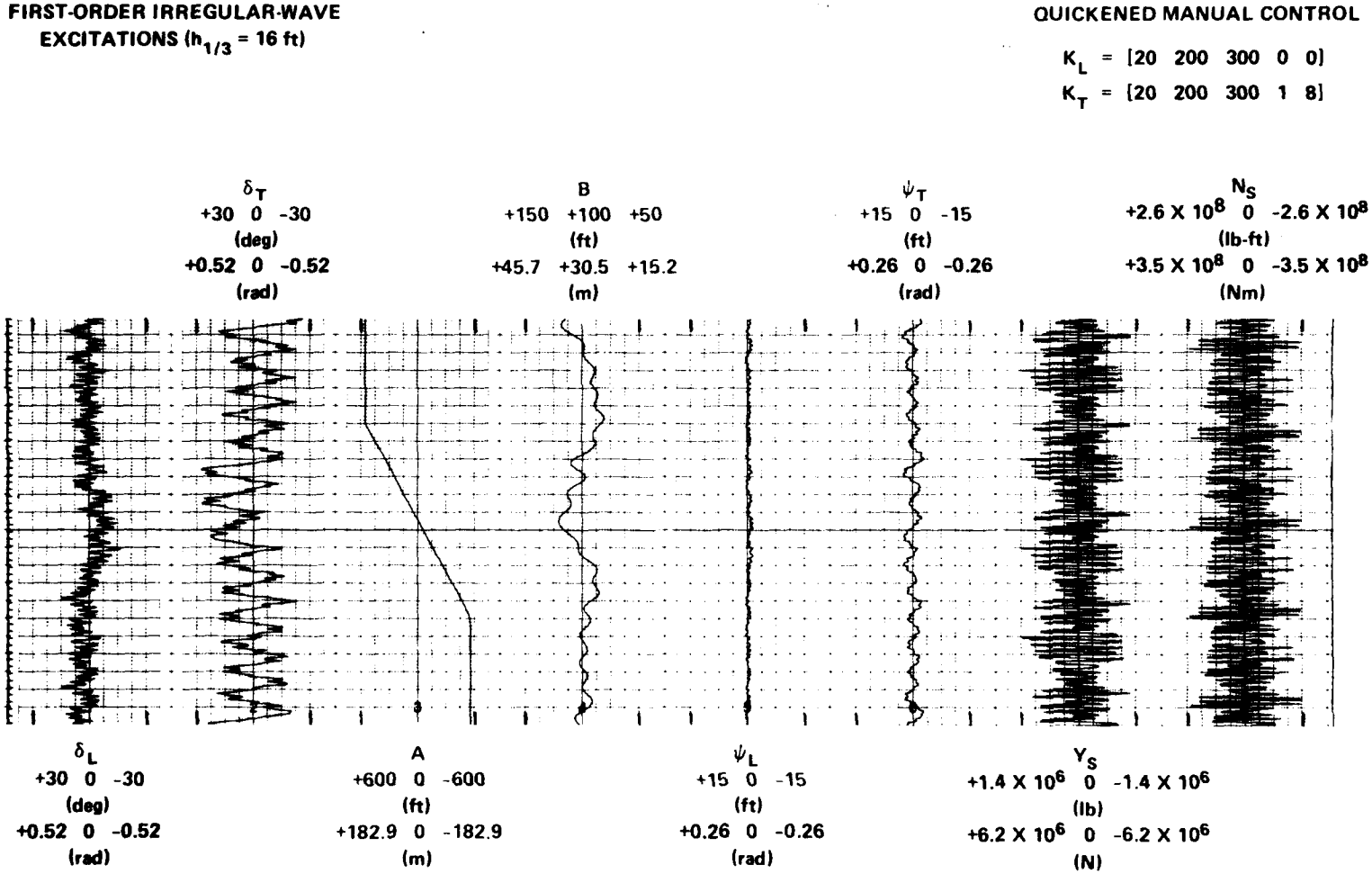

Figure 22 - Underway Replenishment Control Passing Maneuver in First-Order Irregular Waves (Quickened Manual Control)

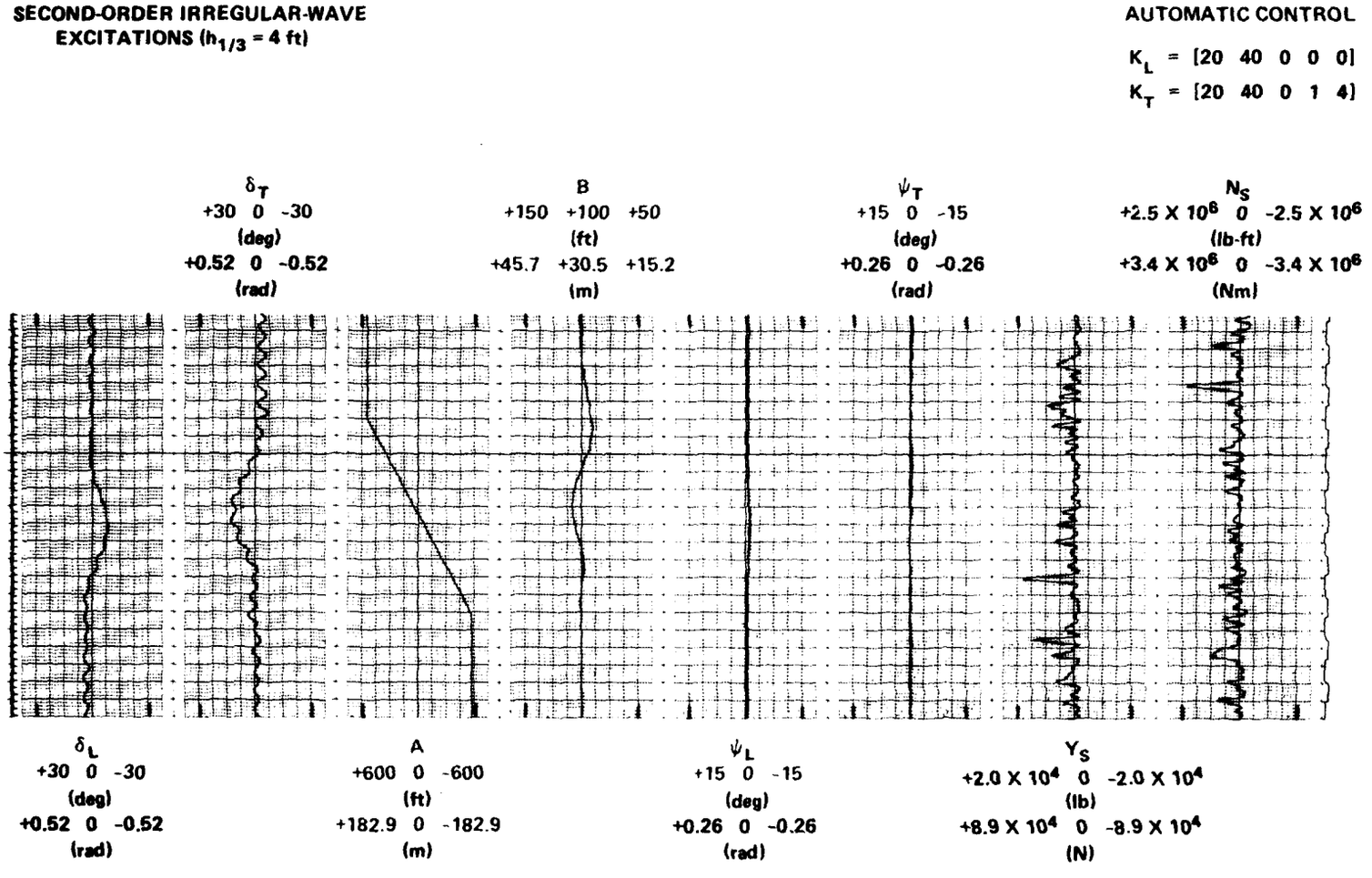

Figure 23 - Underway Replenishment Control Passing Maneuver in Low Second-Order Irregular Waves (Automatic Control)

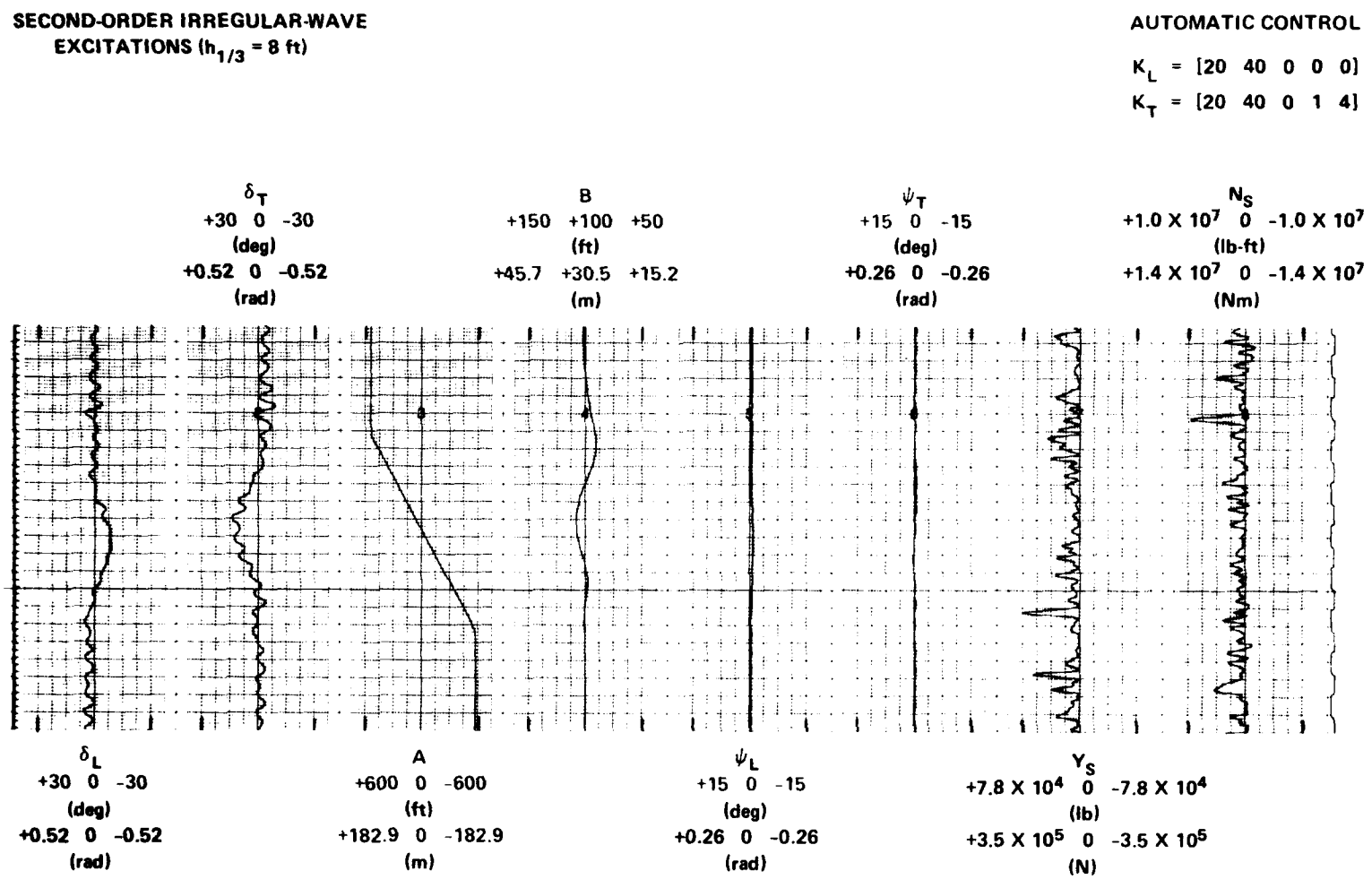

Figure 24 - Underway Replenishment Control Passing Maneuver in Medium Second-Order Irregular Waves (Automatic Control)

for 16-ft significant height waves with quickened manual control and automatic control are shown in Figures 25 and 26, respectively. The lateral separation traces for all four cases are virtually identical, with lateral separation varying smoothly from 90 to 109 ft.

The results obtained with 4-ft waves (Figure 23) are essentially identical to results obtained with no waves (Figure 14). Rudder excursions increase slightly in amplitude with increasing wave amplitude, but are of much lower frequency and rate them with first-order excitations only. Heading control with quickened manual steering is slightly smoother than with automatic control, but the control system coefficients are also different.

FIRST- AND SECOND-ORDER IRREGULAR-WAVE EXCITATION RESULTS

Figures 27 and 28 show the comparative effectiveness of automatic and quickened manual control with both first- and second-order wave excitations under simulated severe sea conditions with 16-ft significant wave heights. When compared with Figures 21 and 22 and with Figures 25 and 26, they also provide a basis for estimating the relative importance of first-order and second-order excitations, respectively, to the overall control problem of UNREP.

Figures 27 and 28 show the relative effectiveness of automatic and quickened manual controls under identical conditions of severe, irregular, first- and second-order sea excitations with identical control system coefficients. It may be observed by inspection that lateral separation; heading; and rudder excursion amplitudes, frequencies, and rates are essentially identical with automatic and quickened manual control. With automatic control, lateral separation varies between 86 and 118 ft. With quickened manual control, it varies between 85 and 118 ft.

UNREP simulation results with both first- and second-order, irregular wave excitations (as shown in Figures 27 and 28) are very similar to results with first-order excitations only (as shown in Figures 22 and 23); but are not similar to results with second-order excitations only (as shown in Figures 23 through 26). The higher amplitudes, frequencies, and rates of lateral separation, heading, and rudder excursions found in

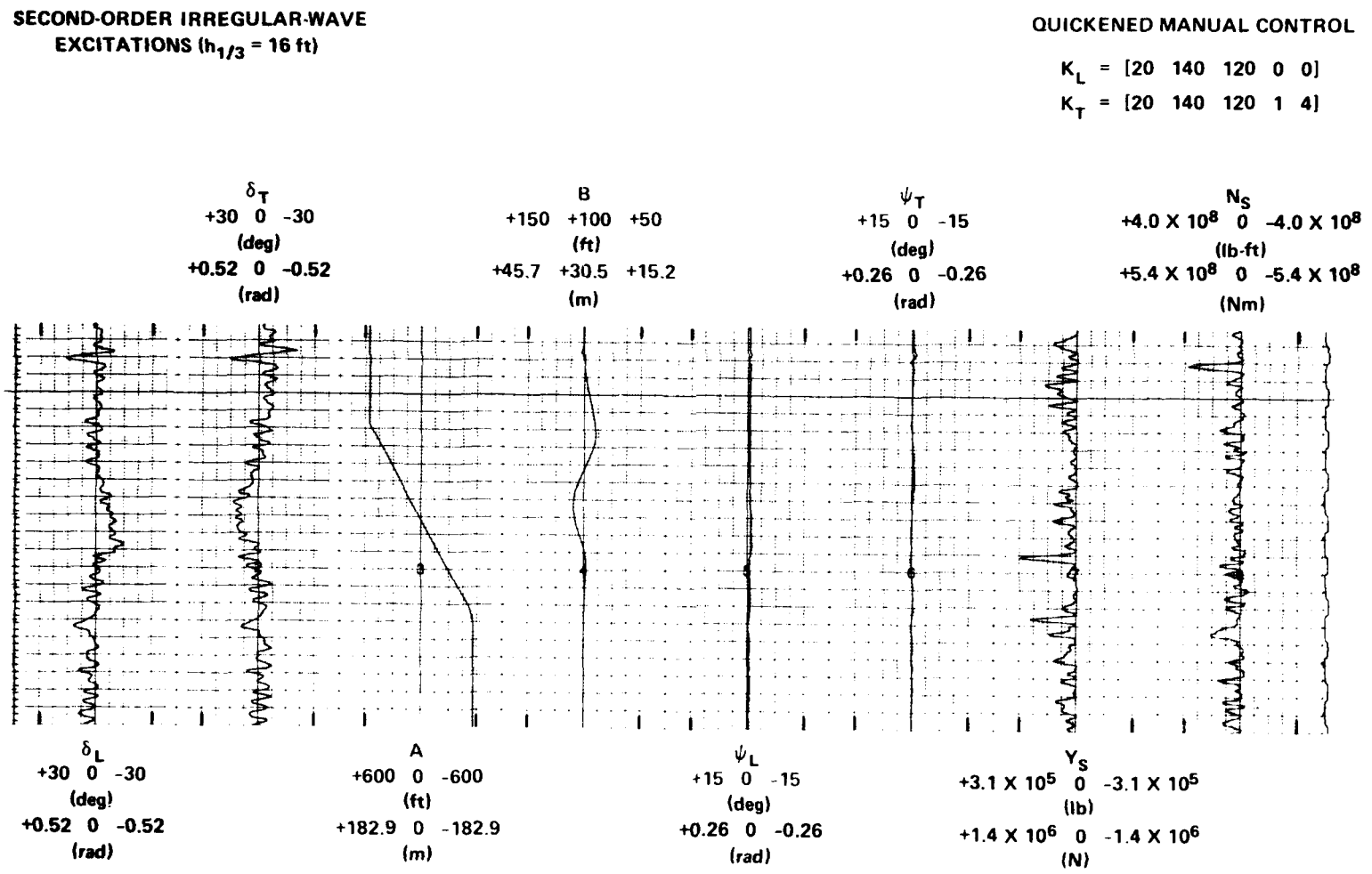

Figure 25 - Underway Replenishment Control Passing Maneuver in High Second-Order Irregular Waves (Quickened Manual Control)

SECOND-ORDER IRREGULAR-WAVE EXCITATIONS ($h_{1/3}$ = 16 ft)

AUTOMATIC CONTROL

K_L = [20 40 0 0 0]

K_T = [20 40 0 1 4]

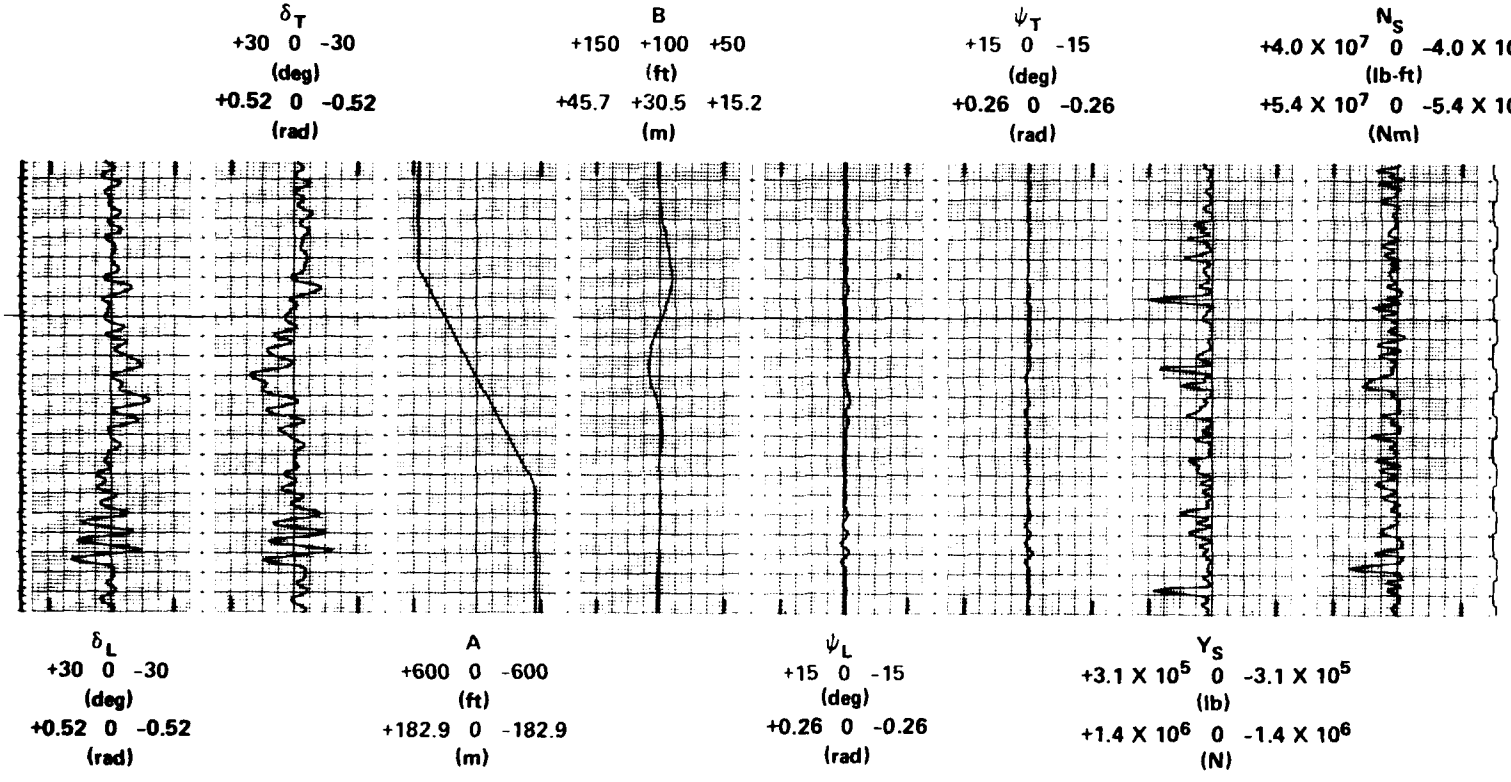

Figure 26 - Underway Replenishment Control Passing Maneuver in High Second-Order Irregular Waves (Automatic Control)

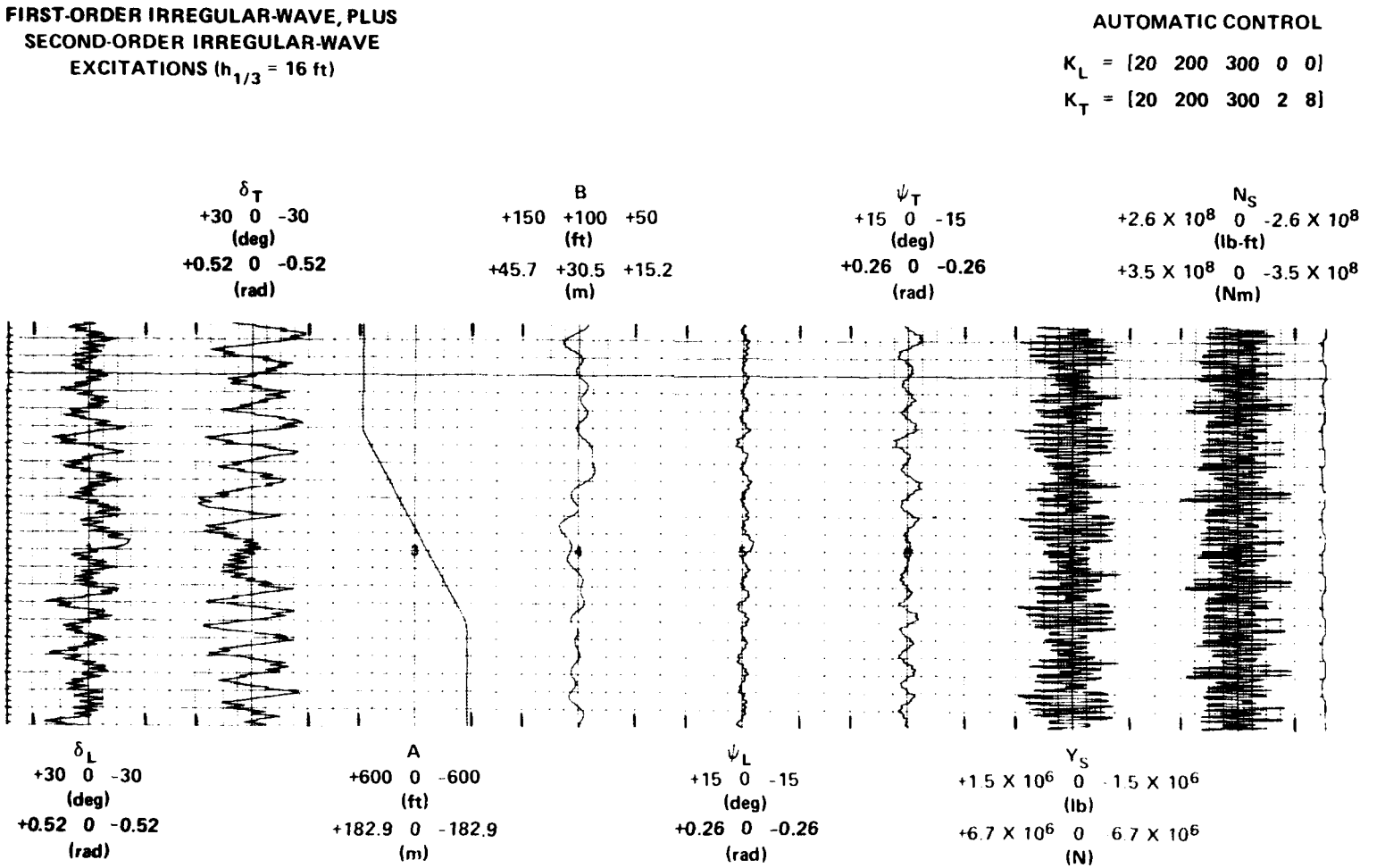

Figure 27 - Underway Replenishment Control Passing Maneuver in Irregular Waves (Automatic Control)

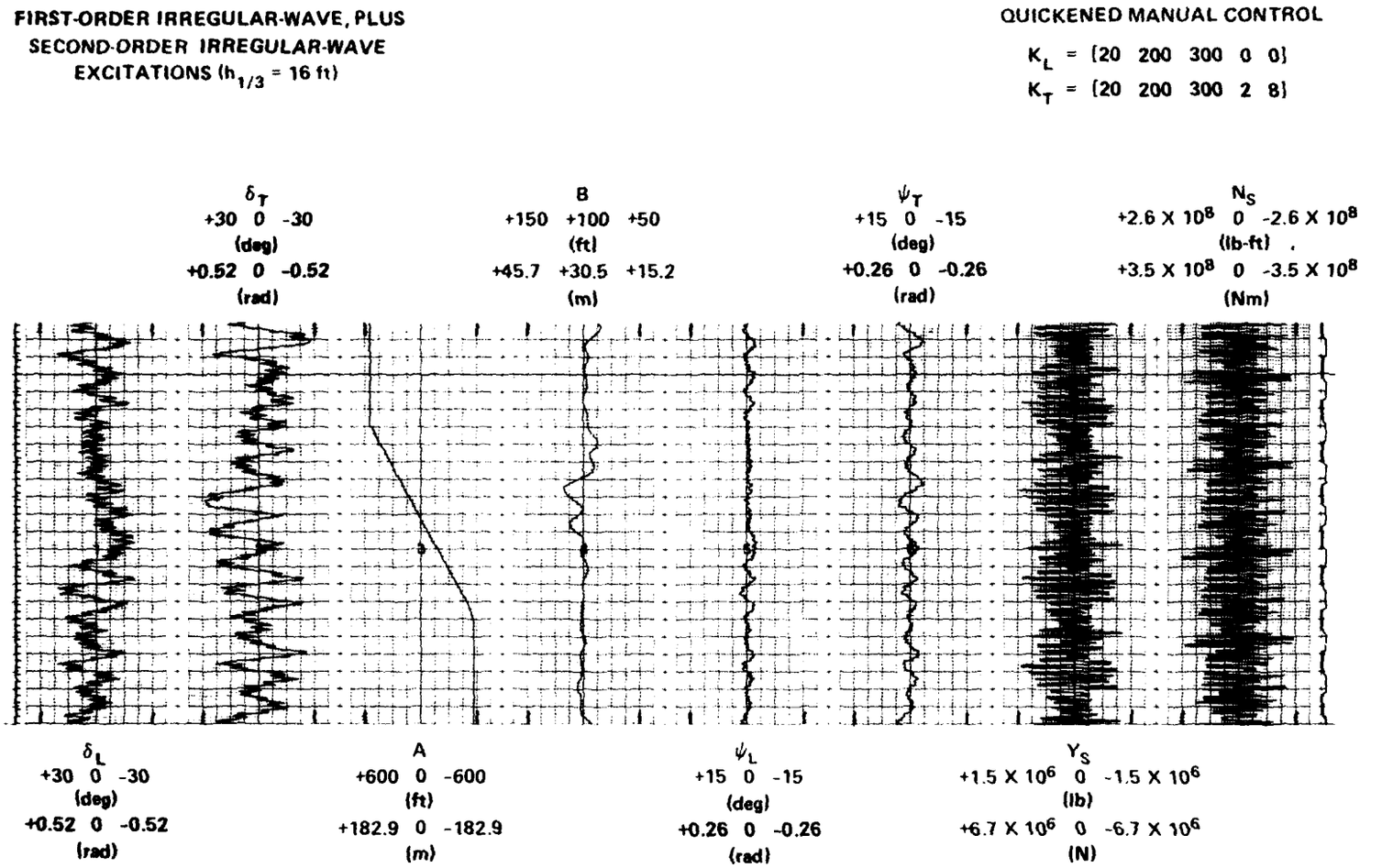

Figure 28 - Underway Replenishment Control Passing Maneuver in Irregular Waves
(Quickened Manual Control)

Figures 21 through 22 and 27 through 33 are not present when the excitation is entirely second-order (as shown in Figures 23 through 26).

TIME-SAMPLED SEPARATION MEASUREMENTS

The effects of sampling lateral separation at discrete time intervals of 1.0, 1.5, and 2.0 seconds are illustrated by Figures 29, 30, and 31, respectively. All three UNREP simulations were conducted under identical conditions of severe, first- and second-order sea state excitations with identical automatic control system coefficients. With 1.0 and 1.5 second sampling intervals, lateral separation varies between 80 and 115 ft and between 78 and 118 ft, respectively. Heading and rudder control parameters are similar to those observed under similar simulation conditions with essentially continuous measurement of lateral separation (as shown in Figures 28 and 29). With 2.0 second sampling intervals, however, lateral separation varies rapidly between 65 and 133 ft, implying the onset of control loss.

LOW-PASS FILTER ON RUDDER INPUT

All simulation conditions for Figures 32 and 33 were identical, except that a low-pass filter with a cutoff of 0.1 rad/s was added to the input of the rudder control system of the tracking ship to attempt to eliminate some of the high-frequency oscillations resulting from response to the zero-mean, first-order sea state excitations. With the low-pass filter, leading-ship rudder excursion amplitudes and rates are greatly reduced, but lateral separation varies between 65 and 128 ft, with the largest excursions beginning at longitudinal separations corresponding to the reversal points of the hydrodynamic interaction forces and moments. Without the low-pass filter, lateral separation excursions are greatly reduced, varying between 85 and 115 ft.

CONCLUSIONS

Simulations were conducted to analyze factors not considered in earlier work and to attempt to confirm some provisional assumptions and results. In general, previous results were found to be valid, but the

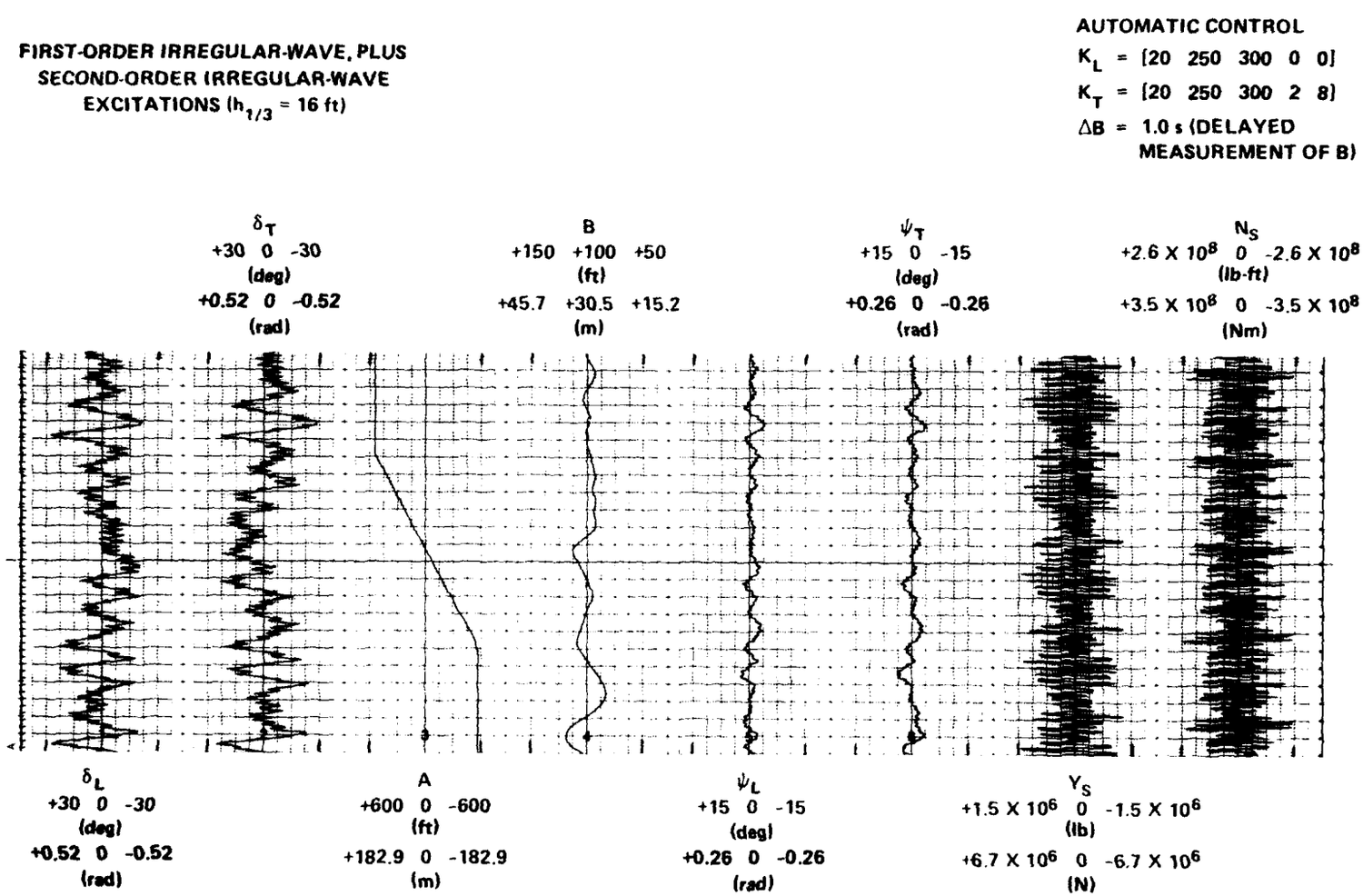

Figure 29 - Underway Replenishment Control Passing Maneuver (1.0-Second Delayed Measurement of B)

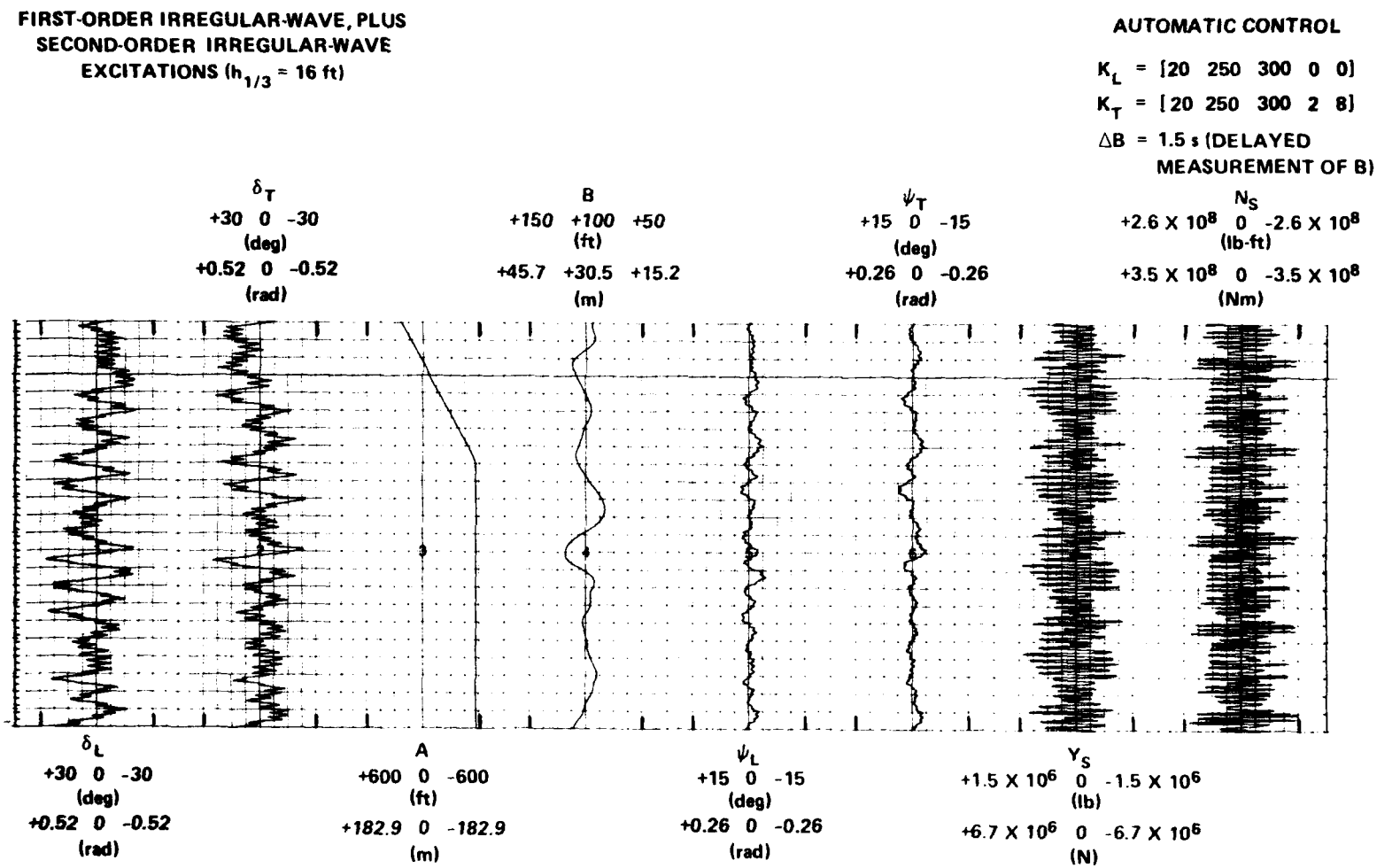

Figure 30 - Underway Replenishment Control Passing Maneuver (1.5-Second Delayed Measurement of B)

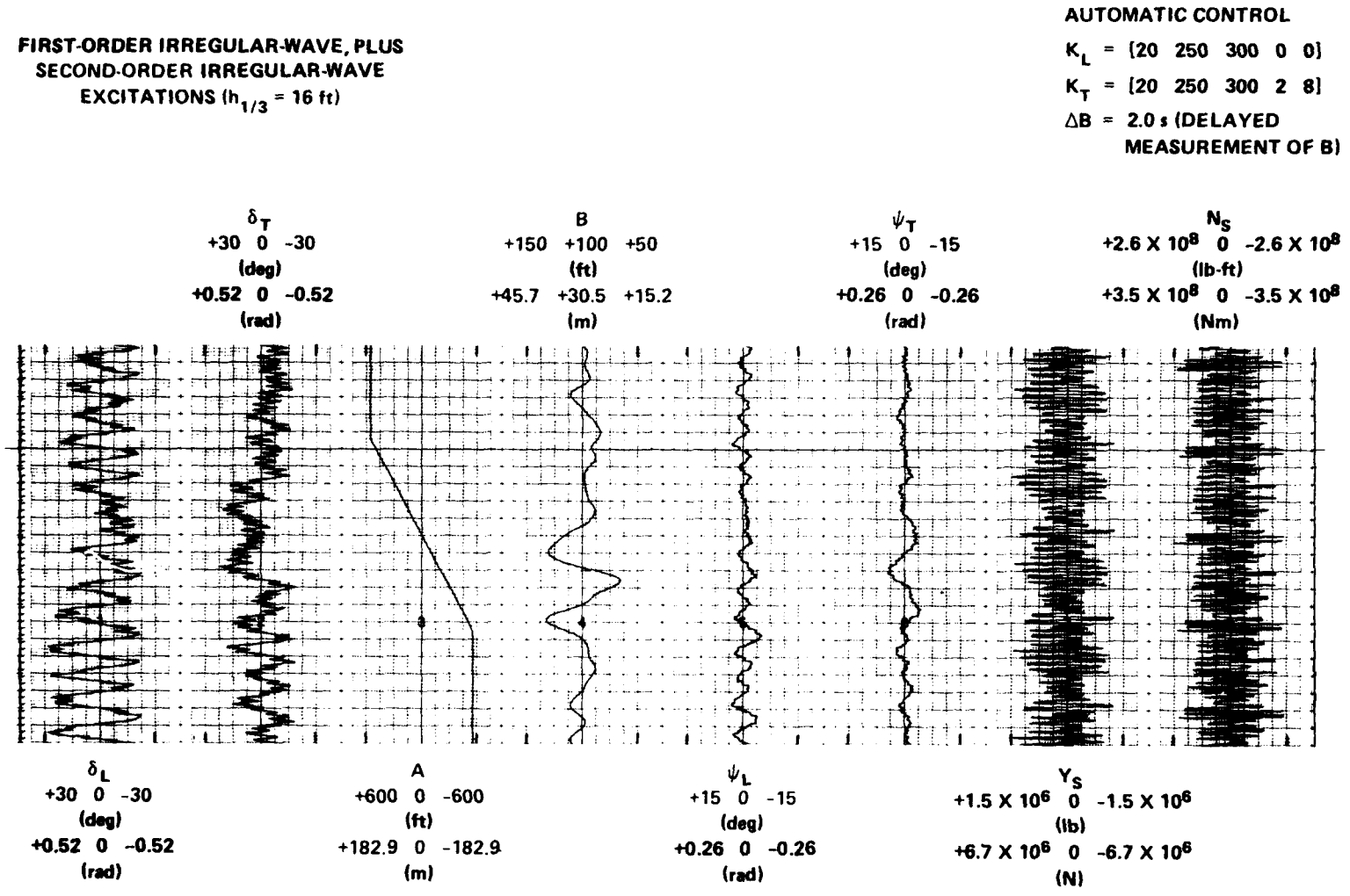

Figure 31 - Underway Replenishment Control Passing Maneuver (2.0-Second Delayed Measurement of B)

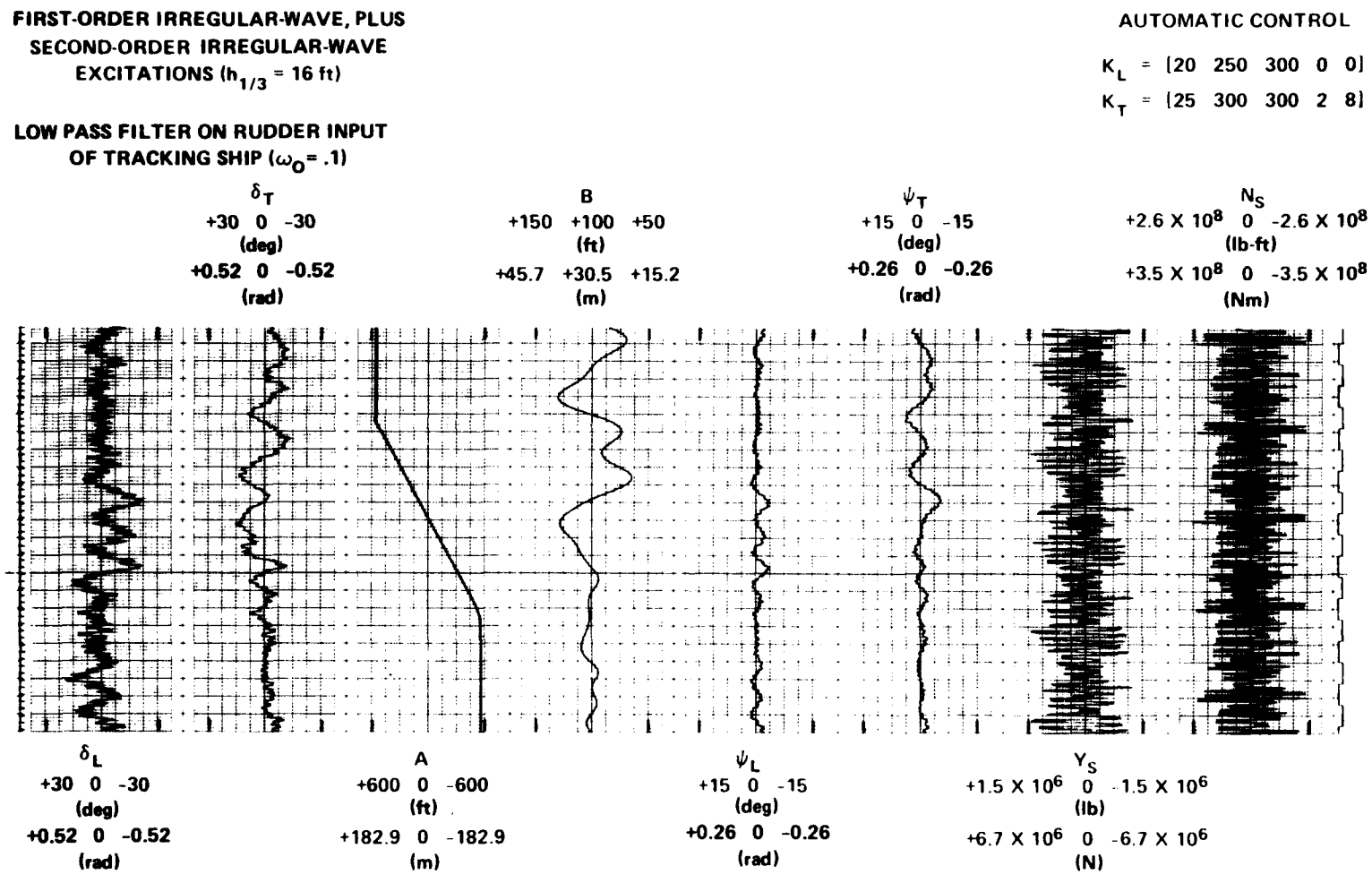

Figure 32 - Underway Replenishment Control Passing Maneuver (Low-Pass Filter on Tracking Ship Rudder Input)

FIRST-ORDER IRREGULAR-WAVE, PLUS
SECOND-ORDER IRREGULAR-WAVE
EXCITATIONS ($h_{1/3}$ = 16 ft)

NO LOW-PASS FILTER

AUTOMATIC CONTROL

K_L = [20 250 300 0 0]

K_T = [25 300 300 2 8]

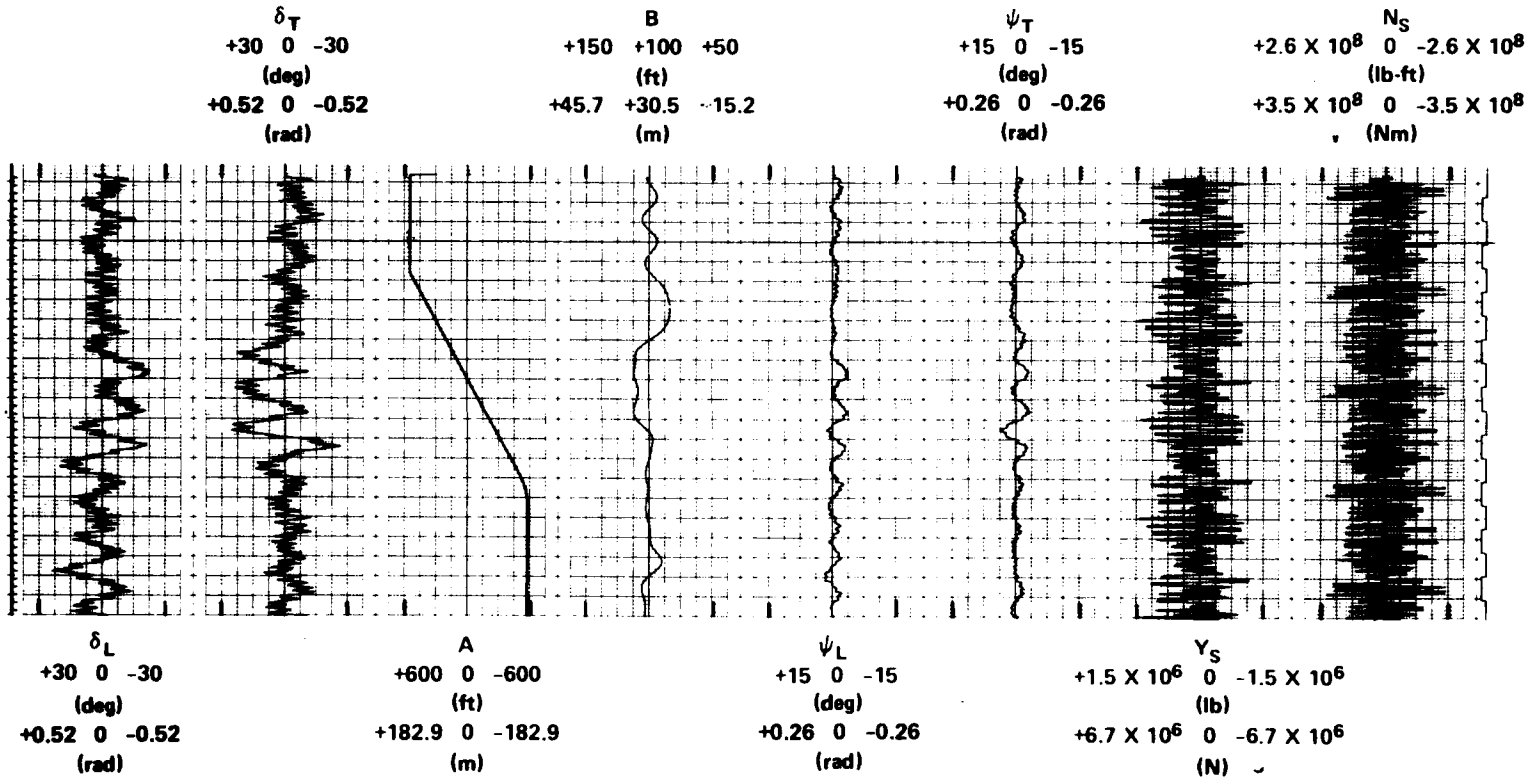

Figure 33 - Underway Replenishment Control Passing Maneuver (No Low-Pass Filter)

current work contradicts some earlier assumptions and points out the need for additional work in the areas of displays, human factors engineering, and automatic controls.

It has been assumed throughout the previous work[6-11] that the drifting type of second-order, irregular sea state excitations were more important than the higher-frequency, first-order, irregular sea state excitations. The current work, which includes detailed studies on the first-order, irregular sea state excitations for the first time, indicates that the opposite is true--first-order sea state excitations dominate the UNREP steering control problem. This new finding is based on analysis of results of simulations conducted with first- and second-order irregular effects considered separately and in combination. Those results with both effects in combination are very similar to results with first-order effects only, but are not similar to results with second-order effects only. Simulations with first-order, irregular excitations, singly or in combination, result in significantly higher amplitudes; frequencies; and rates of lateral separation, headings, and rudder excursions than simulations with second-order, irregular excitations only.

In simulations with second-order, irregular excitations only, the hydrodynamic interaction forces and moments dominate control of lateral separation, even in severe sea states of 16-ft significant wave heights. Lateral separation excursions with severe second-order excursions are equivalent to lateral separation excursions with no sea state excitation. Second-order effects of severe, irregular seas slightly increase rudder activity and heading excursions with respect to the calm sea (no excitation) condition, but have no significant effect on lateral separation control.

Assuming that a reasonable criterion for satisfactory lateral separation control is to maintain separation within 20 ft of the set point ($80 \leq B \leq 120$ ft), unsatisfactory lateral separation control occurred under several conditions. With regular wave excitations, lateral separation control was unsatisfactory with: (a) automatic control, 10-ft waves, and the encounter frequency which maximizes sway force (Figure 17); and (b) quickened manual control, 5-ft waves, and the encounter frequency which maximizes yaw moment. With severe, irregular wave excitations and

automatic control, lateral separation control was unsatisfactory, with lateral separation measurements occurring at intervals in excess of 1.0 second and with a low-pass filter at the input to the rudder control system of the simulated tracking ship.

Previous results, which were based on lower-frequency, second-order irregular excitations only, indicated that lateral separation measurement intervals of as long as 30 seconds could be tolerated; but with first-order excitations included, it is now clear (Figures 29 and 31) that the measurement interval should be no longer than 1.0 second. This finding is consistent with the conclusion that first-order excitations dominate the UNREP steering control problem in realistic sea conditions.

Under some conditions, the quality of control, as described by lateral separation, rudder, and heading excursion amplitudes, frequencies and rates, is as good with quickened manual steering as it is with automatic steering; but this is not always the case. One case of unsatisfactory lateral separation control (Figure 19) was with quickened manual steering. With all conditions identical except for automatic steering (Figure 18), lateral separation excursions were reduced by 23 ft and were within the criterion of $80 \leq B \leq 120$ ft. However, since the simulations were not designed to be statistically valid comparisons of automatic and quickened manual steering, it is reasonable to conclude that quickened manual steering control shows promise of being as satisfactory as automatic control, and that some additional human factors engineering experiments are needed to define its advantages and disadvantages more accurately.

The unsatisfactory lateral separation control (Figure 32) which resulted from putting a low-pass filter on the input to the rudder control system of the simulated tracking ship is entirely consistent with the conclusion that the higher-frequency, first-order irregular excitations dominate the UNREP steering control problem. With the low-pass filter installed on the tracking ship rudder input during an UNREP passing maneuver, the lateral separation was not as well maintained as in the case without the filter (Figures 32 and 33).

It is highly probable that better results could be obtained with a better automatic controller. Improving the automatic controller, possibly

by adding adaptive capabilities, should also improve the quality of quickened manual control.

In summary, the major conclusions of this final report are:

- First-order excitations of irregular seas dominate the UNREP steering control problem.
- Lateral separation measurement intervals should not exceed 1.0 second.
- Quickened manual steering shows promise for UNREP, but requires further study and human factors engineering experiments.
- The quality of UNREP steering control could be improved by redesigning the automatic controller used in this work.

RECOMMENDATIONS

Completion of the current simulation work has provided a good definition of the parameters which must be measured and used to improve lateral separation control during UNREP. The next objective should be to design and evaluate the required sensing systems, specifically for lateral separation and separation rate. If the sensing system chosen makes measurements at discrete time intervals, the intervals should be 1.0 second or less.

If the sensing system development is successful, it should be integrated with an automatic or quickened manual controller to provide the best performance. Both the automatic controller design and the quickened manual controller design described in this report are practical, but they must be modified to suit the maneuvering characteristics of any Navy ship in which they may be installed. Adaptive automatic controller gains would significantly enhance performance.

Additional human factors engineering experiments should be conducted to define the capabilities of quickened manual control and to identify specific areas needing improvement.

The methodology available as a result of the current work is valuable for simulation and analysis of interaction effects among different ship types. All future work using this or similar methodologies should include first-order irregular sea state excitations. Before additional ships or

combinations of ships can be simulated, hydrodynamic data must be made available.

Finally, it must be strongly cautioned that, although results for different ships are expected to be qualitatively similar, the quantitative results must not be applied to different ships or to the same ships at different speeds or other conditions.[36] In particular, safe speeds, separation distances, and sea conditions for the ships simulated in the current work should not be assumed to apply equally to other ships. Since the simulations were applicable only for UNREP operations in open seas, the results are not valid for shallow water nor for ships moving in close proximity to vertical obstructions such as channel banks.[36] The effects of ship size, speed, maneuverability, reserve power, and rudder turning moments, as well as sea state effects, water depth, channel width, and UNREP rig forces and moments are all large[36] and must be considered on a case-by-case basis in determining safe speeds and lateral separations for overtaking, passing, or UNREP.

ACKNOWLEDGMENTS

The authors appreciate the many technical contributions provided by Dr. C. M. Lee, Dr. N. Salvesen, Dr. W. McCreight, Dr. M. Martin, Mr. G. Cox, and Mr. G. Hagen of the Ship Performance Department. The information on the range and bearing transmitter systems for the UNREP quickened display was supplied by Mr. H. K. Whitesel of the Sensors Branch. Mr. G. L. Stump of the Control and Simulation Branch contributed to programming the analog portions of the simulation.

APPENDIX A

UNDERWAY REPLENISHMENT MANEUVERING MATHEMATICAL MODEL IN WAVES

The UNREP simulation[6-11] incorporates approximate irregular sea state excitations (or linear regular sea excitations) on the ships' hulls and the hydrodynamic interaction forces and moments acting on both the leading and tracking ships (Figure 2). The UNREP simulation has the capability of controlling either the leading or tracking ship's rudder and propeller shaft speed "manually" or "automatically," but only automatic control and quickened manual[11] control are considered in this work. The basic Mariner study ship characteristics are presented in Table 1.

BASIC MATHEMATICAL MANEUVERING MODEL

The ship dynamic mathematical model for each of the two Mariner study ships consists of a set of nonlinear equations in the horizontal plane (i.e., surge, sway, and yaw). The hydrodynamic coefficients[24] in each set of maneuvering equations are presented in Table A.1. Most of the coefficients were taken from Smitt and Chislett.[24] The hydrodynamic coefficients X_n, Y_n, and N_n, however, were calculated by Calvano.[20] The nonlinear hydrodynamic interaction forces and moments and the linear and nonlinear effects[9,10] of the oblique seas (30 deg off the port bow, Figure 2) are added to the model as additional forces and moments. The effects of the forces and moments on the ship's hull on ship control during UNREP in both regular and irregular waves were simulated. The nonlinear equations for the leading ship are presented below in Equations A.1 to A.3 (' represents nondimensional value):

SURGE EQUATION

$$(m - X_{\dot{u}'})\dot{u}' = F_1(\underline{u}', v', r', \delta) \tag{A.1}$$

SWAY EQUATION

$$(m' - Y_{\dot{v}'})\dot{v}' + (m'x'_G - Y'_{\dot{r}'})\dot{r} = F_2(\underline{u}', v', r', \delta) \tag{A.2}$$

YAW EQUATION

$$(m'X_G - N'_{\dot{v}'})\dot{v}' + (I'_Z - N'_{\dot{r}'})\dot{r}' = F_3(u', v', r', \delta) \tag{A.3}$$

where

$$F_1(\underline{u}', v', r', \delta) = X'_{u'}\underline{u}' + X_{\eta'}\Delta\eta'$$

$$\begin{aligned} F_2(\underline{u}', v', r', \delta) = {} & Y_\eta\Delta\eta + Y'_\delta\delta + Y'_{\delta\delta\delta}\delta^3 \\ & + Y'_{v'}v' + Y'_{v'|v'|v'|v'|} + Y'_{vrr}v'r'^2 \\ & (Y'_{r'} - m'u')r' + Y'_{rrr}r'^3 + Y'_{rvv}r'v'^2 \\ & Y'(A,B) + Y^{(1)r}_S(\chi') + Y^{(2)r}_S(\chi') \end{aligned}$$

$$\begin{aligned} F_3(\underline{u}', v', r', \delta) = {} & N'_\eta\Delta\eta' + N'_\delta\delta \\ & N'_{\delta\delta\delta}\delta^3 + N'_{v'}v' + N'_{v|v|v'|v'|} \\ & N'_{vrr}v'r'^2 + (N'_{r'} - m'x_G u')r' \\ & + N'_{rvv}r'\,v'^2 + N(A,B) + N^{(1)r}_S(\chi') \\ & + N^{(2)r}_S(\chi') \end{aligned}$$

where: $Y'(A,B)$ = nondimensional, hydrodynamic interaction force caused by tracking ship on the leading ship

$N'(A,B)$ = nondimensional, hydrodynamic interaction moment caused by tracking ship on the leading ship

$Y_s^{(1)'}(\chi)$ = nondimensional, first-order sway force due to sea state acting on ship's hull (χ = 150 deg)

$N_s^{(1)'}(\chi)$ = nondimensional, first-order yaw moment due to sea state acting on ship's hull (χ = 150 deg)

$Y_s^{(2)'}(\chi)$ = nondimensional, low-frequency, second-order sway force due to sea state acting on ship's hull (χ = 150 deg)

$N_s^{(2)'}(\chi)$ = nondimensional, low-frequency, second-order yaw moment due to the sea state acting on the ship's hull (χ = 150 deg)

χ = ship-to-wave angle equals 150 deg (2.618 rad), see Figure 3.

The sea state excitations $Y_s^{(1)'}(\chi)$, $N_s^{(1)'}(\chi)$, $Y_s^{(2)'}(\chi)$, and $N_s^{(2)'}(\chi)$ are discussed in detail in Appendix B.

HYDRODYNAMIC INTERACTION CURVES

The terms Y'(A,B) and N'(A,B) are functions of the longitudinal separation A measured between the centers of mass of the two ships[20] and lateral side-to-side distance B measured between the two ships' centers of mass. Since the two study ships are of the same class (both leading and tracking ship), the maneuvering equations are the same for each ship except that the nondimensional interaction force Y'(A,B) and moment N'(A,B) are changed to -Y'(-A,B) and -N'(-A,B) when applied to the equations of the tracking ship. The values of A and B are constantly calculated and updated in the simulation.

The steady-state ship interaction curves used in the maneuvering equations (A.1 to A.3) are for two Mariner ships traveling at 15 knots on parallel paths. Figures A.1 and A.2 show curves of the hydrodynamic interaction force Y'(A,B) and interaction moment N'(A,B), respectively. The curves for B = 50 ft (15.24 m) and B = 100 ft (30.48 m) were determined from model testing by Calvano.[20] The curves for B = 110 ft (33.53 m)

TABLE A.1 - MANEUVERING COEFFICIENTS USED FOR MATHEMATICAL MODEL[24] (Equations A.1 to A.3)

X—EQUATION NONDIMENSIONAL COEFFICIENT X10^5		Y—EQUATION NONDIMENSIONAL COEFFICIENT X10^5		N—EQUATION NONDIMENSIONAL COEFFICIENT X10^5	
$X_{\dot{u}}$	−36.3	$Y_{\dot{v}}$	−740.0	$N_{\dot{v}}$	−11.0
X_u	−160.8	$Y_{\dot{r}}$	−12.3	$N_{\dot{r}}$	−44.0
X_n	4.62	Y_δ	262.0	N_δ	−135.2
		$Y_{\delta\delta\delta}$	−257.3	$N_{\delta\delta\delta}$	133.7
		Y_v	−1121.0	N_v	−385.4
		$Y_{v\|v\|}$	−2038.6	$N_{v\|v\|}$	539.6
		Y_{vrr}	−2220.0	N_{vrr}	500.0
		Y_r	322.7	N_r	−201.5
Note: No Taylor Expansion Factorials are used except for X_n Y_n N_n		Y_{rrr}	552.8	N_{rrr}	−2700.0
		Y_{rvv}	2833.0	N_n	0.26
		Y_n	−0.52		
m′		$x_G \cong o$		$I'_z = 35.2$	
		$y_G \cong o$			

MASS NON-DIM WITH $\frac{1}{2}\varrho L_{pp}^3$

INERTIA NON-DIM WITH $\frac{1}{2}\varrho L_{pp}^5$

X AND Y FORCES NON-DIM WITH $\frac{1}{2}\varrho L_{pp}^2 U^2$

N MOMENTS NON-DIM WITH $\frac{1}{2}\varrho L_{pp}^3 U^2$

$u' = (u - u_0)$/WHERE u_0 IS INITIAL SPEED

u, u-, and V NON-DIMENSIONAL WITH U

r	—	U/L_{pp}
δ	—	rads
$\dot{u}$ and $\dot{v}$	—	U^2/L_{pp}
$\dot{r}$	—	U^2/L_{pp}^2

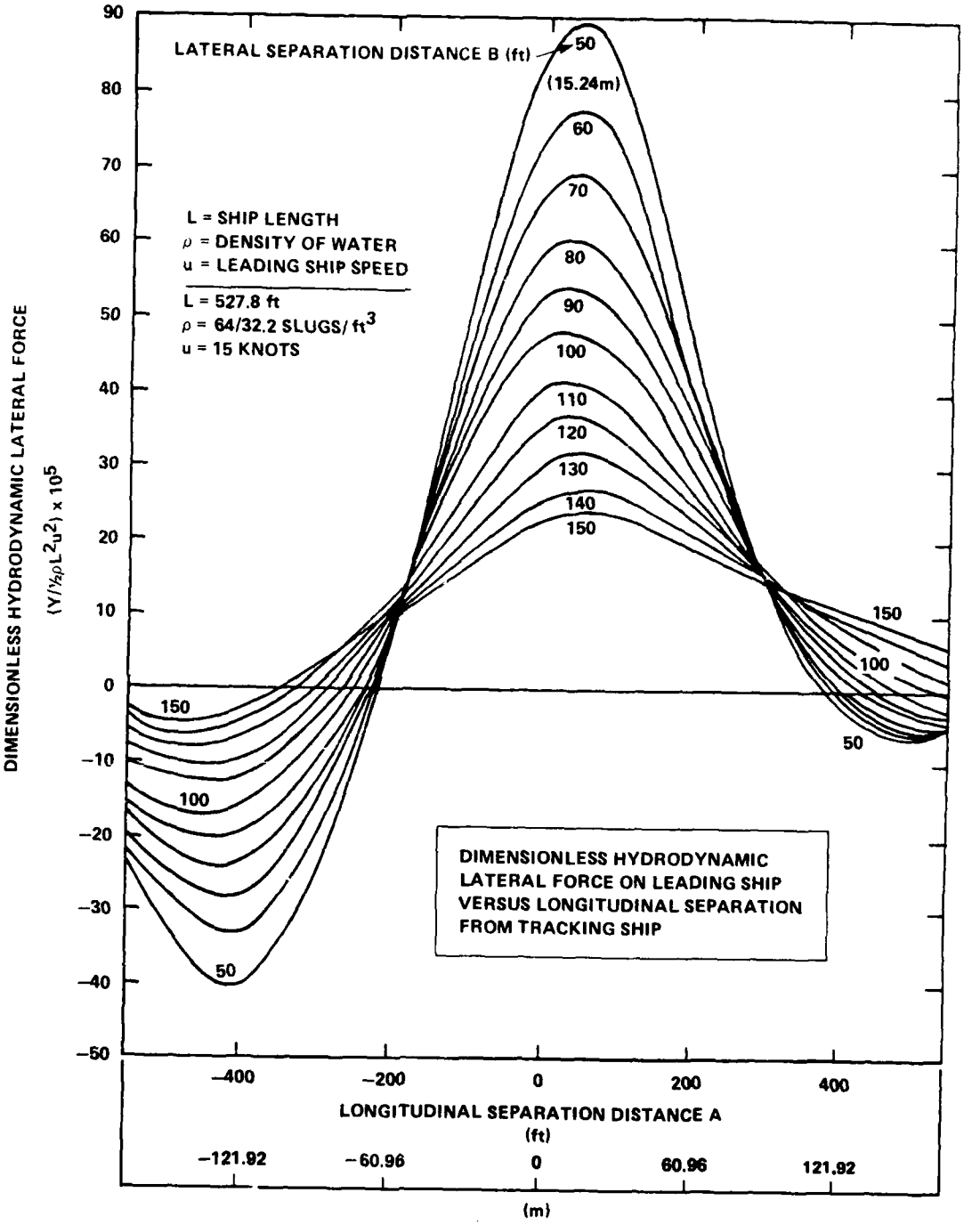

Figure A.1 - Dimensionless Hydrodynamic Interaction Force Y versus Longitudinal Separation[20]

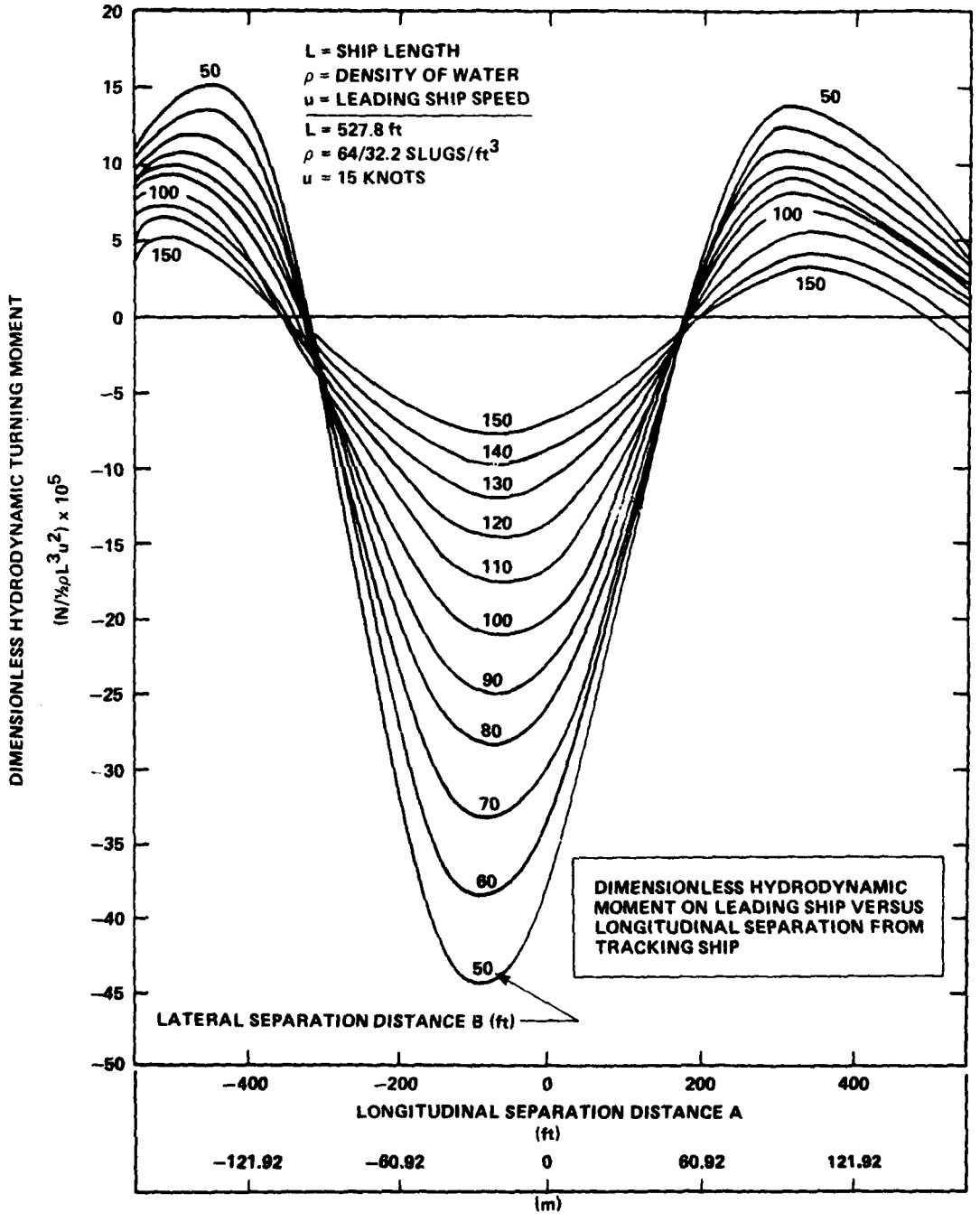

Figure A.2 - Dimensionless Hydrodynamic Interaction Moment N versus Longitudinal Separation[20]

through B = 150 ft (45.72 m) were determined by extrapolation by Alvestad and Brown.[6,7] During the UNREP simulation, the effects of the yawing of either ship on the interaction forces and moments are assumed negligible since the interaction curves are measured for parallel paths of the two ships. Since, in general, transients are relatively small for the UNREP simulations, the steady state and transient interaction forces and moments are assumed to be nearly equal.

SIMULATION OF RUDDER DYNAMICS

The lag time in the rudder dynamics and "dead band" when a rudder angle (helm angle) is commanded is an important aspect of the maneuvering mathematical model.[9,10] The rate of change of the rudder angle was assumed to be directly proportional to the error signal ($\dot{\delta} = -K\delta_e$). The rate constant was set equal to 0.50 (1/s) and the maximum error signal was not allowed to exceed 7 deg (0.122 rad) (Figure A.3). The rudder "dead band" was set at ±0.5 deg. Figure A.4 shows the response of the rudder to step commands.

The rudder analog design (Figure A.3) was designed by C. L. Patterson, Jr., of the Control and Simulation Branch of the Center.

COORDINATE SYSTEM

The coupled equations of planar motion are solved in ship velocity coordinates (u, y) and then transformed to the space coordinates (x_o, y_o) (Figure 2). This mathematical transformation was performed since the information of primary interest in an UNREP simulation is related to the space coordinates (i.e., longitudinal and lateral separation distances and yaw angle). In the work presented here, the space coordinate system is given an initial velocity of 15 knots, equal to the equilibrium velocity. Therefore, changes in the transverse and/or longitudinal position coordinates with respect to the space coordinates system (x_o, y_o) are due to perturbations above or below the ship equilibrium velocity.

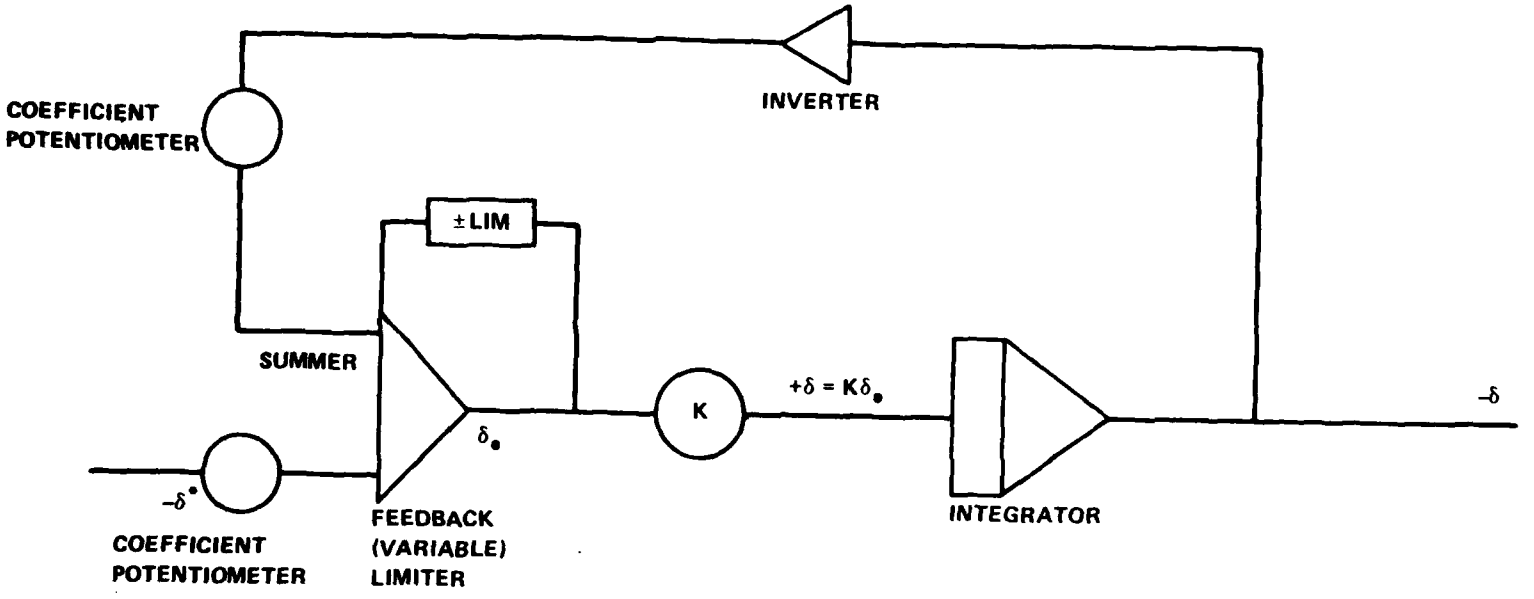

δ^* = RUDDER COMMAND
$\delta_\bullet$ = ERROR SIGNAL (MAXIMUM VALUE = 7°)
δ = ACTUAL RUDDER RESPONSE
K = 0.5/SEC
MAXIMUM RUDDER RATE = 3.5°/SEC

Figure A.3 - Analog Diagram Representing Rudder Dynamics[9]

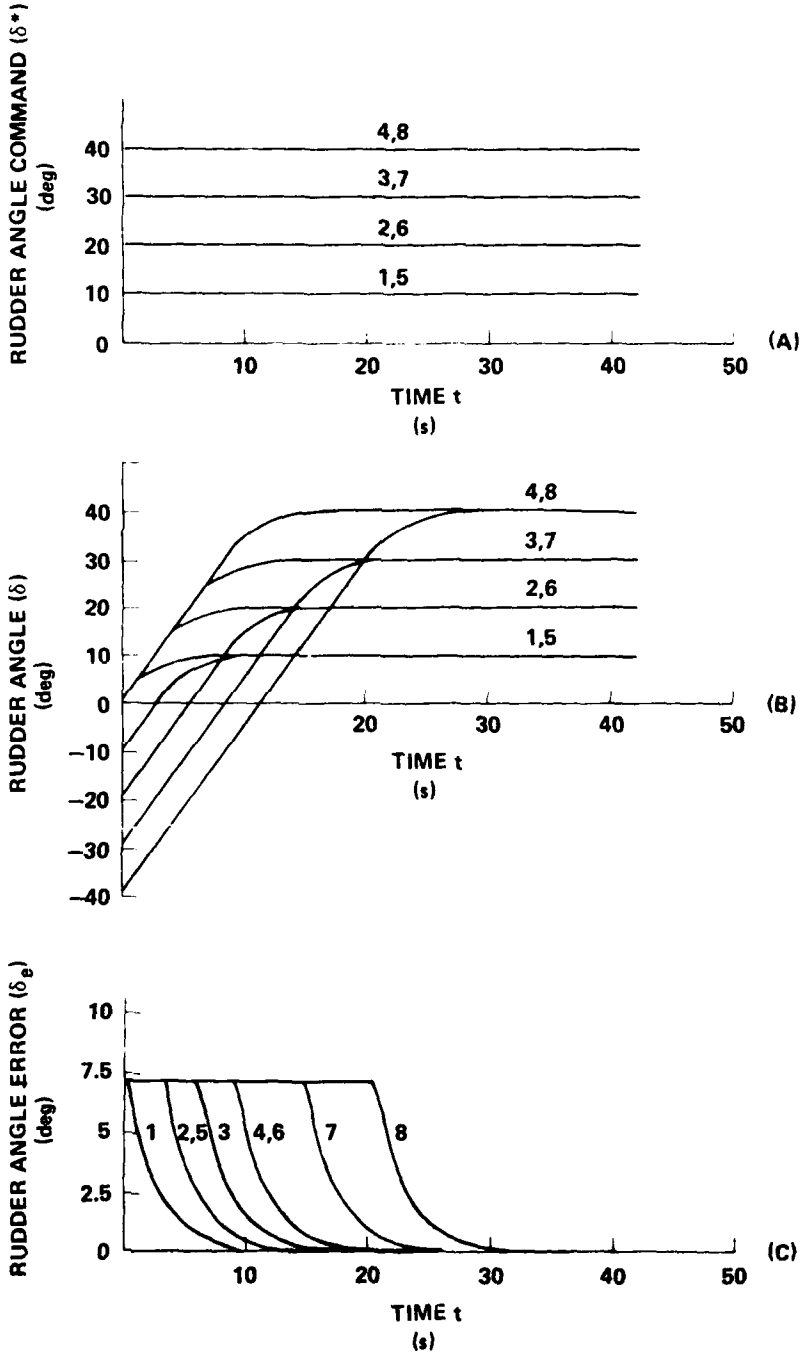

Figure A.4 - Response of Rudder System to Step Commands

The mathematical transformation from ship to space coordinates is represented by

$$\dot{x}_o = u \cos \psi - v \sin \psi$$

$$\dot{y}_o = u \sin \psi + v \cos \psi \qquad \text{(A.4)}$$

ASSUMPTIONS AND LIMITATIONS OF MATHEMATICAL MODEL

The UNREP mathematical model contains the following assumptions[9,10] and limitations:

1. Only oblique irregular and regular seas are simulated. Ship control is assumed to be more difficult for this sea condition than in the head-sea condition which is generally the sea condition for performing UNREP.

2. Under the simulation conditions it is assumed that the ship-to-wave angle χ does not change significantly.

3. $Y_s^{(1)'}(\chi)$, $N_s^{(1)'}(\chi)$, $Y_s^{(2)'}(\chi)$, and $N_s^{(2)'}(\chi)$ are assumed independent of v, $\dot{v}$, $\dot{u}$, $\dot{\psi}$, and $\ddot{\psi}$ during the simulation. It is assumed that these variables are kept small by the automatic controller.

4. The propeller loading and power plant loading are not considered in this work, because these effects manifest themselves in longitudinal control which is not of primary concern in this study. The reliability of X_n, Y_n, and N_n obtained by calculations by Calvano[20] from full-scale trials data in open seas are uncertain under the conditions of the simulation. The reason is that propeller performance in a calm water condition and in a sea state can be somewhat different.

5. It is assumed that the leading and tracking ships are subjected to the same irregular wave system at any specified instant of time.

APPENDIX B

GENERATION OF SWAY FORCE AND YAW MOMENT EXCITATIONS

MATHEMATICAL BACKGROUND

The fundamental mathematical techniques of Volterra series were used to model the sway force and yaw moment acting on the ship's hull in irregular waves. The fundamental ideas for applying Volterra series were originally expressed by Wiener.[23] His work was applied later to ship hydrodynamics by such authors as Vassilopoulos,[26] Tick,[27] and Hasselmann.[28] The Volterra series represents a causal physical system. The theory of the Volterra series to second-order will be used in this work, because the analysis of the sway force and yaw moment will include excitation effects only through second-order. Equations B.1 to B.3 are the fundamental mathematical model[25] and are termed "a truncated functional power series" (or "functional polynomial"). It is assumed that the nonlinear system is time invariant so that the kernel functions depend only on time differences.

$$Y(t) = Y^{(0)}(t) + Y^{(1)}(t) + Y^{(2)}(t_1) \tag{B.1}$$

$$= h_o + \int_{-\infty}^{\infty} h_1(t-t_1)X(t_1)dt_1 \tag{B.2}$$

$$+ \int_{-\infty}^{\infty}\int_{-\infty}^{\infty} h_2(t-t_1,t-t_2)X(t_1)X(t_2)dt_1dt_2$$

$$= h_o + \int_{-\infty}^{\infty} h_1(\tau)X(t-\tau)d\tau \qquad (B.3)$$

$$+ \int_{-\infty}^{\infty}\int_{-\infty}^{\infty} h_2(\tau_1,\tau_2)X(t-\tau_1)X(t-\tau_2)d\tau_1 d\tau_2$$

where $h_n(\tau_1,\ldots\tau_n)$ = symmetric kernel function

$X(t)$ = excitation may be stochastic or deterministic.

This quadratic series can be used to analyze wave forces and moment excitations that are proportional to the wave amplitude and wave amplitude squared. The system must also be assumed to be time invariant. Because it includes both a first-order and second-order term, Tick[27] termed Equation B.1 a time-invariant quadratic system.

In the truncated series (Equation B.2), h_o is set equal to zero. The first-order term $Y^{(1)}(t)$ is the familiar convolution integral for linear, time-invariant systems.[25] This term will be used to represent the first-order sway or first-order yaw moment induced on the ship hull. The first-order irregular sway force (and moment) acting on the ship hull have both high- and low-frequency components and are a zero-mean process.

The second-order term[25] $Y^{(2)}(t)$ is used to study the second-order force (and moment) wave excitations on the ship hull in this work. The second-order excitations each consist of two components: (1) the rapidly varying (high-frequency) component; and (2) the slowly varying (low-frequency) component. The high-frequency excitations are a zero-mean process and are thus neglected. It is the slowly varying (low-frequency) component which is the only component of the second-order term which was considered in this work. The slowly varying component also has a DC offset (non-zero mean).

The Gaussian stochastic integral representation[25] is used to represent the irregular sea:

$$X(t) = \int_0^\infty \cos(\omega t - \varepsilon(\omega)) \sqrt{2S_x(\omega)\,d\omega} \qquad (B.4)$$

$$\cong \lim \sum_n \cos\left[\omega_n t - \varepsilon(\omega_n)\right] \left[2S_x(\omega_n)\delta\omega\right]^{1/2}$$

where the radical $\left[2S_x(\omega)\delta\omega\right]^{1/2}$ represents the amplitude of each harmonic wave where:

ω = radian frequency

$S_x(\omega)$ = one-sided wave energy spectrum for irregular sea state (Pierson-Moskowitz wave energy spectrum)

$\varepsilon(\omega)$ = uniformly distributed phase angle from 0 to 2π.

Substituting X(t), Equation B.4 into the first-order term Equation B.2, results in the expression:[25]

$$Y^{(1)}(t) = \int_0^\infty \cos(\omega t - \varepsilon(\omega) + \phi(\omega)) \sqrt{2\left|H(\omega)\right|^2 S_x(\omega)\,d\omega} \qquad (B.5)$$

where $H(\omega)$ is a complex-valued function called the frequency response factor or transfer function of the linear system and is defined as

$$H(\omega) = \int_{-\infty}^{\infty} h(\tau) e^{i\omega\tau} d\tau \qquad (B.6)$$

The transfer function $H(\omega)$ can be written in terms of the amplitude and phase components as:

$$H(\omega) = |H(\omega)| e^{i\phi(\omega)} \qquad (B.7)$$

In ship hydrodynamics the function $|H(\omega)|^2$ is called the response amplitude operator (RAO). Equation B.5 will be used as the mathematical model to simulate the first-order sway force (and moment) induced on the ship hull by a given irregular sea. The wave will be characterized by the Pierson-Moskowitz spectrum.

Substituting X(t), Equation B.4, into the second-order term Equation B.2 results in the following expression:[25]

$$Y^{(2)}(t) = \text{rapidly varying, second-order term} \qquad (B.8)$$

$$+ \text{ slowly varying, second-order term}$$

$$Y^{(2)}(t) = \int_0^\infty \int_0^\infty \cos\left[(\omega_1+\omega_2)t-(\varepsilon(\omega_1)+\varepsilon(\omega_2))+\phi(\omega_1,\omega_2)\right]$$

$$x\sqrt{|H(\omega_1,\omega_2)|^2 S_x(\omega_1)S_x(\omega_2)d\omega_1 d\omega_2}$$

$$+ \int_0^\infty \int_0^\infty \cos\left[(\omega_1-\omega_2)t-(\varepsilon(\omega_1)-\varepsilon(\omega_2))+\phi(\omega_1-\omega_2)\right]$$

$$x\sqrt{|H(\omega_1)-\omega_2)|^2 S_x(\omega_1)S_x(\omega_2)d\omega_1 d\omega_2}$$

$H(\omega_1,\omega_2)$ is called the second-order transfer function and is defined as[25]

$$H(\omega_1,\omega_2) = \int_{-\infty}^\infty \int_{-\infty}^\infty h(\tau_1,\tau_2)e^{-i\left[\omega_1\tau_1+\omega_2\tau_2\right]}d\tau_1 d\tau_2 \qquad (B.9)$$

The transfer function can be written in terms of the amplitude and phase components[25]

$$H(\omega_1,\omega_2) = |H(\omega_1,\omega_2)|e^{i\phi(\omega_1,\omega_2)} \qquad (B.10)$$

For details of this derivation, see Neal.[25]

The first term in Equation B.8 can be used to mathematically represent the contribution of the wave-frequency pair sums and the second term the contribution of the wave-frequency pair sum differences of the second-order wave forces (and moments) excitation.[25] The second term of Equation B.8 will be used as the basic mathematical model to simulate the second-order slowly varying sway force (and yaw moment) induced on the ship hull by a given irregular sea in this work.

COMPUTER SIMULATION OF SEA STATES

Regular Wave Simulation

The first-order sway force and first-order yaw moment induced on the Mariner study ship in oblique regular waves (χ = 150 deg) were calculated by a computer program using a strip theory developed by Salvesen, Tuck, and Faltinson,[21] by the DTNSRDC Ship Performance Department. The nondimensional first-order sway force and nondimensional first-order yaw moment versus regular wave-encounter frequency are presented in Table 2 and graphed in Figure 4. These data were used in the UNREP maneuvering simulation runs in regular waves that are presented later in the report.

First-Order, Irregular Wave Excitations

The first-order, irregular sway force and first-order, irregular yaw moment induced on the hull of the Mariner study ship in an oblique seaway (χ = 150 deg) with a significant wave height ($h^{1/3}$) of 16 ft were calculated on the computer. The first-order irregular sway force $Y^{(1)}(t)$ and first-order, irregular yaw moment $N^{(1)}(t)$ were calculated using Equations B.11 and B.12, respectively, as the mathematical model

$$Y^{(1)}(t) = \int_0^\infty \cos(\omega t - \varepsilon(\omega)) \sqrt{2 S_x(\omega) |H_y(\omega)|^2 d\omega} \qquad \text{(B.11)}$$

AD-A085 924 DAVID W TAYLOR NAVAL SHIP RESEARCH AND DEVELOPMENT CE--ETC F/G 13/10
SIMULATION ANALYSIS OF AUTOMATIC AND QUICKENED MANUAL CONTROL D--ETC(U)
JUN 80 S M BROWN, J G DIMMICK
UNCLASSIFIED DTNSRDC-80/007 NL

2 OF 2

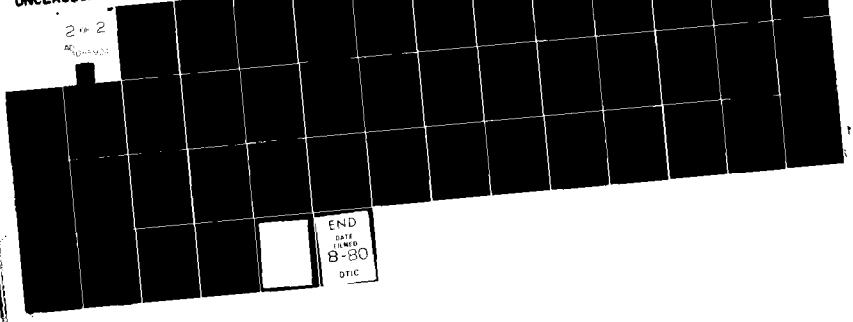

END
DATE FILMED
8-80
DTIC

$$N^{(1)}(t) = \int_0^\infty \cos(\omega t - \varepsilon(\omega)) \sqrt{2S_x(\omega) |H_n(\omega)|^2 d\omega} \qquad (B.12)$$

where ω is the frequency of encounter in the computer program.

The Pierson-Moskowitz Energy Density Spectrum $S_x(\omega)$ is needed to characterize the sea state. In this work, the Pierson-Moskowitz Spectrum was calculated for a significant wave height of 16 ft for a fully developed, wind-driven sea at the ship frequency of encounter ω_e.

$(|H_y(\omega)|^2)$ and $(|H_n(\omega)|^2)$ are the response amplitude operators (RAOs) at the frequency of encounter for the sway-force excitations and yaw-moment excitations, respectively. The response amplitude operator $|H_y(\omega)|^2$ for the sway force excitation is defined at each frequency as the ratio of the sway-force amplitude squared in a regular wave to the wave amplitude squared. The yaw-moment-response amplitude operator was defined in an analogous manner. The data from Table 2 were used to determine both response amplitude operators.

Figure 5 shows the first-order, sway-force excitation versus time acting on the Mariner study ship hull in an oblique irregular wave (ship-to-wave χ = 150 deg) with a significant wave height of 16 ft. Figure 6 shows the analogous first-order, yaw-moment excitation versus time acting on the ship hull.

Second-Order, Irregular Wave Excitations

Digital computer simulation programs developed by Neal[25] were used to generate the second-order, irregular sea state excitations. The second term of Equation B.8 is used as a basis for the mathematical model. The computer programs were used to generate time series of the nonlinear (second-order with respect to wave amplitude) sway force and the nonlinear yaw moment acting on the Mariner study ship. The transfer function $H(\omega_1,-\omega_2)$ is approximated by $H(\omega_1,-\omega_1)$, which is Neuman's approximation.[34] In the computer calculation ω is the ship encounter frequency. The

computer input required to generate the time series consists of a wave-energy spectrum $S_x(\omega)$ and the approximation to the transfer function associated with the slowly varying sway force (and moment).

The oblique, irregular seaway in the UNREP simulation is assumed to be unidirectional and long-crested. The seaway is statistically represented in this work by the Pierson-Moskowitz wave-energy spectrum representing a state 4 sea on the Beaufort Scale. The sea-state, wave-height time series corresponding to the Pierson-Moskowitz spectrum is shown in Figure 7. A digital approximation to the random phase model[25] ($\varepsilon(\omega)$) was used to generate the wave surfaces with Gaussian distribution properties.

The digital-computer-generated, nonlinear, hydrodynamic sway force versus time, and the nonlinear, yaw moment versus time acting on the Mariner study ship at 15 knots in a bow irregular sea ($h^{1/3}$ = significant wave height = 4 ft) are presented in Figures 8 and 9, respectively.[9,10] The sway-force and yaw-moment time series for 8-ft and 16-ft significant wave heights were approximated by multiplying the above time series amplitudes by a factor of 4 and 16, respectively. (Force and moment are approximately proportional to wave amplitude squared.)

The sway-force and yaw-moment time series appear to generally have the correct statistics. Both records have a dc offset and the frequency is lower than the frequency of the wave-height time series. These computer simulation results indicate that there is some validity in Newman's approximation[34] for estimating the transfer functions.

The transfer function $H(\omega_1,-\omega_2)$ was approximated by $H(\omega_1,-\omega_1)$ which is Newman's approximation. The data for estimating the transfer functions associated with the nonlinear excitations were obtained from work by Chey.[37] These data were plotted by the authors in Figures B.1 and B.2. In this work, Chey[37] presents experimental measurements of the forces and moments acting on a restrained Series 60 (C_b = 0.60) ship model proceeding in oblique regular waves (χ = 150 deg). The propeller did not have a driving motor in the ship model.

Realistic data for the transfer functions would be data taken from an unrestrained Mariner moving at constant mean speed in oblique, regular waves. It would also be necessary to have the constraints of hydrodynamic

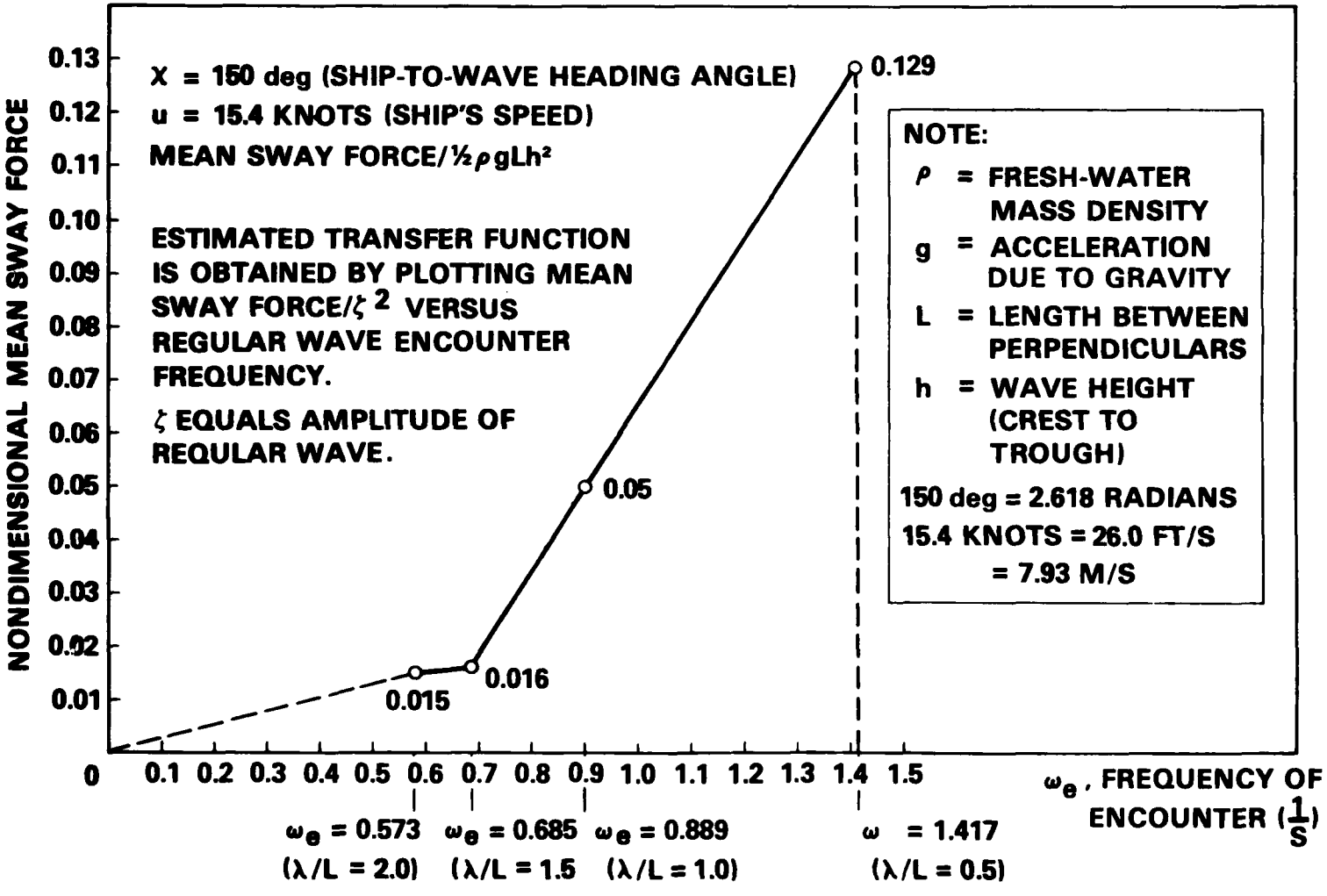

Figure B.1 - Nondimensional Mean Sway Force versus Oblique, Regular-Wave Encounter Frequency[10]

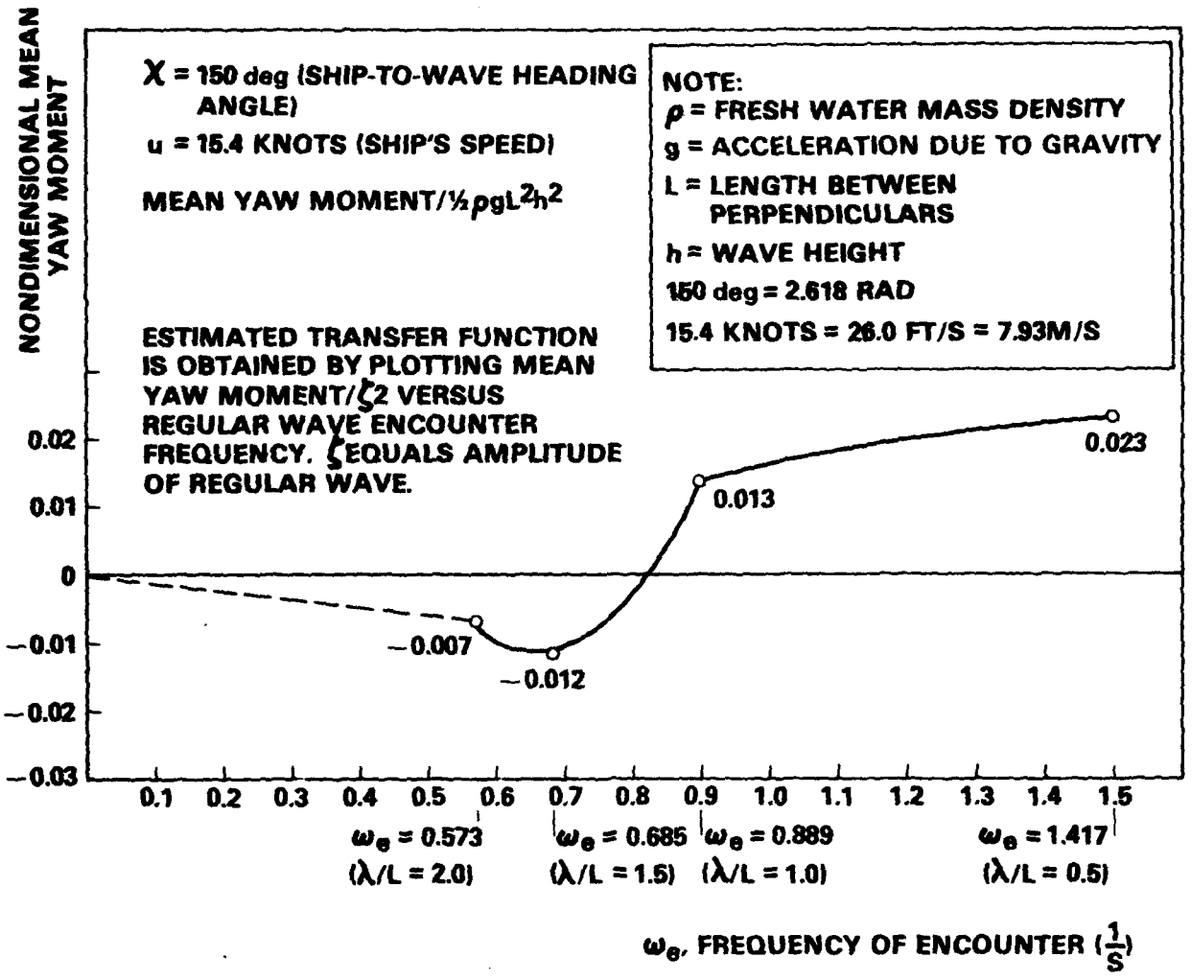

Figure B.2 - Nondimensional Mean Yaw Moment versus Regular-Wave Encounter Frequency[10]

interaction effects of another Mariner and an automatic controller. These data are not currently available.

These experimental data were used because they were the only experimental data available to the authors at the time of the work. However, Lalangas[38] reports that, for a ship in beam seas at zero speed, the drift force on a free-moving model is different from the drift force on a restrained model.[38,39] Thus, it would probably be more realistic to have experimental model data from partially restrained model testing. These data also do not entirely meet the criteria mentioned above and are also only an approximation. Experimentally, partially restrained model data for a single ship or experimentally validated theoretical data were not available to the authors at the time of the work.

The drift force and moment for a Mariner hull at 15 knots in oblique irregular sea (χ = 150 deg) have been calculated by Salvesen.[35] His data were not used in this work because his theory has not been verified against experimental data.

The limitations in the transfer functions used in this control study should not have a large effect on the performance of the automatic controller on each ship during UNREP simulations, the reason being that the controller on each ship is relatively insensitive (several orders of magnitude) to large changes in the amplitude and signs of the amplitude from the nonlinear sea state excitations.[9,10] Thus, the authors realize that the actual ship response to the nonlinear excitations may not be entirely realistic from a theoretical hydrodynamic standpoint. However, it is considered that this work gives a good indication of automatic controller performance when subjected to nonlinear sea state excitations, which is the objective of this work.

APPENDIX C

THE AUTOMATIC CONTROLLERS

The automatic feedback control algorithms on both the leading and tracking ship were primarily developed in earlier work by Alvestad.[8] During UNREP control maneuvers, the leading ship maintains a constant heading, while the tracking ship is responsible for maintaining a constant lateral separation. In the hybrid UNREP control simulation, the algorithms for the two ships are adjusted by taking into account their basic control functions. The basic control block diagrams for each ship are shown in Figure 10.

The main control law for each digital automatic controller is:[8-10]

$$\delta^* = \delta_o + \Delta\delta \tag{C.1}$$

$$\Delta\delta = \underline{K}_1(\Delta\psi) + \underline{K}_2\dot{\psi} + \underline{K}_3\ddot{\psi} + \underline{K}_4(\Delta B) + \underline{K}_5\dot{B}$$

$$+ a_t \int (\Delta B)dt$$

$$= \underline{K}\hat{\underline{Z}} + a_t \int (\Delta B)dt$$

where δ_o = nominal rudder angle

$\Delta\delta$ = rudder perturbations about δ_o the set point ($\Delta\delta$ = rudder output from the automatic controller)

$\underline{K}_i$ = feedback gain constants (i = 1,2,3,4)

$\hat{\underline{Z}}_i = \underline{Z}_i$ + error

$\underline{Z}_i$ = maneuvering control parameters

a_t = gain constant in integral control loop

$\Delta\psi = \psi - \psi_o$

$\Delta\dot{\psi} = \dot{\psi} - \dot{\psi}_o = \dot{\psi}$, since $\dot{\psi}_o = 0$

$\Delta\ddot{\psi} = \ddot{\psi} - \ddot{\psi}_o = \ddot{\psi}$, since $\ddot{\psi}_o = 0$

$\Delta B = B - B_o$

$\Delta\dot{B} = \dot{B} - \dot{B}_o = \dot{B}$, since $\dot{B}_o = 0$

Integral control was added to the tracking ship to improve the control characteristics, but was not needed for the leading ship because its control function is simpler. The gains chosen for $\underline{K}_L$ and $\underline{K}_T$ have the following general form:

$$\underline{K}_L = \left[\underline{K}_1\ \underline{K}_2\ \underline{K}_3\ 0\ \ 0\right],\ a_t = 0 \qquad \text{(C.2)}$$

$$\underline{K}_T = \left[\underline{K}_1\ \underline{K}_2\ \underline{K}_3\ \underline{K}_4\ \underline{K}_5\right],\ a_t$$

and

$$\underline{Z} = \begin{bmatrix} \Delta\psi \\ \dot{\psi} \\ \ddot{\psi} \\ \Delta B \\ \dot{B} \end{bmatrix}$$

where L and T subscripts refer to leading and tracking ship, respectively.

For detailed discussion of the automatic controllers on the leading and tracking ship, the reader should consult the work by Alvestad.[8]

APPENDIX D

HYDRODYNAMIC INTERACTION FORCES AND MOMENTS FOR AO 177 AND DESTROYER STUDY SHIP

The hydrodynamic interaction forces and moments are presented for the destroyer study ship and AO 177 during UNREP operations. Table D.1 presents the hydrodynamic data as a function of lateral and longitudinal separation distance. These data are plotted in Figures D.1 through D.24. These data were calculated on the computer by Glen Ashe,[40] of the U.S. Coast Guard, and given to the authors. The computer program was developed by Abkowitz, Ashe, and Fortson[40,41] at the Massachusetts Institute of Technology.

TABLE D.1 - DIMENSIONLESS HYDRODYNAMIC INTERACTION DATA BETWEEN AO 177 CLASS AND DESTROYER STUDY SHIP

Lateral Separation (ft) (Side to Side)	Longitudinal Separation of Amidships (ft) (Positive Indicates Destroyer Ahead)	Destroyer Study Ship			AO 177 Class		
		Normal Force, $\left(\frac{Y}{1/2\ \rho u^2 L^2}\right)$ Positive = Attraction	Moment, $\left(\frac{N}{1/2\ \rho u^2 L^3}\right)$ Positive = Bow In	Longitudinal Force, $\left(\frac{X}{1/2\ \rho u^2 L^2}\right)$ Positive = Forward	Normal Force, $\left(\frac{Y}{1/2\ \rho u^2 L^2}\right)$ Positive = Attraction	Moment, $\left(\frac{N}{1/2\ \rho u^2 L^3}\right)$ Positive = Bow In	Longitudinal Force, $\left(\frac{X}{1/2\ \rho u^2 L^2}\right)$ Positive = Forward
90	-600	-0.000014	0.0000023	-0.000014	-0.000013	0.0000010	-0.000013
	-540	-0.000025	0.0000036	-0.000017	-0.000023	0.0000022	-0.000016
	-480	-0.000041	0.0000066	-0.000017	-0.000038	0.0000030	-0.000015
	-420	-0.000050	0.0000140	-0.0000068	-0.000054	0.0000013	-0.0000062
	-360	-0.000070	0.0000260	0.000015	-0.000064	-0.0000059	0.000014
	-300	-0.000064	0.0000420	0.000046	-0.000059	-0.000020	0.000042
	-240	-0.000034	0.0000560	0.000077	-0.000032	-0.000039	0.000072
	-180	0.000010	0.0000600	0.000098	0.000017	-0.000057	0.000090
	-120	0.000083	0.0000480	0.000096	0.000077	-0.000064	0.000089
	-60	0.000140	0.0000210	0.000067	0.000130	-0.000055	0.000062
	0	0.000170	-0.0000150	0.000016	0.000160	-0.000030	0.000015
	60	0.000160	-0.0000460	-0.000041	0.000150	0.0000049	-0.000038
	120	0.000120	-0.0000640	-0.000084	0.000110	0.000037	-0.000078
	180	0.000055	-0.0000670	-0.000100	0.000051	0.000055	-0.000094
	240	-0.0000075	-0.0000560	-0.000093	-0.0000069	0.000057	-0.000086
	300	-0-000053	-0.0000350	-0.000067	-0.000049	0.000046	-0.000062
	360	-0.000075	-0.0000150	-0.000033	-0.000069	0.000030	-0.000030
	420	-0.000071	-0.0000016	-0.0000022	-0.000066	0.000016	-0.000002
	480	-0.000053	-0.0000030	0.000015	-0.000049	0.0000076	0.000014
	540	-0.000033	-0.0000027	0.000020	-0.000031	0.0000030	0.000018
	600	-0.000019	-0.0000013	0.000017	-0.000018	0.0000025	0.000016
110	-600	-0.000014	0.0000026	-0.0000120	-0.000013	0.0000007	0.0000110
	-540	-0.000023	0.0000041	-0.0000130	-0.000021	0.0000013	0.0000120
	-480	-0.000035	0.0000071	-0.0000110	-0.000032	0.0000015	0.0000110
	-420	-0.000048	0.0000130	-0.0000023	-0.000044	-0.0000006	0.0000021
	-360	-0.000055	0.0000230	0.0000160	-0.000051	-0.0000069	-0.0000140
	-300	-0.000049	0.0000350	0.0000400	-0.000045	-0.0000180	-0.0000370
	-240	-0.000024	0.0000450	0.0000640	-0.000022	-0.0000330	-0.0000600
	-180	0.000017	0.0000480	0.0000790	0.000016	-0.0000450	-0.0000730
	-120	0.000067	0.0000380	0.0000770	0.000062	-0.0000500	-0.0000710
	-60	0.000110	0.0000160	0.0000530	0.000100	-0.0000430	-0.0000490
	0	0.000140	-0.0000110	0.0000130	0.000130	-0.0000230	-0.0000120
	60	0.000130	-0.0000360	-0.0000320	0.000120	0.0000037	0.0000300
	120	0.000095	-0.0000510	-0.0000670	0.000088	0.0000280	0.0000620
	180	0.000045	-0.0000530	-0.0000820	0.000042	0.0000430	0.0000760
	240	-0.0000032	-0.0000450	-0.0000770	-0.000003	0.0000450	0.0000710
	300	-0.000040	-0.0000300	-0.0000570	-0.000037	0.0000380	0.0000520
	360	-0.000058	-0.0000140	-0.0000300	-0.000053	0.0000260	0.0000280
	420	-0.000057	-0.0000036	-0.0000055	-0.000053	0.0000150	0.0000051
	480	-0.000044	-0.0000009	0.0000095	-0.000041	0.0000061	-0.0000038
	540	-0.000030	-0.0000014	0.0000150	-0.000027	0.0000045	-0.0000140
	600	-0.000018	-0.0000008	0.0000140	-0.000017	0.0000028	-0.0000130

TABLE D.1 (Continued)

Lateral Separation (ft) (Side to Side)	Longitudinal Separation of Amidships (ft) (Positive Indicates Destroyer Ahead)	Destroyer Study Ship			AO 177 Class		
		Normal Force, $\left(\frac{Y}{1/2\ \rho u^2 L^2}\right)$ Positive = Attraction	Moment, $\left(\frac{N}{1/2\ \rho u^2 L^3}\right)$ Positive = Bow In	Longitudinal Force, $\left(\frac{X}{1/2\ \rho u^2 L^2}\right)$ Positive = Forward	Normal Force, $\left(\frac{Y}{1/2\ \rho u^2 L^2}\right)$ Positive = Attraction	Moment, $\left(\frac{N}{1/2\ \rho u^2 L^3}\right)$ Positive = Bow In	Longitudinal Force, $\left(\frac{X}{1/2\ \rho u^2 L^2}\right)$ Positive = Forward
	-600	-0.000013	0.0000028	-0.0000096	-0.000012	0.0000004	0.0000089
	-540	-0.000020	0.0000044	-0.0000100	-0.000019	0.0000006	0.0000094
	-480	-0.000030	0.0000073	-0.0000075	-0.000028	0.0000003	0.0000070
	-420	-0.000039	0.0000130	-0.0000008	-0.000036	-0.0000019	-0.0000007
	-360	-0.000044	0.0000210	0.0000160	-0.000040	-0.0000073	-0.0000150
	-300	-0.000037	0.0000300	0.0000350	-0.000035	-0.0000160	-0.0000330
	-240	-0.000017	0.0000370	0.0000540	-0.000016	-0.0000280	-0.0000500
	-180	0.000016	0.0000380	0.0000650	0.000015	-0.0000370	-0.0000600
	-120	0.000056	0.0000300	0.0000620	0.000052	-0.0000400	-0.0000570
	-60	0.000090	0.0000130	0.0000420	0.000084	-0.0000340	-0.0000390
130	0	0.000110	-0.0000089	0.0000100	0.000100	-0.0000180	-0.0000093
	60	0.000100	-0.0000280	-0.0000260	0.000096	0.0000028	0.0000240
	120	0.000077	-0.0000400	-0.0000540	0.000071	0.0000220	0.0000500
	180	0.000038	-0.0000430	-0.0000660	0.000036	0.0000340	0.0000610
	240	-0.0000001	-0.0000370	-0.0000630	-0.0000001	0.0000360	0.0000590
	300	-0.000030	-0.0000260	-0.0000480	-0.000027	0.0000310	0.0000440
	360	-0.000045	-0.0000140	-0.0000270	-0.000041	0.0000230	0.0000250
	420	-0.000046	-0.0000049	-0.000008	-0.000042	0.0000140	0.0000070
	480	-0.000037	-0.0000006	-0.000005	-0.000034	0.0000081	-0.0000049
	540	-0.000026	0.0000004	-0.0000110	-0.000024	0.0000048	-0.0000098
	600	-0.000017	0.0000003	0.0000110	-0.000016	0.0000030	-0.0000100
	-600	-0.000012	0.0000030	-0.0000077	-0.000011	0.00000005	0.0000071
	-540	-0.000018	0.0000045	-0.0000076	-0.000017	0.00000006	0.0000070
	-480	-0.000026	0.0000073	-0.0000046	-0.000024	-0.00000057	0.0000043
	-420	-0.000033	0.0000120	0.0000029	-0.000030	-0.00000280	-0.0000027
	-360	-0.000035	0.0000180	0.0000150	-0.000032	-0.00000750	-0.0000140
	-300	-0.000029	0.0000250	0.0000310	-0.000026	-0.00001500	-0.0000290
	-240	-0.000011	0.0000310	0.0000460	-0.000011	-0.00002300	-0.0000420
	-180	0.000016	0.0000310	0.0000540	0.000014	-0.00003000	-0.0000500
	-120	0.000047	0.0000240	0.0000500	0.000043	-0.00003200	-0.0000470
	-60	0.000074	0.0000099	0.0000340	0.000068	-0.00002700	-0.0000320
150	0	0.000088	-0.0000071	0.0000080	0.000081	-0.00001400	-0.0000074
	60	0.000084	-0.0000230	-0.0000210	0.000078	0.00000210	0.0000190
	120	0.000063	-0.0000320	-0.0000430	0.000058	0.00001700	0.0000400
	180	0.000033	-0.0000350	-0.0000540	0.000030	0.00002700	0.0000500
	240	0.0000021	-0.0000310	-0.0000530	0.000002	0.00003000	0.0000490
	300	-0.000022	-0.0000220	-0.0000410	-0.000020	0.00002600	0.0000350
	360	-0.000035	-0.0000130	-0.0000250	-0.000032	0.00002000	0.0000280
	420	-0.000037	-0.0000056	-0.000088	-0.000034	0.00001300	0.0000081
	480	-0.000031	-0.0000017	0.0000022	-0.000029	0.00000800	-0.0000020
	540	-0.000023	-0.0000004	0.0000074	-0.000021	0.00000490	-0.0000069
	600	-0.000016	-0.0000001	0.0000086	-0.000014	0.00000320	-0.0000079

TABLE D.1 (Continued)

Lateral Separation (ft) (Side to Side)	Longitudinal Separation of Amidships (ft) (Positive Indicates Destroyer Ahead)	Destroyer Study Ship			AO 177 Class		
		Normal Force, $\left(\frac{Y}{1/2\ \rho u^2 L^2}\right)$ Positive = Attraction	Moment, $\left(\frac{N}{1/2\ \rho u^2 L^3}\right)$ Positive = Bow In	Longitudinal Force, $\left(\frac{X}{1/2\ \rho u^2 L^2}\right)$ Positive = Forward	Normal Force, $\left(\frac{Y}{1/2\ \rho u^2 L^2}\right)$ Positive = Attraction	Moment, $\left(\frac{N}{1/2\ \rho u^2 L^3}\right)$ Positive = Bow In	Longitudinal Force, $\left(\frac{X}{1/2\ \rho u^2 L^2}\right)$ Positive = Forward
	-600	-0.000015	0.0000016	-0.0000200	-0.000014	0.0000017	0.000019
	-540	-0.000030	0.0000021	-0.0000280	-0.000027	0.0000042	0.000026
	-480	-0.000056	0.0000042	-0.0000320	-0.000052	0.0000079	0.000030
	-420	-0.000089	0.0000130	-0.0000220	-0.000083	0.0000082	0.000020
	-360	-0.000110	0.0000330	0.0000095	-0.000100	-0.0000025	-0.000010
	-300	-0.000110	0.0000630	0.0000590	-0.000100	-0.0000250	-0.000055
	-240	-0.000065	0.0000900	0.0001100	-0.000061	-0.0000530	-0.000110
	-180	0.000024	0.0001000	0.0001500	0.000022	-0.0000930	-0.000140
	-120	0.000140	0.0000840	0.0001500	0.000130	-0.0001100	-0.000140
	-60	0.000240	0.0000370	0.0001100	0.000220	-0.0000970	-0.000100
50	0	0.000300	-0.0000270	0.0000280	0.000280	-0.0000550	-0.000026
	60	0.000280	-0.0000810	-0.0000690	0.000260	0.0000085	0.000064
	120	0.000200	-0.0001100	-0.0001400	0.000180	0.0000660	0.000130
	180	0.000087	-0.0001100	-0.0001600	0.000080	0.0000950	0.000150
	240	-0.000019	-0.0000900	-0.0001400	-0.000017	0.0000930	0.000130
	300	-0.000095	-0.0000520	-0.0000970	-0.000088	0.0000700	0.000090
	360	-0.000130	-0.0000150	-0.0000390	-0.000120	0.0000410	0.0000360
	420	-0.000120	0.0000063	0.0000110	-0.000110	0.0000170	-0.0000100
	480	-0.000077	0.0000100	0.0000350	-0.000072	0.0000051	-0.0000320
	540	-0.000041	0.0000059	0.0000350	-0.000038	0.0000021	-0.0000320
	600	-0.000020	0.0000024	0.0000250	-0.000019	0.0000016	-0.0000230
	-600	-0.000015	0.0000020	-0.000017	-0.000014	0.0000015	0.000016
	-540	-0.000027	0.0000029	-0.000022	-0.000025	0.0000031	0.000021
	-480	-0.000048	0.0000057	-0.000023	-0.000044	0.0000051	0.000022
	-420	-0.000072	0.0000140	-0.000013	-0.000067	0.0000041	0.000012
	-360	-0.000089	0.0000290	0.000013	-0.000082	-0.0000041	-0.000012
	-300	-0.000084	0.0000510	0.000052	-0.000078	-0.000022	-0.000048
	-240	-0.000048	0.0000710	0.000094	-0.000044	-0.000048	-0.000086
	-180	0.000020	0.0000770	0.000120	0.000018	-0.000072	-0.000110
	-120	0.000100	0.0000630	0.000120	0.000097	-0.000083	-0.000110
	-60	0.000180	0.0000280	0.000086	0.000170	-0.000072	-0.000080
70	0	0.000230	-0.0000190	0.000021	0.000210	-0.000040	-0.000020
	60	0.000210	-0.0000600	-0.000053	0.000200	0.0000065	0.000049
	120	0.000150	-0.0000830	-0.000110	0.000140	0.000049	0.000089
	180	0.000067	-0.0000860	-0.000130	0.000062	0.000072	0.000120
	240	-0.000013	-0.0000700	-0.000110	-0.000012	0.000072	0.000110
	300	-0.000071	-0.0000420	-0.000080	-0.000066	0.000056	0.000074
	360	-0.000097	-0.0000150	-0.000036	-0.000090	0.000035	0.000033
	120	-0.000090	0.0000017	0.000003	-0.000083	0.000017	-0.0000015
	480	-0.000064	0.0000061	0.000024	-0.000059	0.0000067	-0.0000120
	540	-0.000037	0.0000042	0.000026	-0.000034	0.0000032	-0.0000240
	600	-0.000020	0.0000018	0.000021	-0.000018	0.0000021	-0.0000190

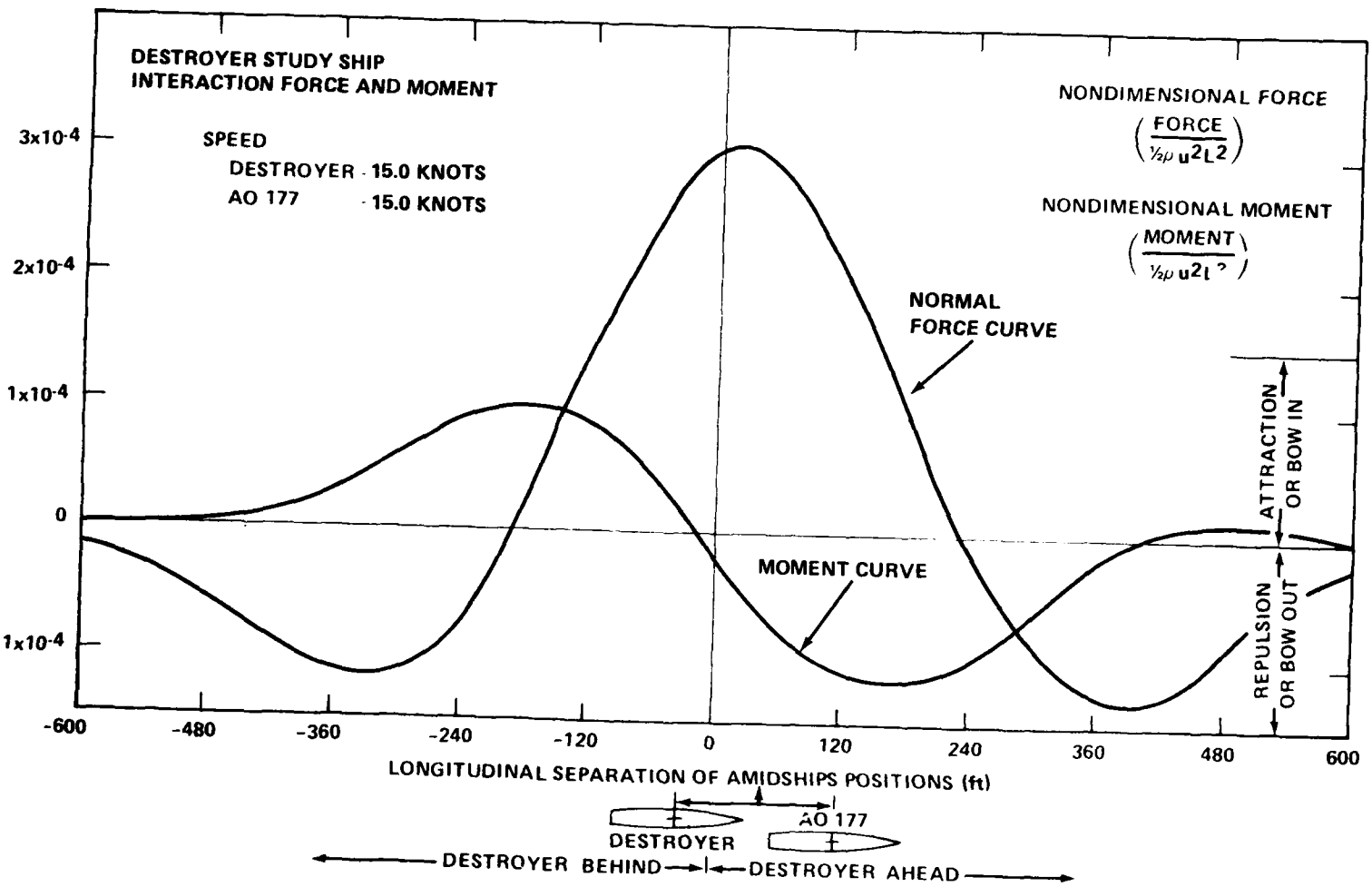

Figure D.1 - Destroyer Study Ship: Interaction Force and Moment
(Lateral Separation Between Amidships - 121.5 ft, Between Sides - 50.0 ft)

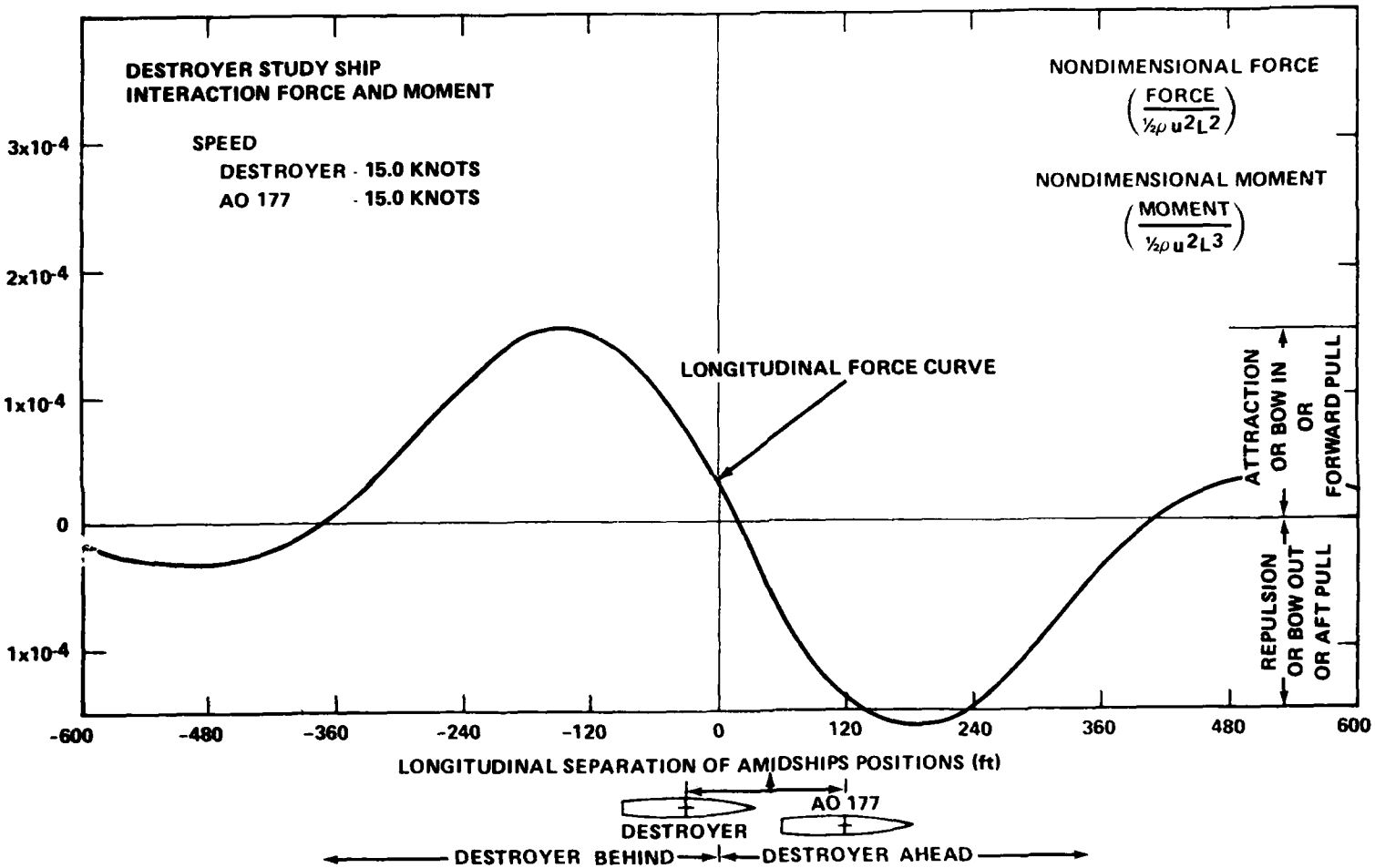

Figure D.2 - Destroyer Study Ship: Longitudinal Interaction Force
(Lateral Separation Between Amidships - 121.5 ft, Between Sides - 50.0 ft)

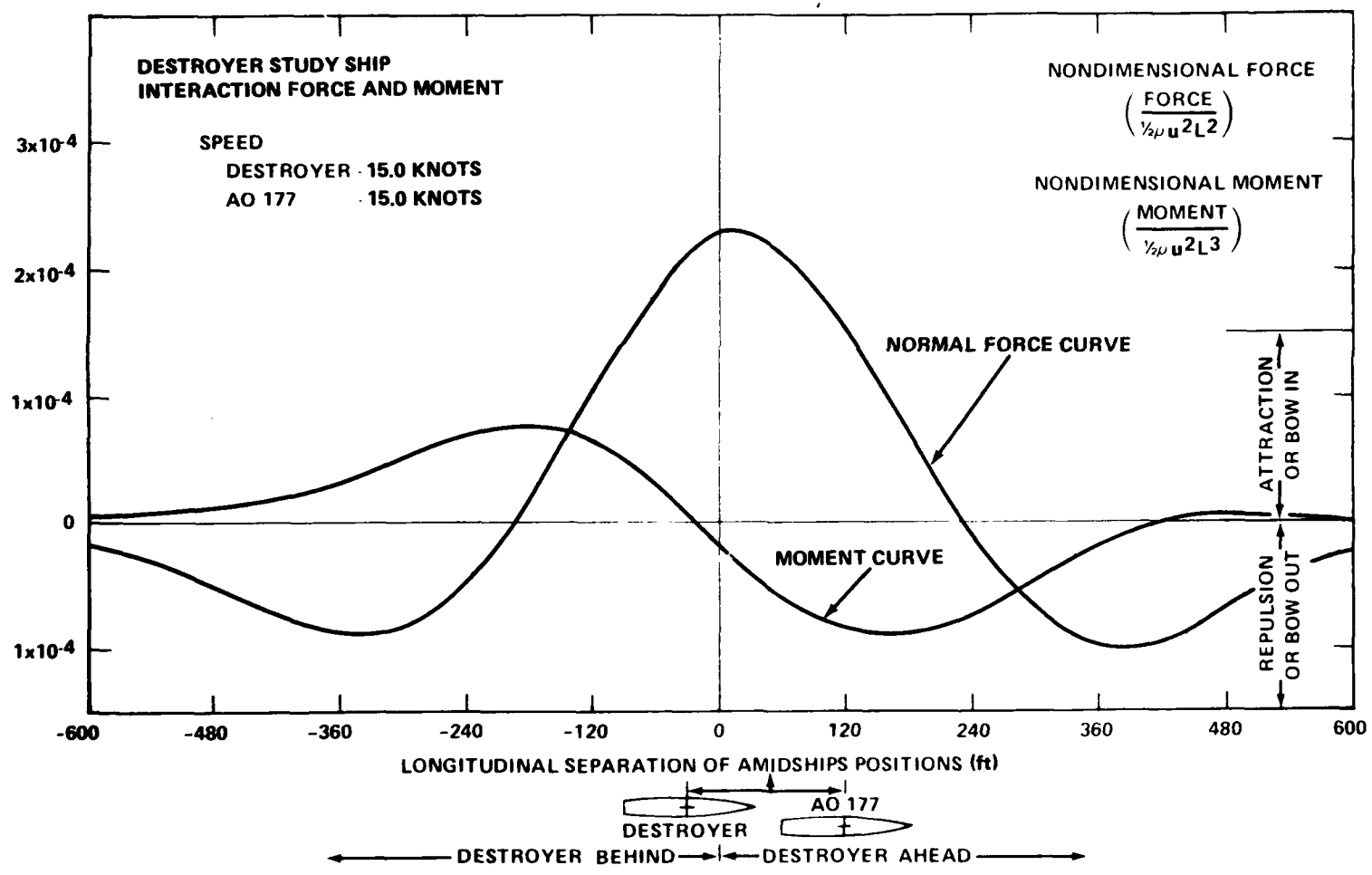

Figure D.3 - Destroyer Study Ship: Interaction Force and Moment
(Lateral Separation Between Amidships - 141.5 ft, Between Sides - 70.0 ft)

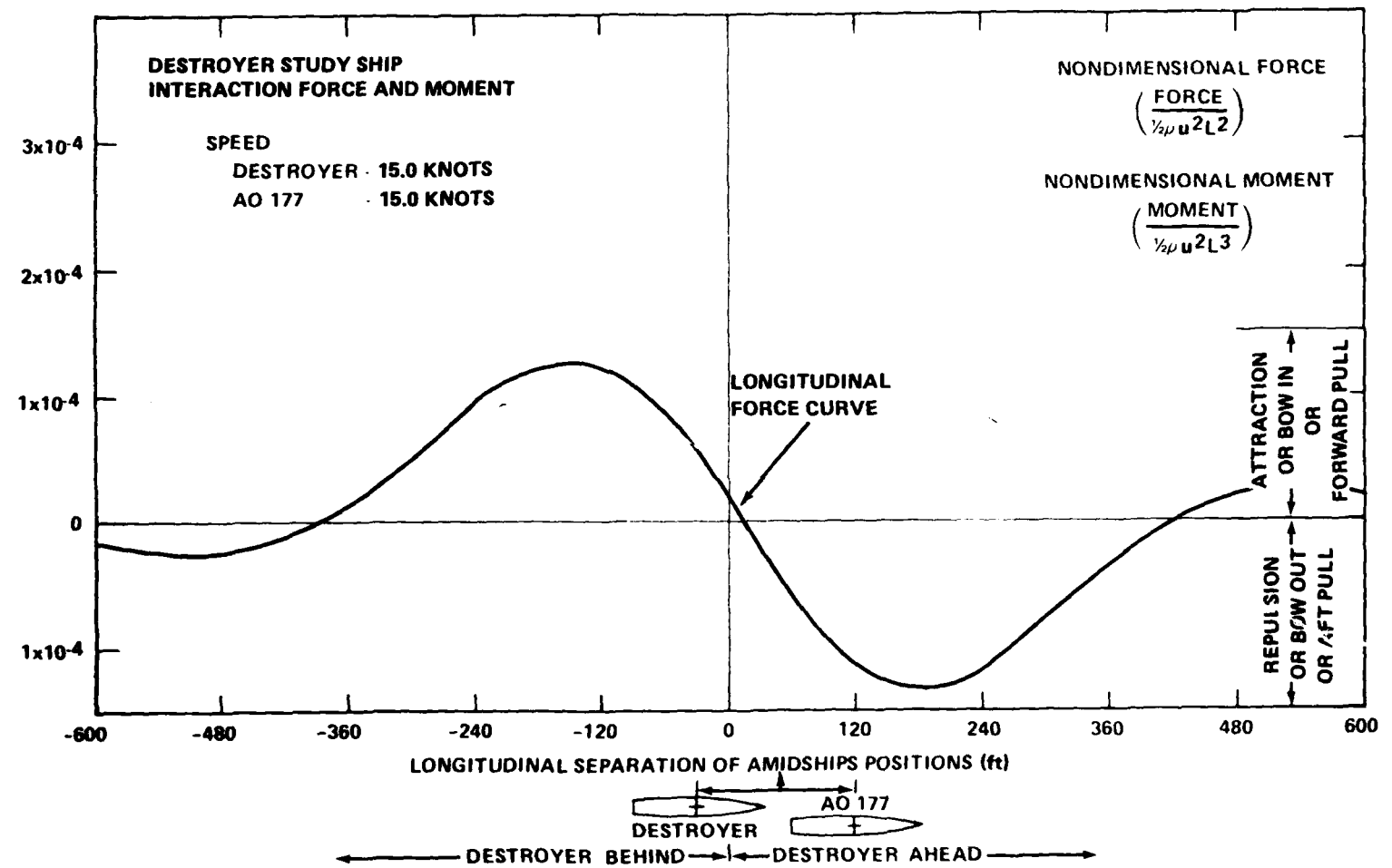

Figure D.4 - Destroyer Study Ship: Longitudinal Interaction Force
(Lateral Separation Between Amidships - 141.5 ft, Between Sides - 70.0 ft)

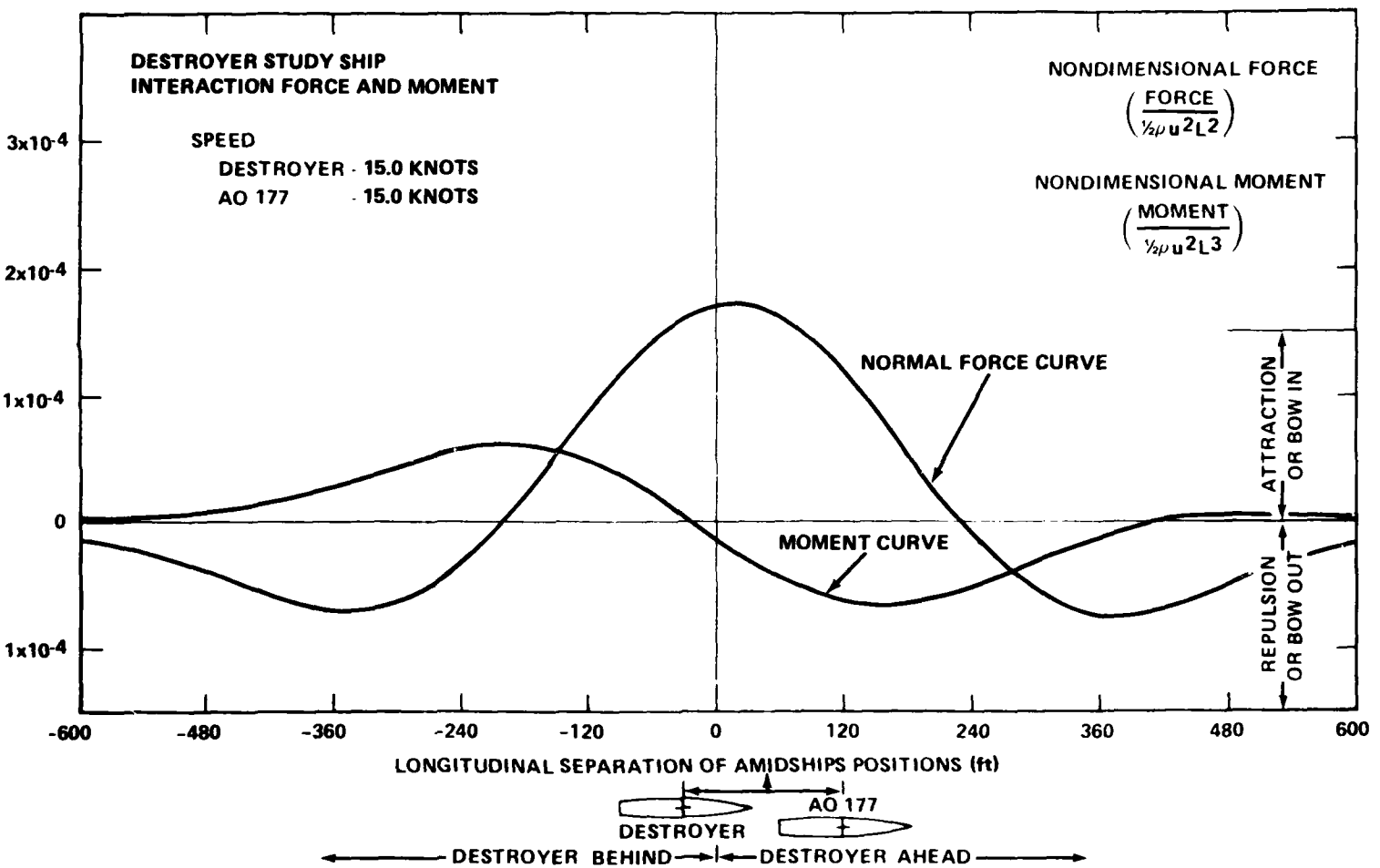

Figure D.5 - Destroyer Study Ship: Interaction Force and Moment
(Lateral Separation Between Amidships - 161.5 ft, Between Sides - 90.0 ft)

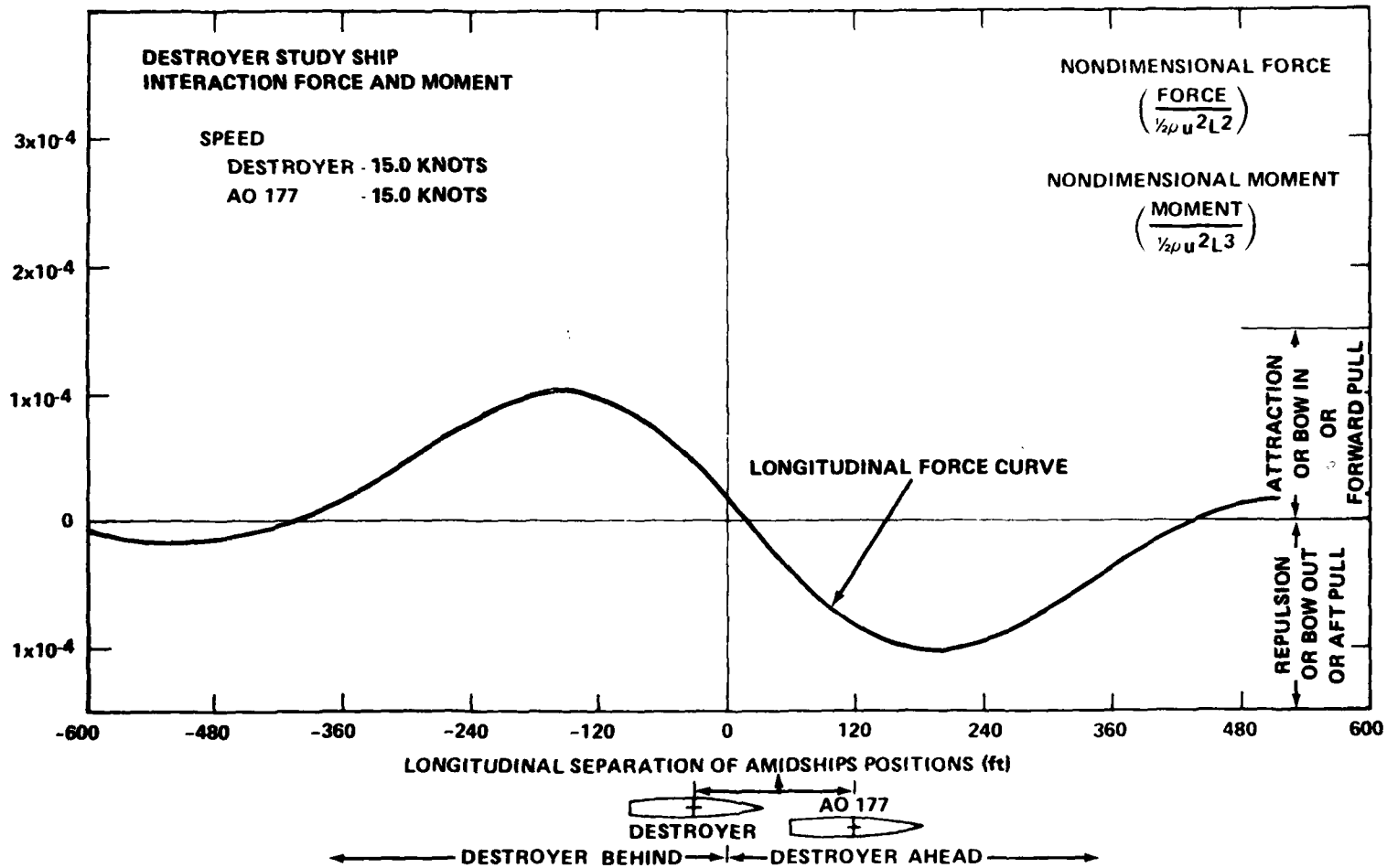

Figure D.6 - Destroyer Study Ship: Longitudinal Interaction Force
(Lateral Separation Between Amidships - 161.5 ft, Between Sides - 90.0 ft)

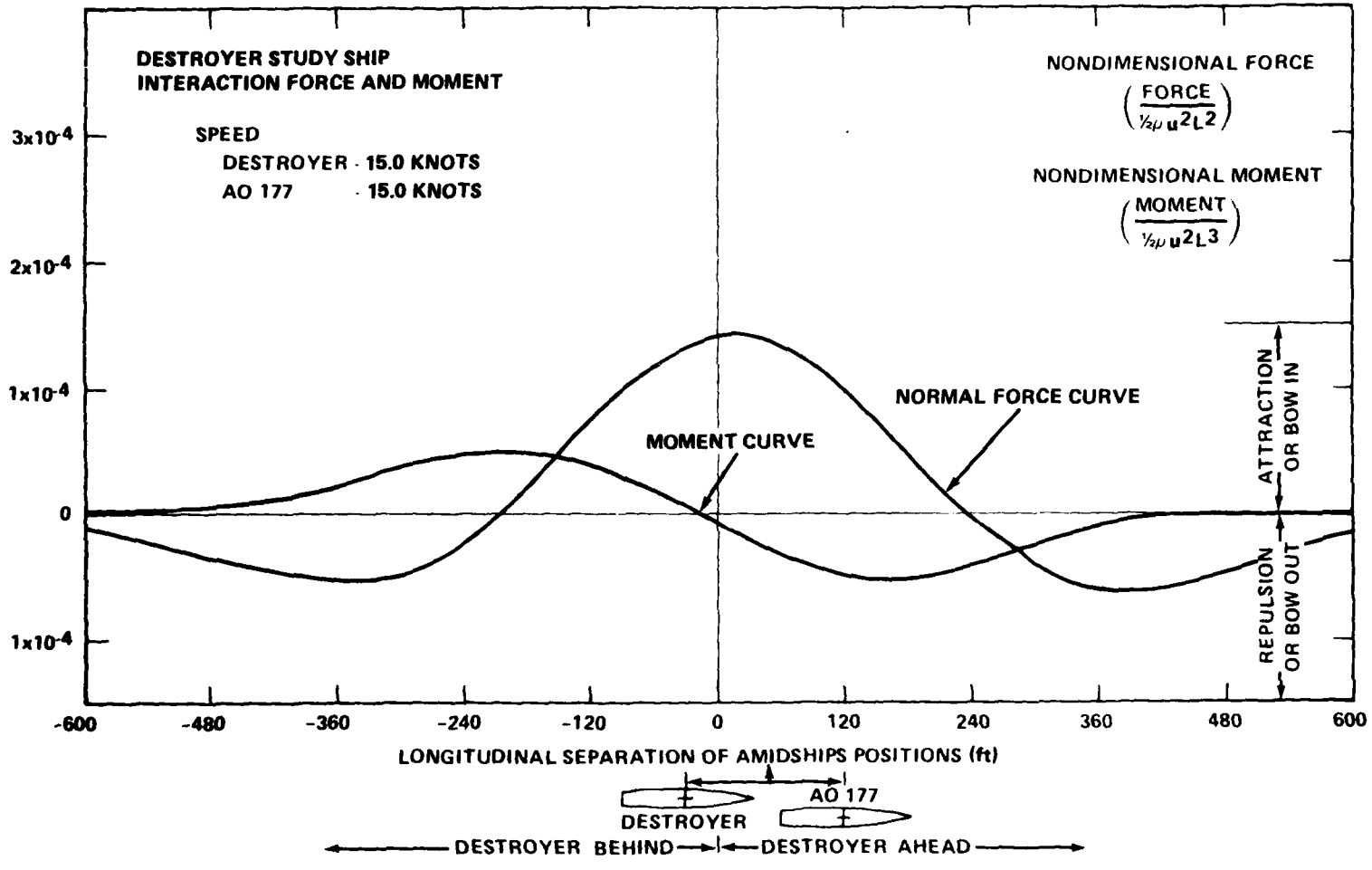

Figure D.7 - Destroyer Study Ship: Interaction Force and Moment
(Lateral Separation Between Amidships - 181.5 ft, Between Sides - 110.0 ft)

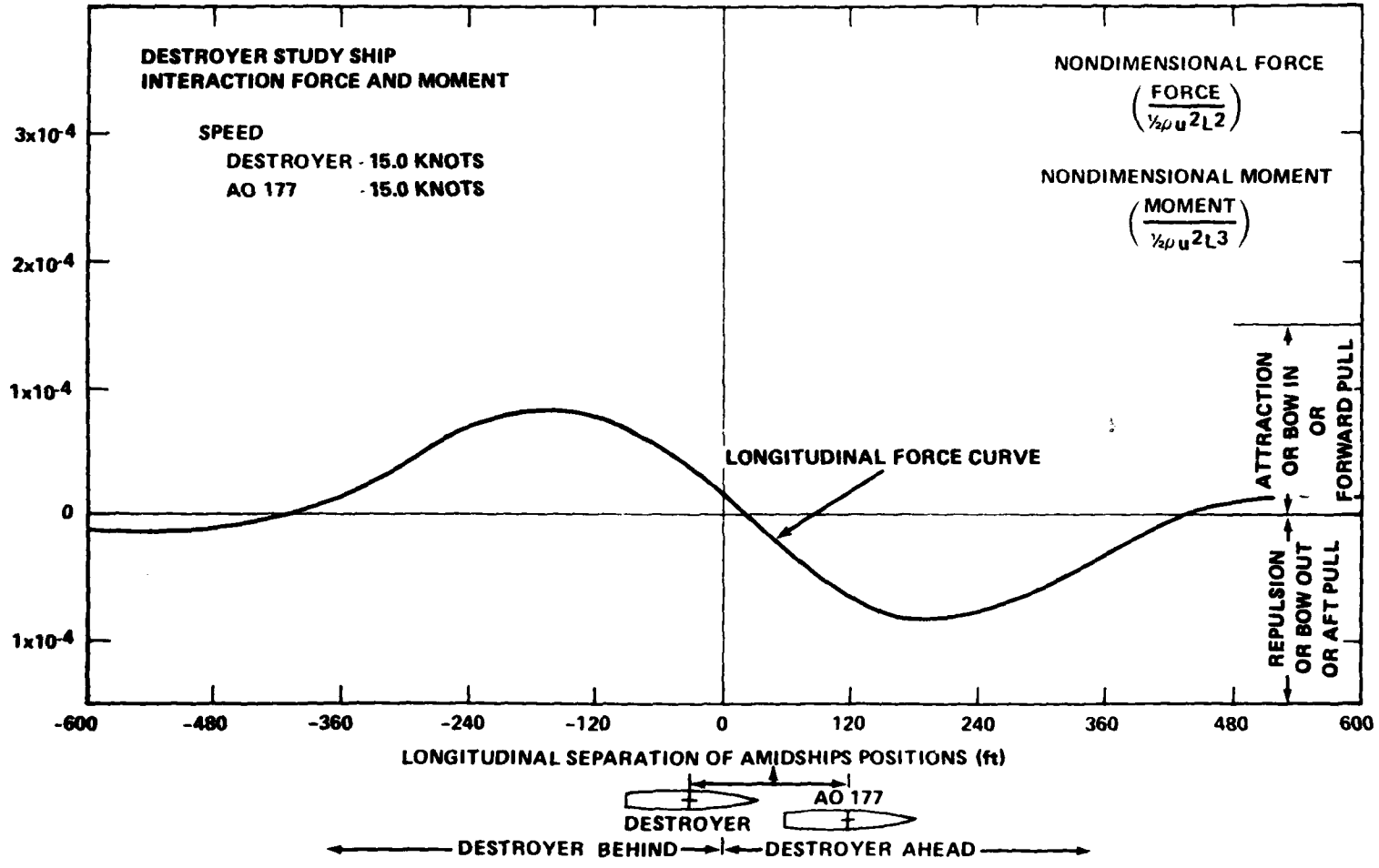

Figure D.8 - Destroyer Study Ship: Longitudinal Interaction Force
(Lateral Separation Between Amidships - 181.5 ft, Between Sides - 110.0 ft)

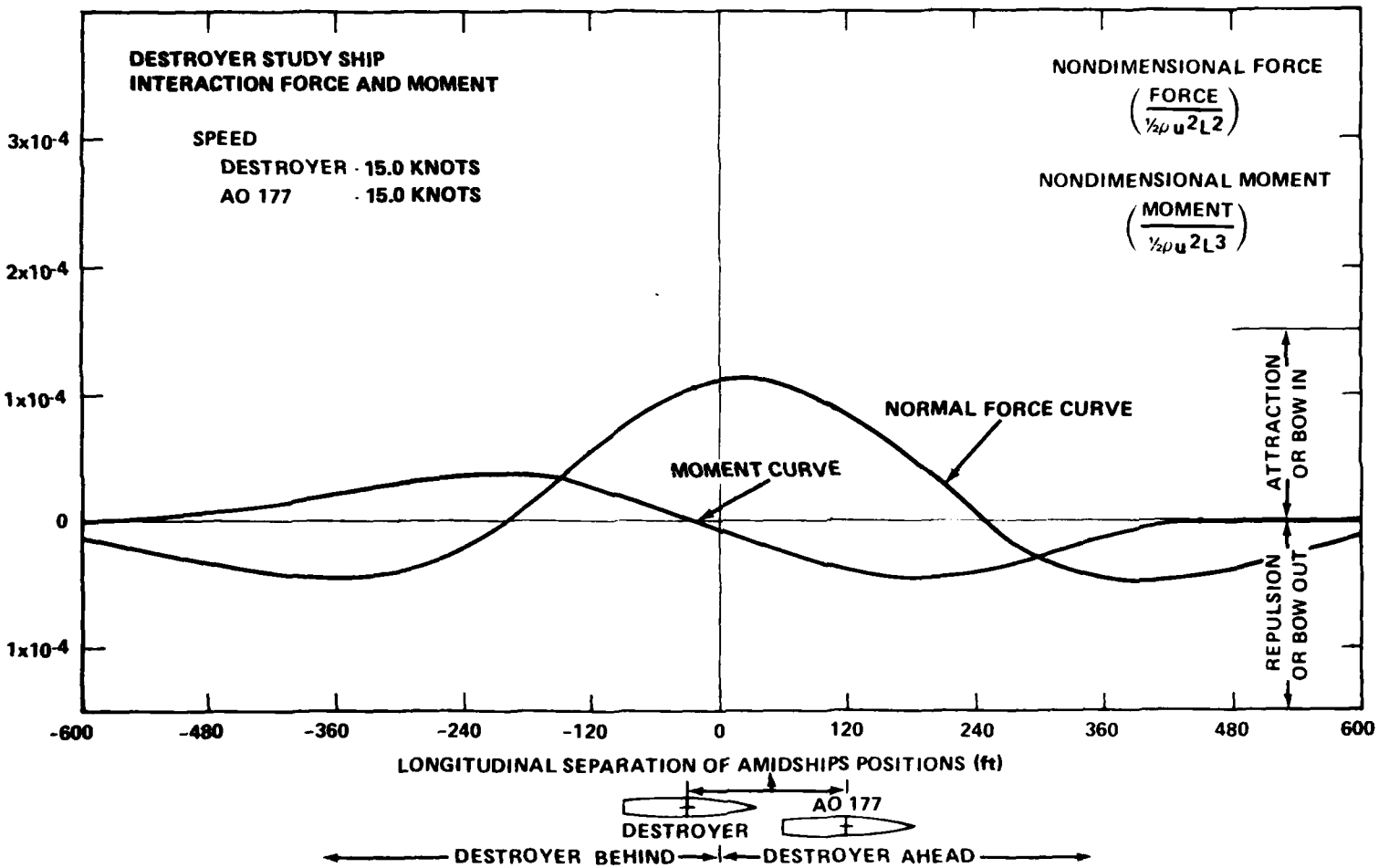

Figure D.9 - Destroyer Study Ship: Interaction Force and Moment
(Lateral Separation Between Amidships - 201.5 ft, Between Sides - 130.0 ft)

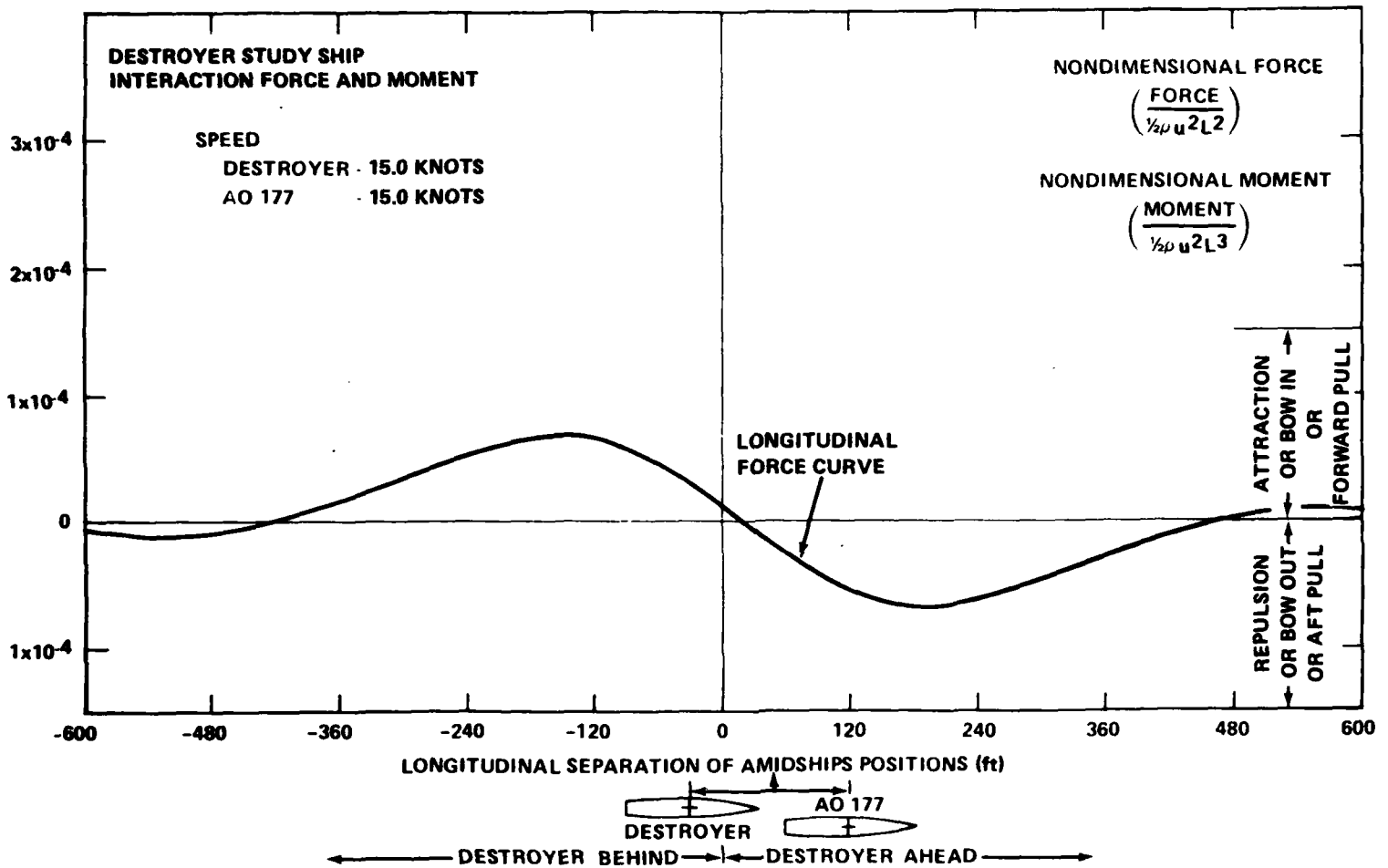

Figure D.10 - Destroyer Study Ship: Longitudinal Interaction Force
(Lateral Separation Between Amidships - 201.5 ft, Between Sides - 130.0 ft)

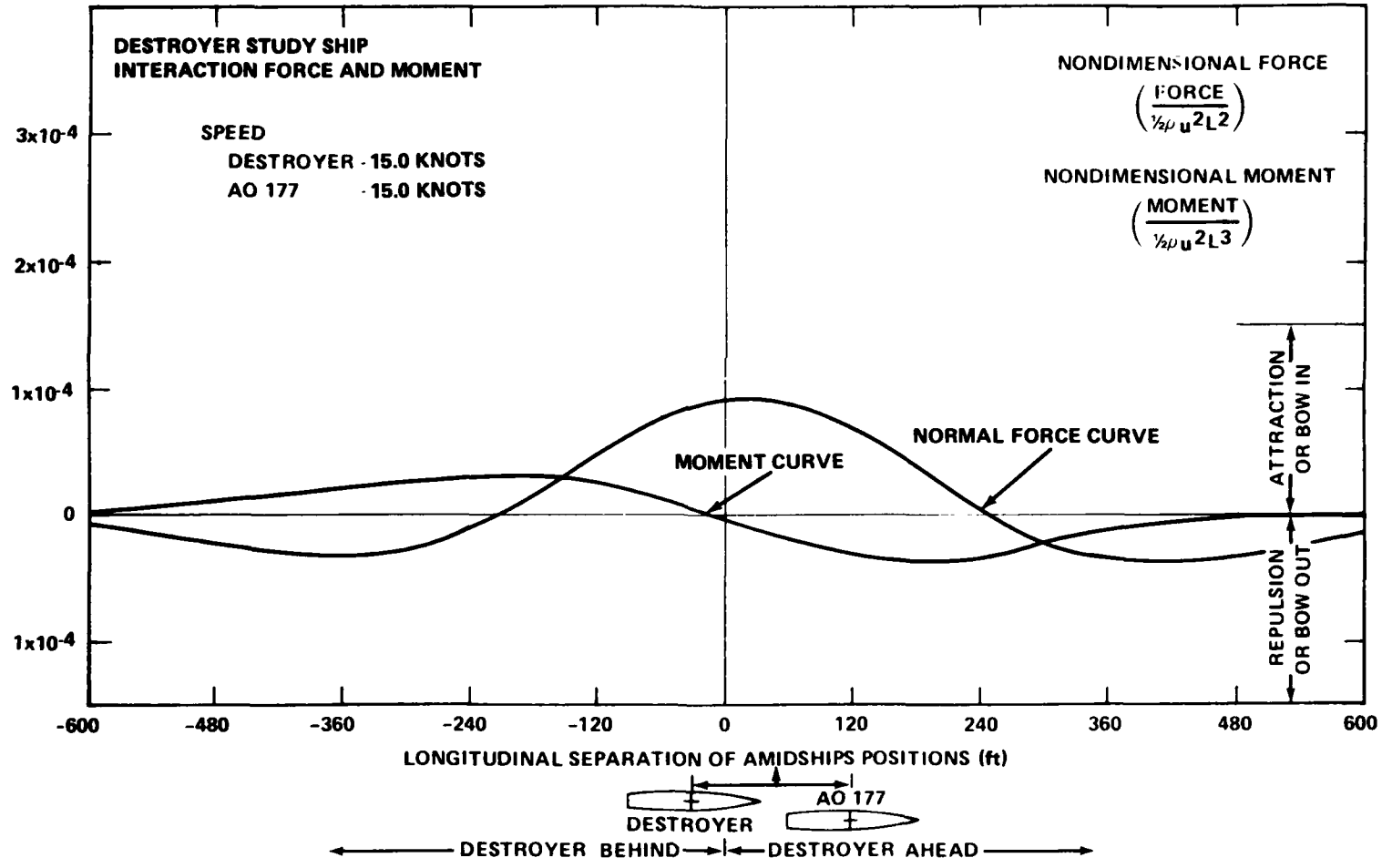

Figure D.11 - Destroyer Study Ship: Interaction Force and Moment
(Lateral Separation Between Amidships - 221.5 ft, Between Sides - 150.0 ft)

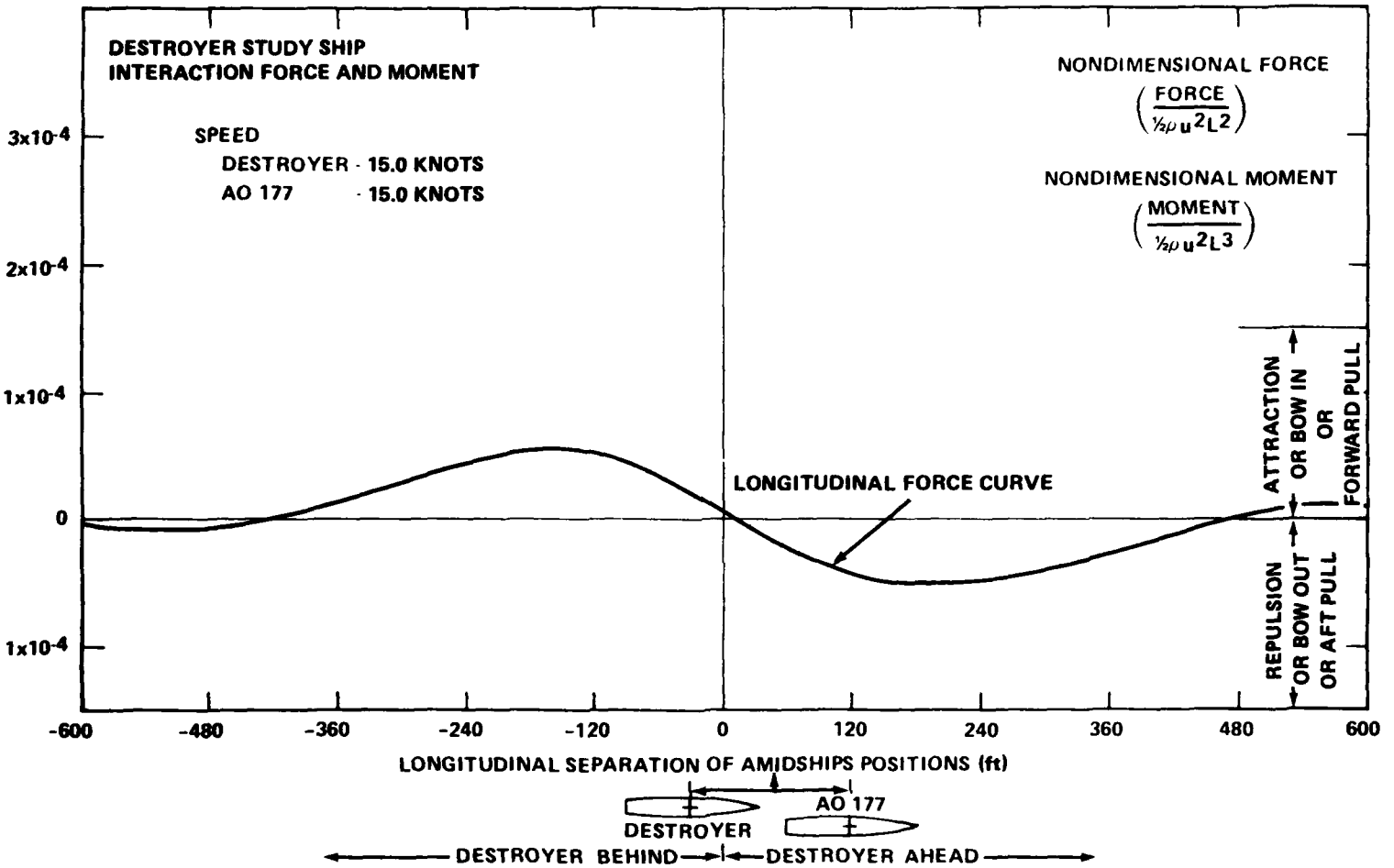

Figure D.12 - Destroyer Study Ship: Longitudinal Interaction Force
(Lateral Separation Between Amidships - 221.5 ft, Between Sides - 150.0 ft)

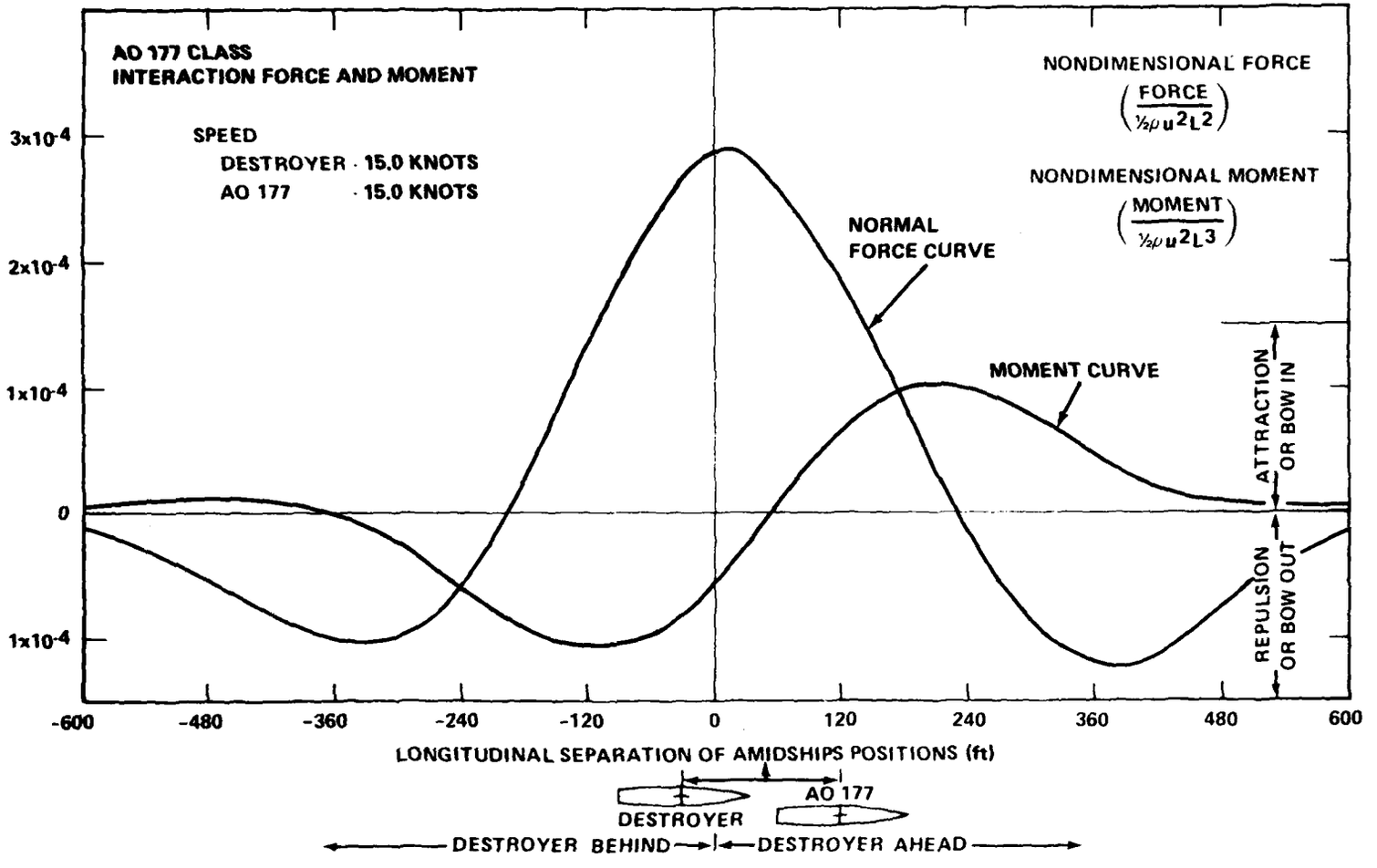

Figure D.13 - AO 177 Class: Interaction Force and Moment
(Lateral Separation Between Amidships - 121.5 ft, Between Sides - 50.0 ft)

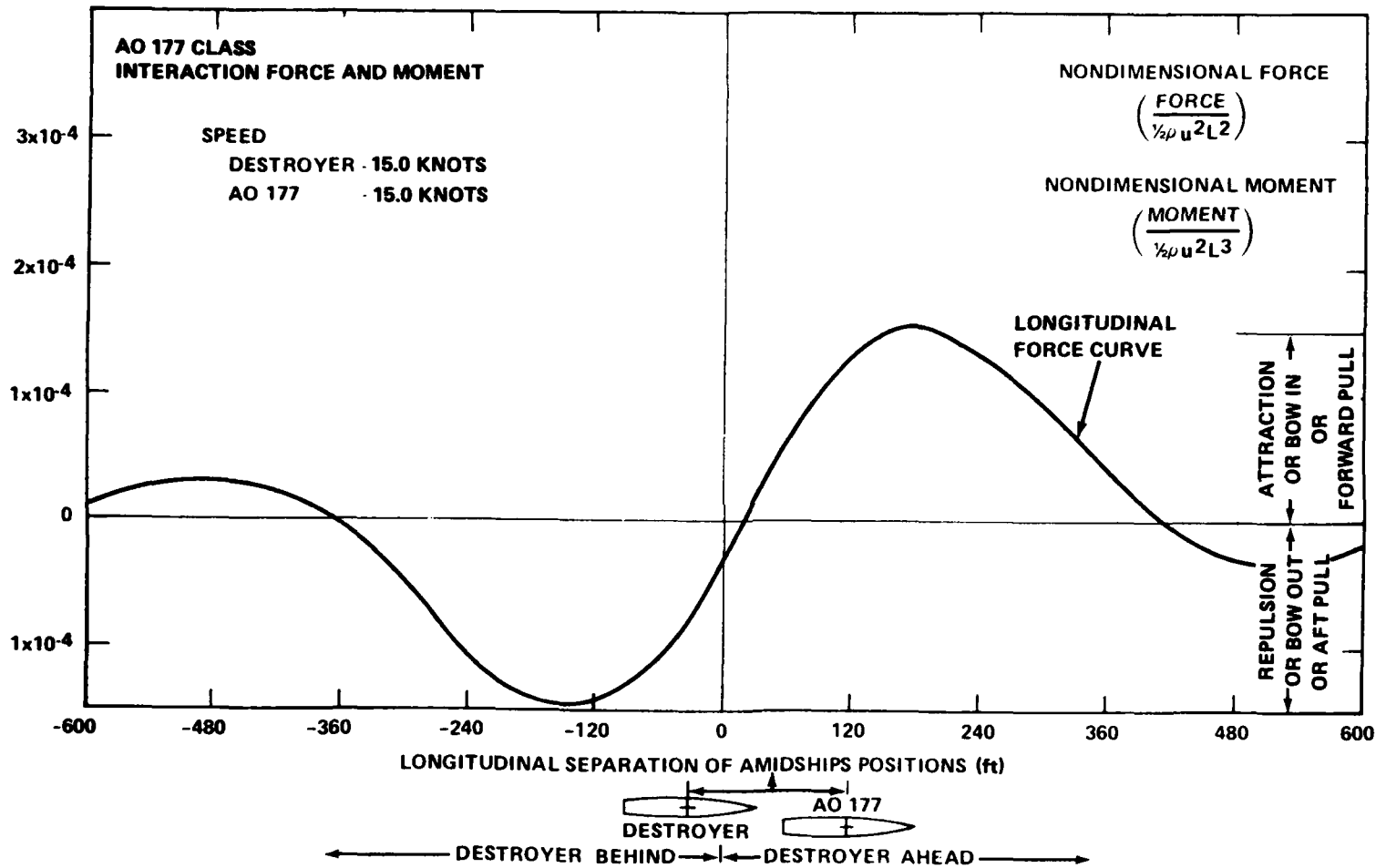

Figure D.14 - AO 177 Class: Longitudinal Interaction Force
(Lateral Separation Between Amidships - 121.5 ft, Between Sides - 50.0 ft)

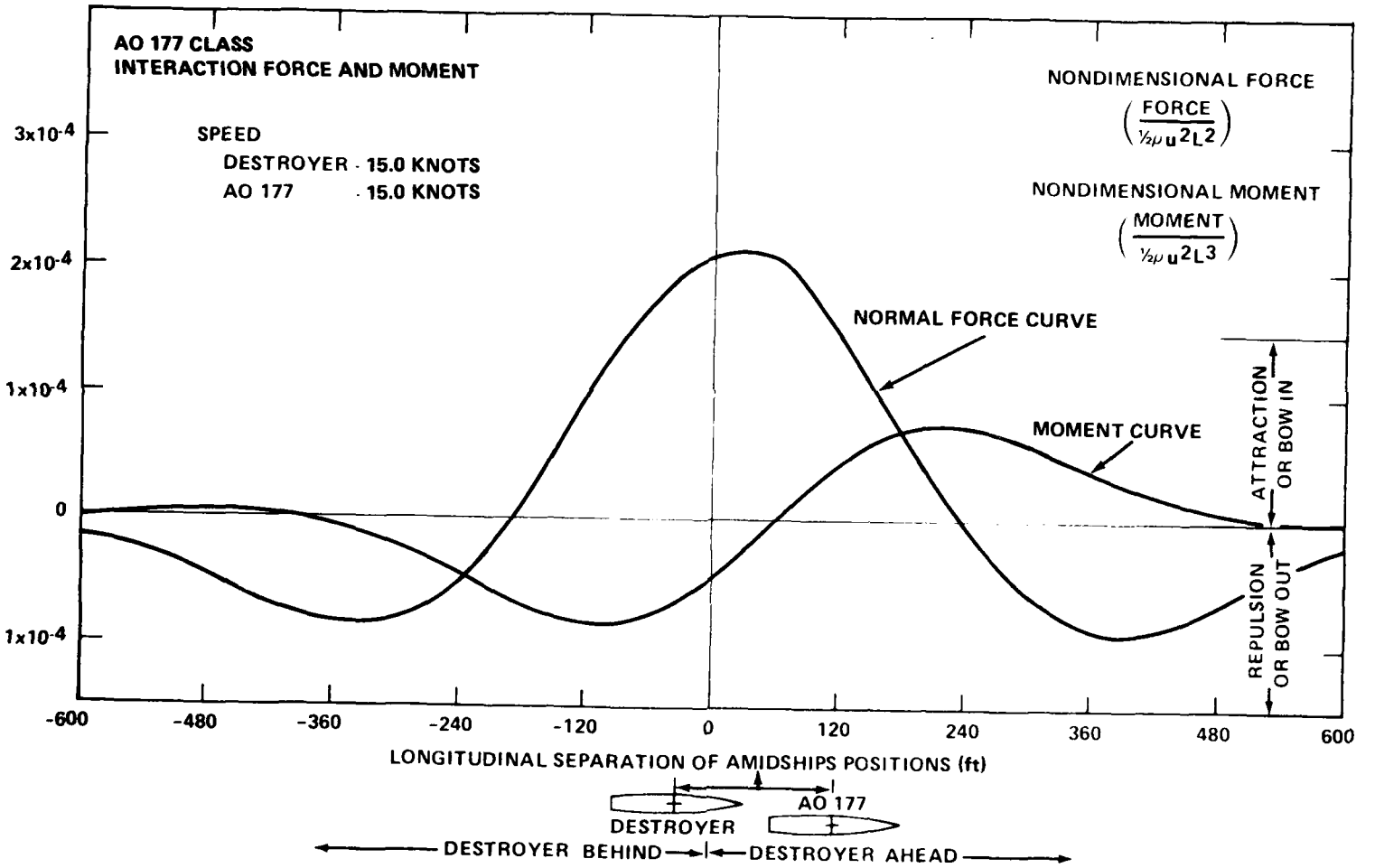

Figure D.15 - AO 177 Class: Interaction Force and Moment
(Lateral Separation Between Amidships - 141.5 ft, Between Sides - 70.0 ft)

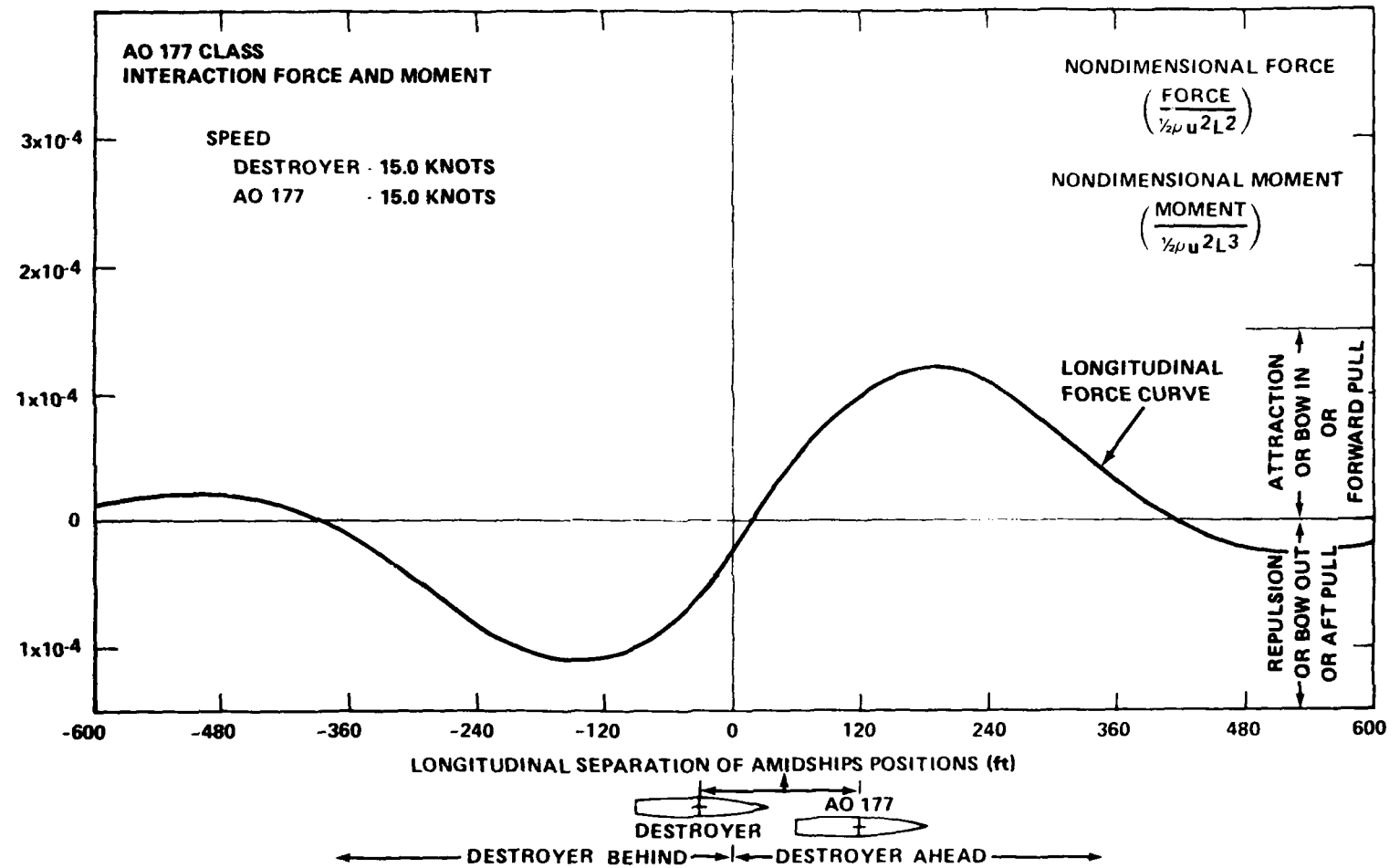

Figure D.16 - AO 177 Class: Longitudinal Interaction Force
(Lateral Separation Between Amidships - 141.5 ft, Between Sides - 70.0 ft)

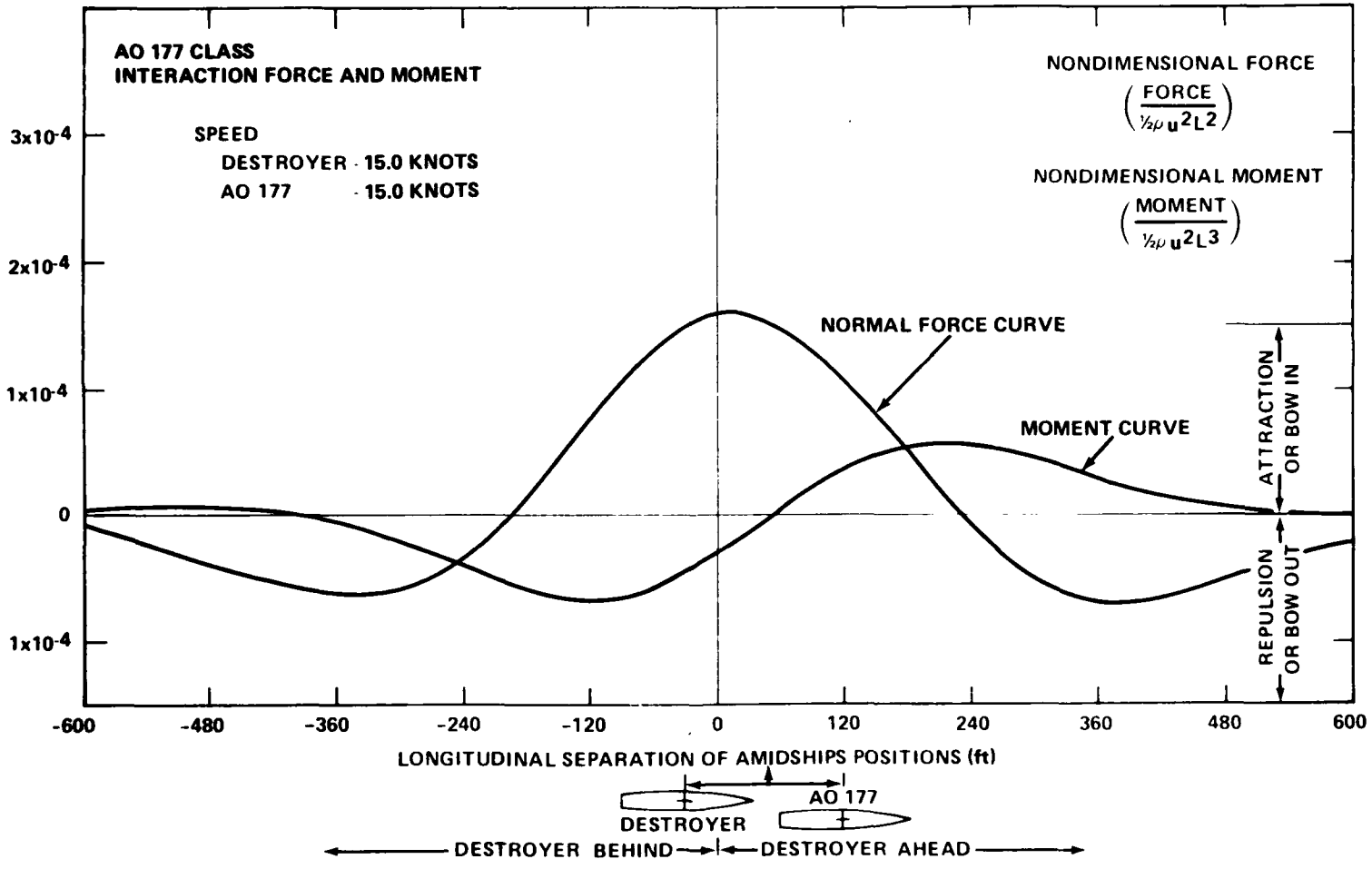

Figure D.17 - AO 177 Class: Interaction Force and Moment
(Lateral Separation Between Amidships - 161.5 ft, Between Sides - 90.0 ft)

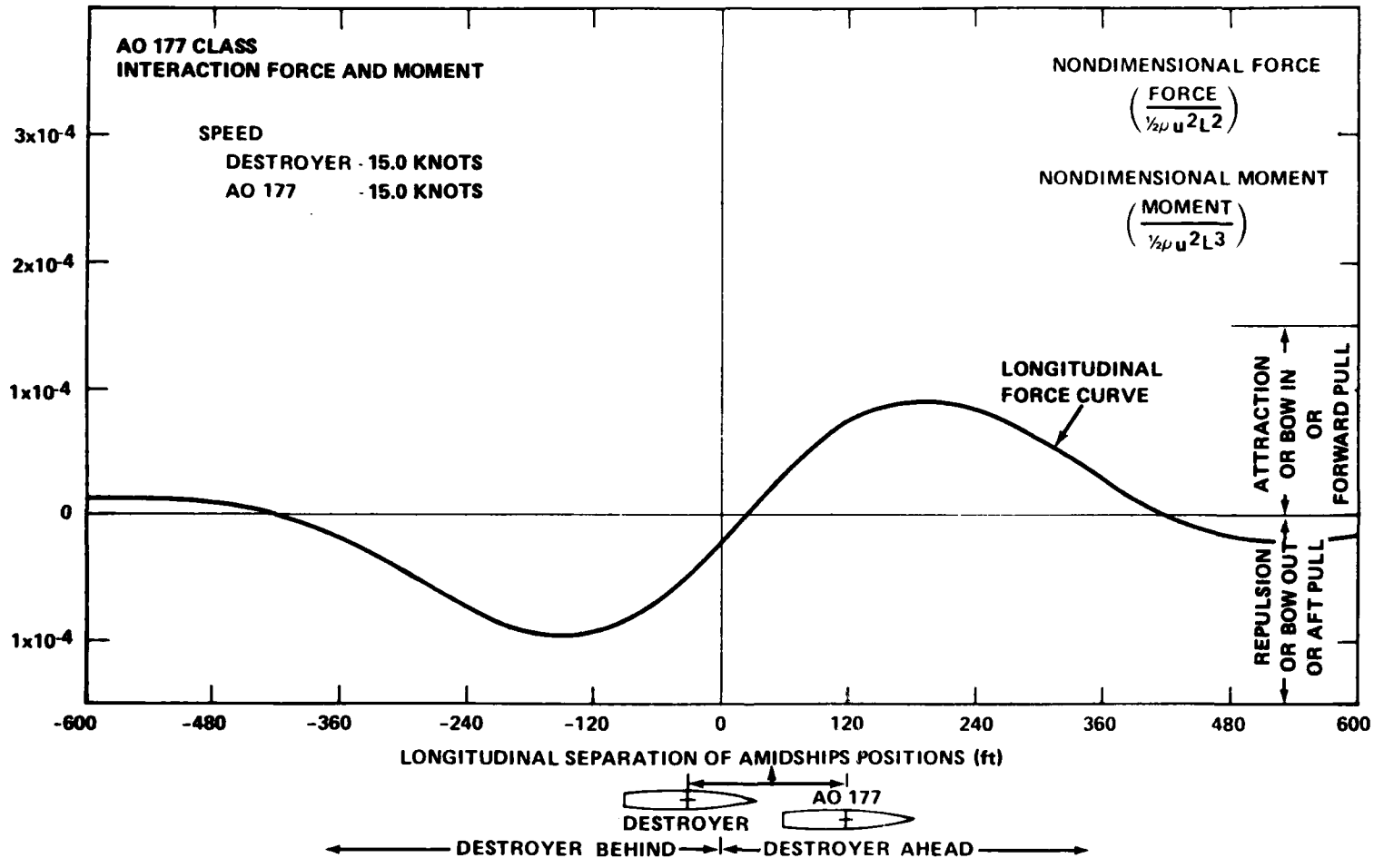

Figure D.18 - AO 177 Class: Longitudinal Interaction Force
(Lateral Separation Between Amidships - 161.5 ft, Between Sides - 90.0 ft)

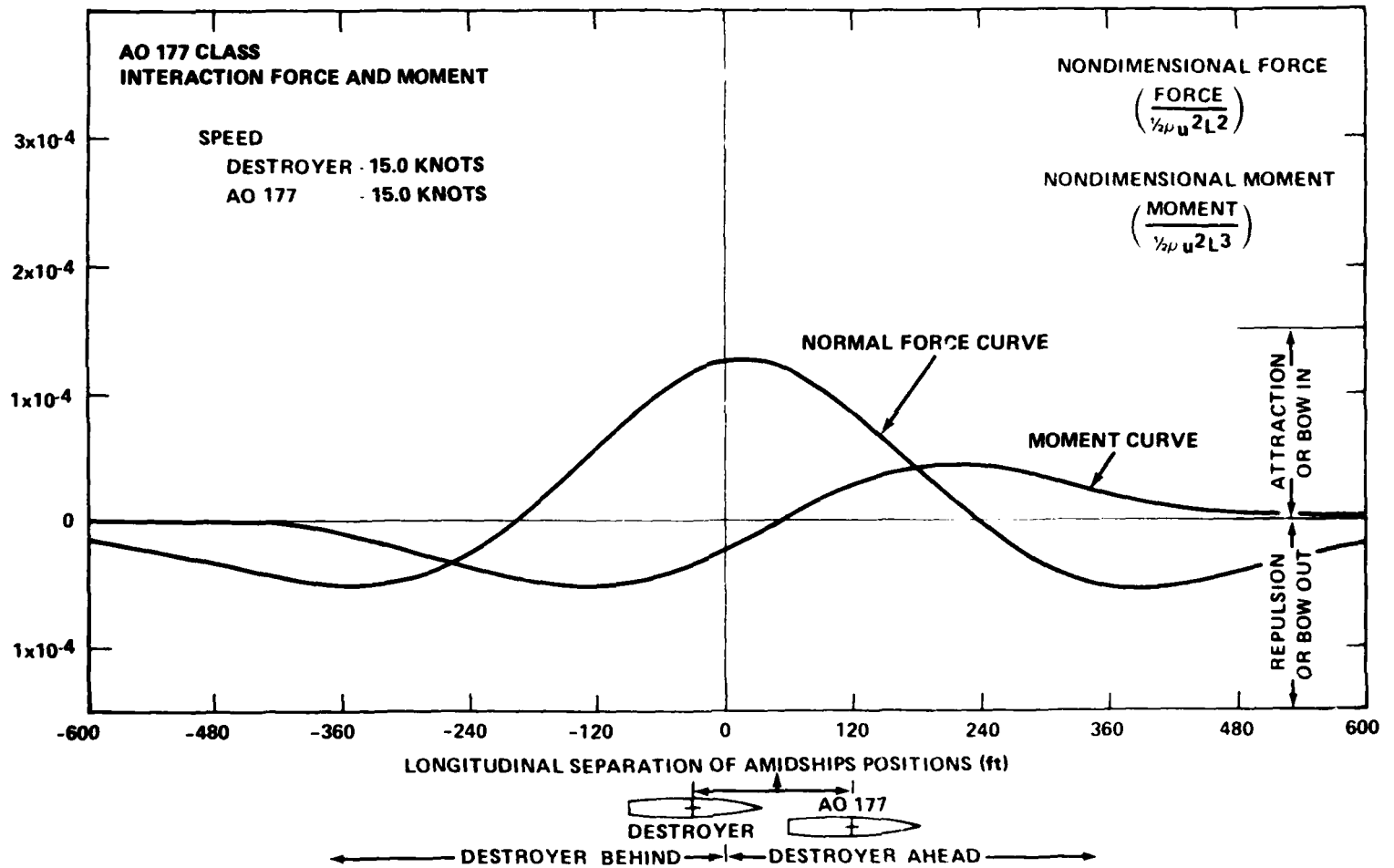

Figure D.19 - AO 177 Class: Interaction Force and Moment
(Lateral Separation Between Amidships - 181.5 ft, Between Sides - 110.0 ft)

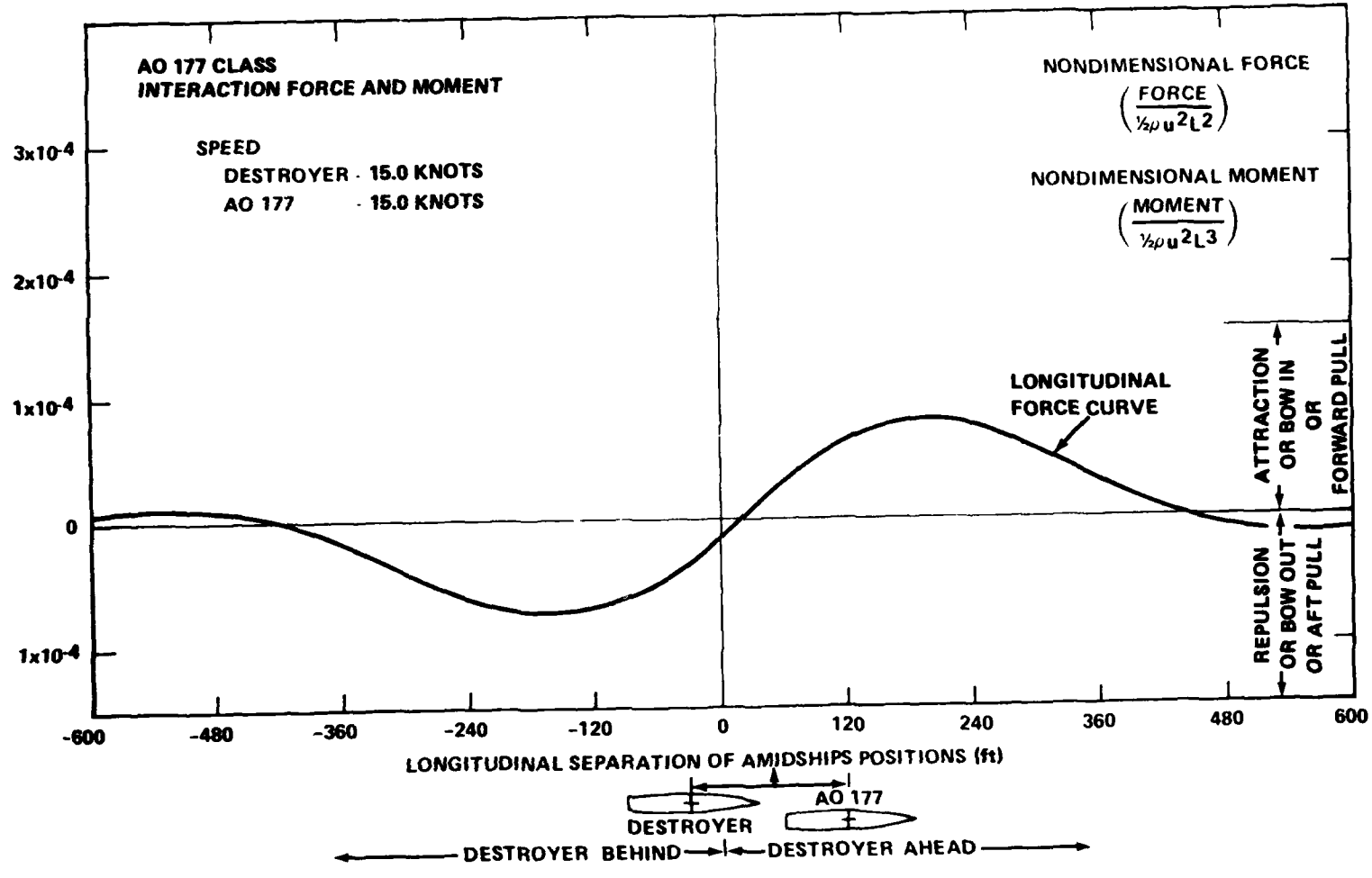

Figure D.20 - AO 177 Class: Longitudinal Interaction Force
(Lateral Separation Between Amidships - 181.5 ft, Between Sides - 110.0 ft)

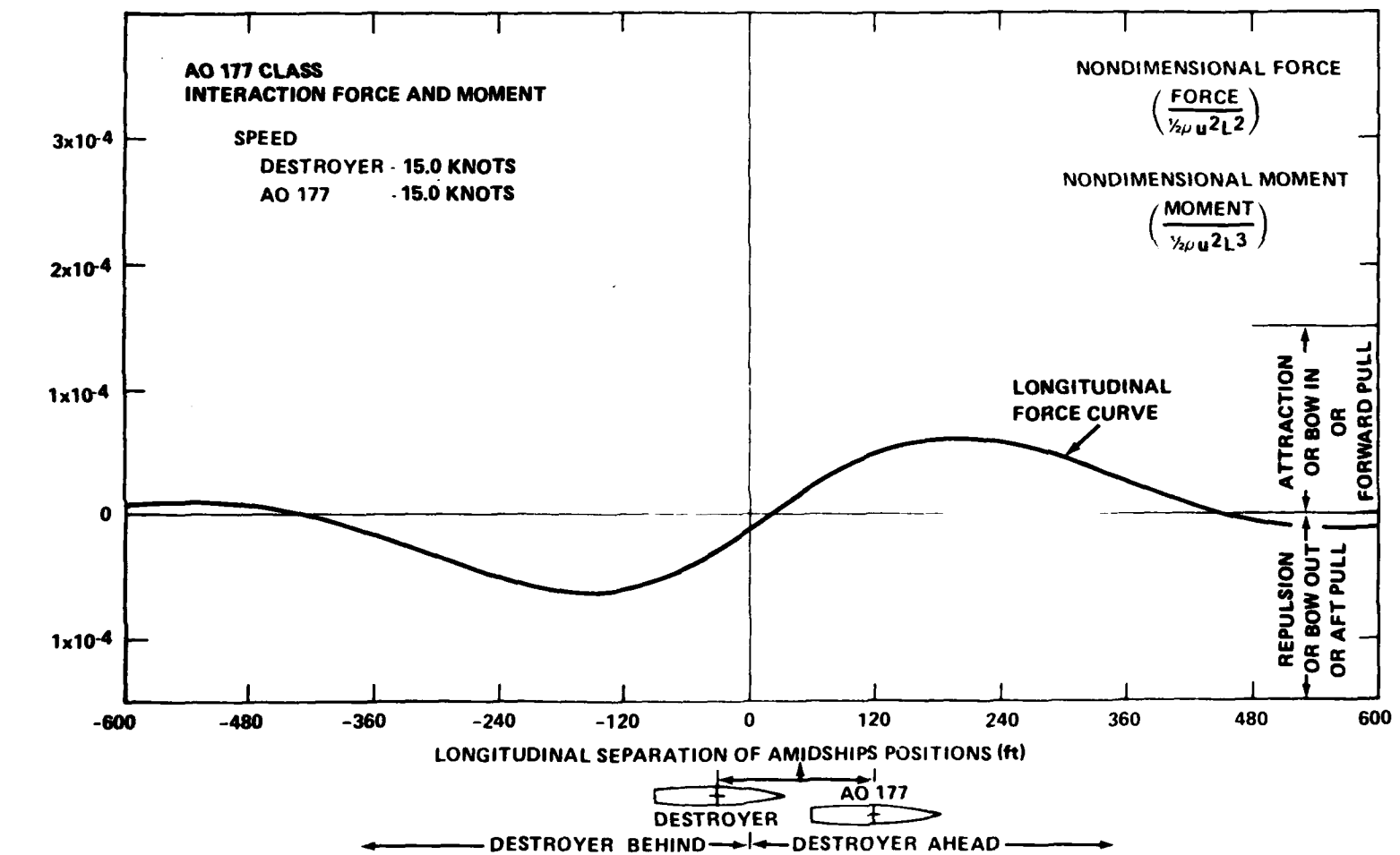

Figure D.21 - AO 177 Class: Longitudinal Force and Moment
(Lateral Separation Between Amidships - 201.5 ft, Between Sides - 130.0 ft)

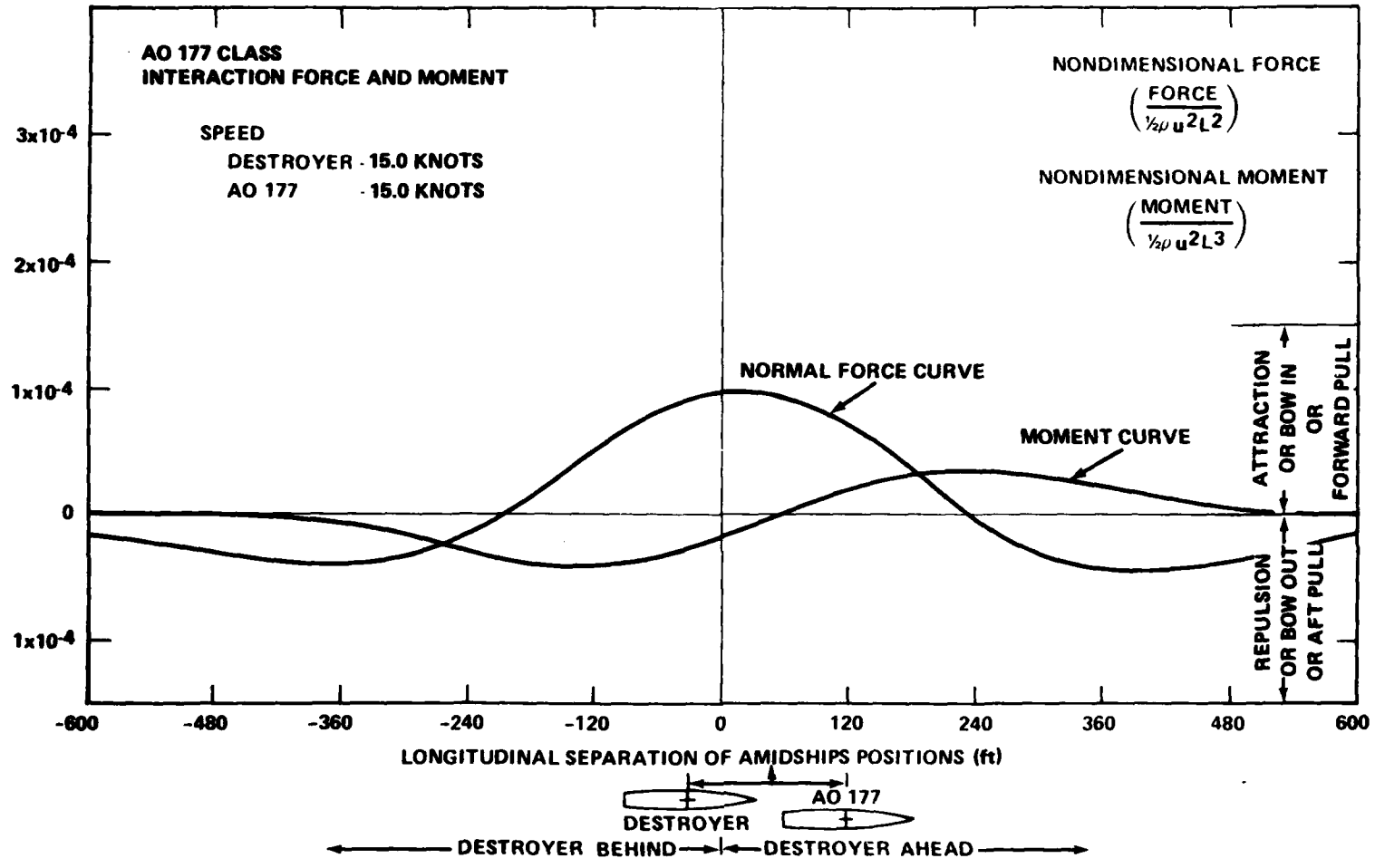

Figure D.22 - AO 177 Class: Interaction Force and Moment
(Lateral Separation Between Amidships - 201.5 ft, Between Sides - 130.0 ft)

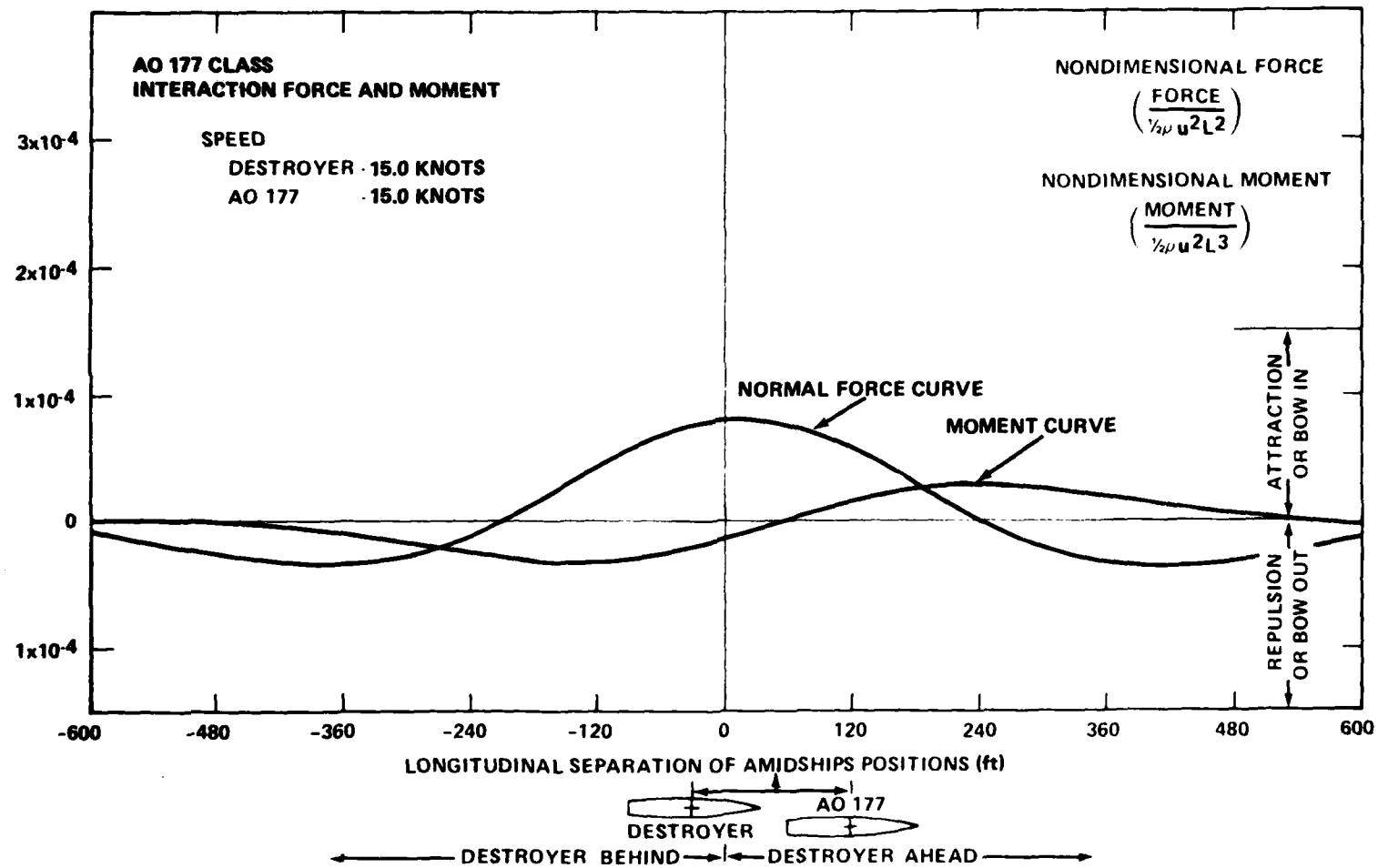

Figure D.23 - AO 177 Class: Interaction Force and Moment
(Lateral Separation Between Amidships - 221.5 ft, Between Sides - 150.0 ft)

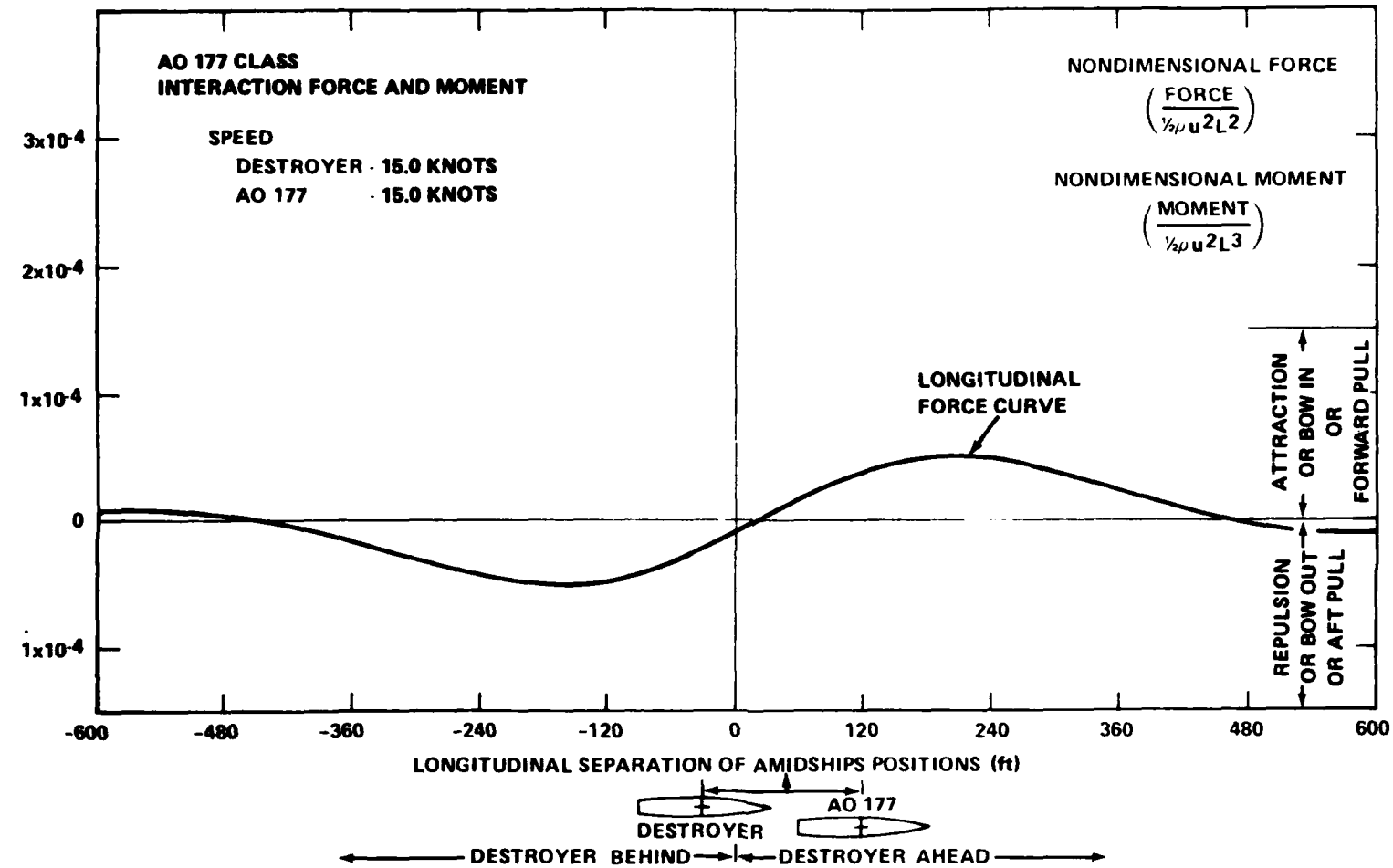

Figure D.24 - AO 177 Class: Longitudinal Interaction Force
(Lateral Separation Between Amidships - 221.5 ft, Between Sides - 150.0 ft)

APPENDIX E

PRELIMINARY SIMULATION CONTROL RESULTS FOR AO 177 CLASS AND DESTROYER STUDY SHIP

The UNREP simulation computer program was used to simulate maneuvering control during UNREP for the AO 177 class and a destroyer study ship. The AO 177 class was used as the leading ship and the destroyer study ship was used as the tracking ship. The passing UNREP control simulation runs were performed at 15 knots.

The maneuvering coefficients for the AO 177 were obtained from the technical report by Cox and Motter.[42] These hydrodynamic maneuvering coefficients are shown in Table E.1. The hydrodynamic maneuvering coefficients for the destroyer study ship were furnished to the authors by Cox and Motter of the DTNSRDC Ship Performance Department and are not presented in this report. The only maneuvering coefficients used are those that can be substituted into the maneuvering equations in Appendix A, Equations A.1 to A.3. The analog computer did not have the capacity to incorporate more maneuvering coefficients into the UNREP maneuvering model.

The hydrodynamic interaction forces and moments between the AO 177 class and destroyer study ship that were used are presented in Appendix D.

Only two initial UNREP maneuvering control runs were performed. More work was not performed because of lack of funds, time, and sufficient hydrodynamic data. Figure E.1 shows the UNREP control results in calm water. Figure E.2 shows the UNREP control results with arbitrary excitations acting on each ship hull. In both cases, good lateral control is demonstrated with automatic control. As expected, the control simulation results are similar to those of the Mariner except the ship maneuvering response times to changes in propeller shaft revolution and changes in rudder angle are somewhat different.

TABLE E.1 - AO 177 CLASS NONDIMENSIONAL COEFFICIENTS (Data Taken from Cox and Motter)[42]

X-Equation Nondimensional Coefficient x 10^5		Y-Equation Nondimensional Coefficient x 10^5		N-Equation Nondimensional Coefficient x 10^5	
$X'_{\dot{u}}$	-51.8	$Y'_{\dot{v}}$	-1264.5	$N'_{\dot{v}}$	-42.1
$X'_{\dot{}}$	7.6	$Y'_{\dot{r}}$	-74.5	$N'_{\dot{r}}$	-87.6
$X'_{\dot{}}$	-165.5	Y'_{o}	24.4	N'_{o}	-8.1
$X'_{\dot{}\delta u}$	308.2	Y'_{ou}	-63.4	N'_{ou}	21.0
X'_{v}	15.4	$Y'_{}$	341.6	$N'_{}$	-159.5
X'_{vv}	-634.4	$Y'_{}$	-122.7	$N'_{}$	61.2
X'_{vr}	895.0	$Y'_{}$	-216.9	$N'_{}$	92.0
$X'_{}$	133.8	$Y'_{\delta u}$	-515.7	$N'_{\delta u}$	261.5
		$Y'_{\delta\delta u}$	201.1	$N'_{\delta\delta u}$	-100.3
		$Y'_{\delta\delta\delta u}$	355.6	$N'_{\delta\delta\delta u}$	-150.8
		$Y'_{\delta\|v\|}$	176.7	$N'_{\delta\|v\|}$	0.0
		$Y'_{\delta v}$	65.6	$N'_{\delta v}$	0.0
		Y'_{v}	-1604.6	N'_{v}	-727.0
		Y'_{vv}	588.6	N'_{vv}	-133.0
		$Y'_{v\|v\|}$	-2566.8	$N'_{v\|v\|}$	156.3
		Y'_{r}	1060.9	N'_{r}	-250.8
		Y'_{rrr}	552.8	N'_{rrr}	-199.4
		Y'_{rvv}	4057.0	N'_{rvv}	-4820.0
m'	1151.7	$m'X_6'$	-9.3	I'_{z}	52.7

Mass nondimensional with	$1/2\ \rho L_{pp}^3$
Inertia	$1/2\ \rho L_{pp}^5$
X and Y forces	$1/2\ \rho L_{pp}^2 U^2$
N moments	$1/2\ \rho L_{pp}^3 U^2$
L_{pp}	550 ft
Beam	88.0 ft
u, u, and v nondimensional with U	
r	U/L_{pp}
δ	rad
$\dot{u}$ and $\dot{v}$	U^2/L_{pp}
$\dot{r}$	U^2/L_{pp}^2

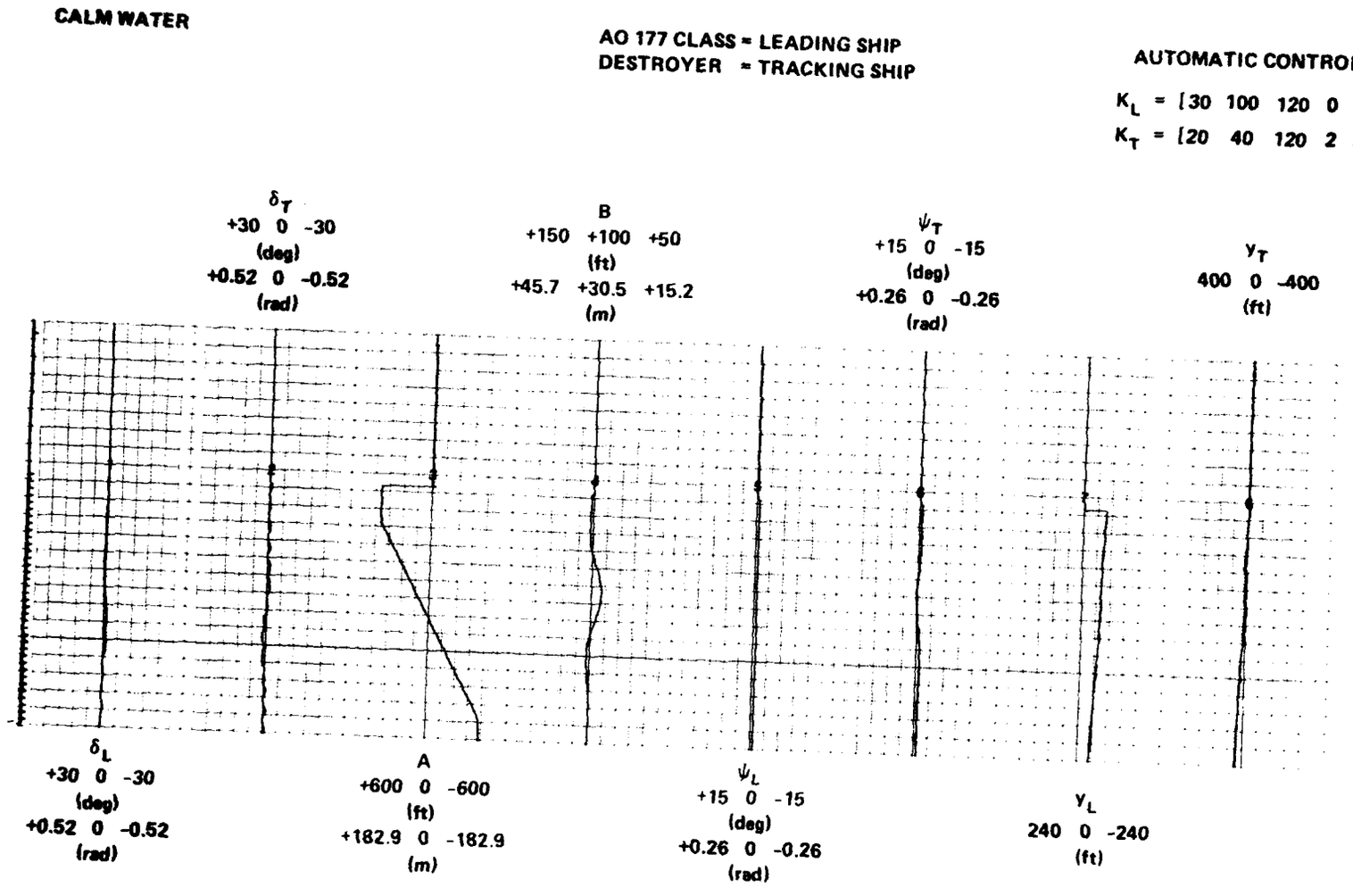

Figure E.1 - Underway Replenishment Control Passing Maneuver (AO 177 Class and Destroyer Study Ship) (Automatic Control)

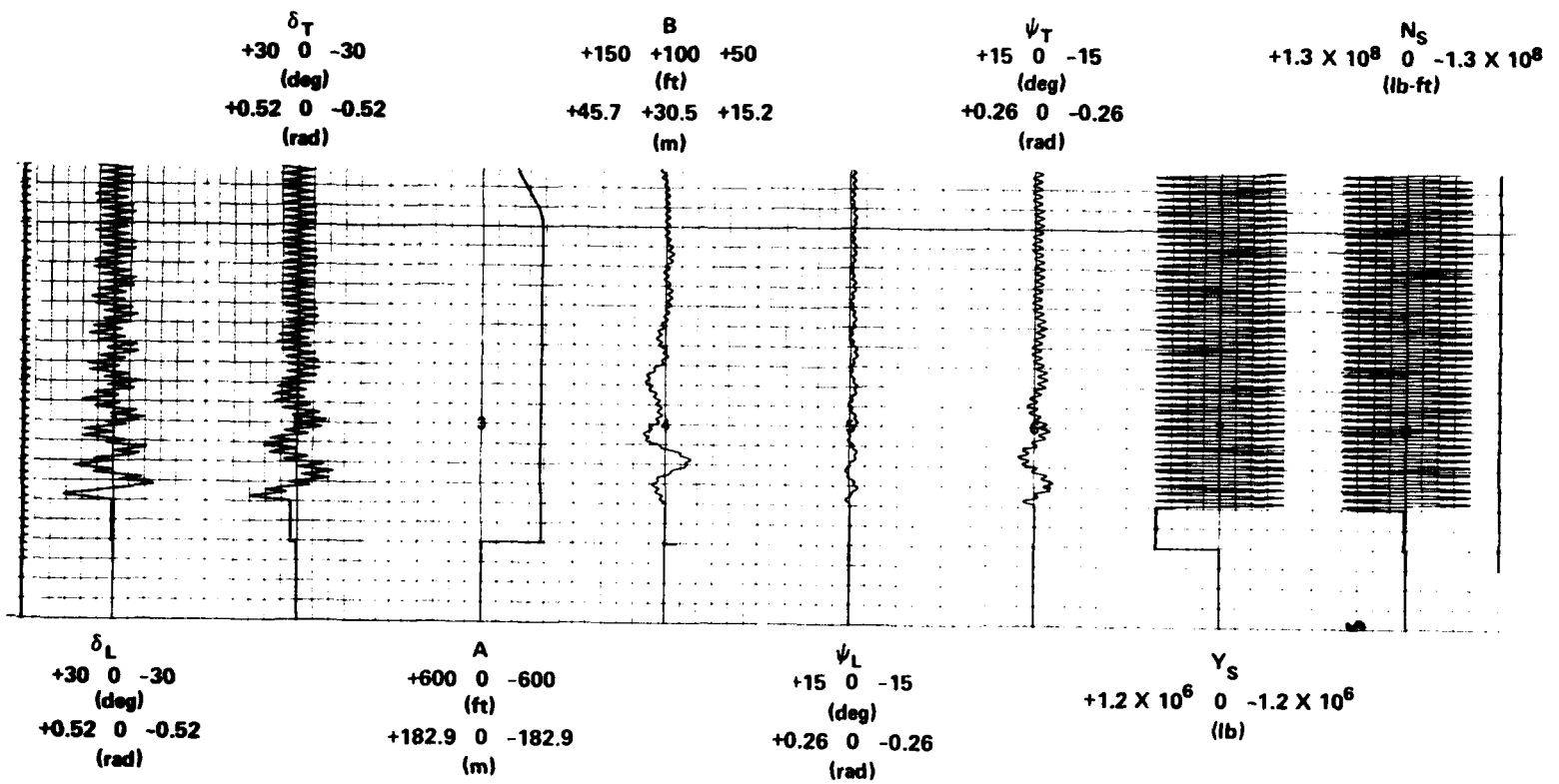

Figure E.2 - Underway Replenishment Control Passing Maneuver (AO 177 Class and Destroyer Study Ship) (Automatic Control)

REFERENCES

1. Tichvinsky, L. M. and Thal-Larsen, H., "Replenishment at Sea, Experiments and Comments," University of California, Berkeley, Inst. of Engr. Research, Report 154, Issue 1 (1 June 1960).

2. Thal-Larsen, H., "Manual Steering of Two Ships in Close Proximity During Replenishment at Sea Exercises," presented at the ASME Winter Annual Meeting, Los Angeles, CA (Nov 1969).

3. Paulling, L. R. and L. W. Wood, "The Dynamic Problem of Two Ships Operating on Parallel Courses in Close Proximity," University of California, Berkeley, CA, Technical Report, Series 189, Issue 1 (July 1962).

4. Lienhard, B. A., CAPT, USN, "Shipbuilding in Modern Underway Replenishment," NAVSHIPS Tech News, Vol. 21, No. 4, NAVSHIPS 0900 000 2085 (Apr 1972).

5. Morisseau, K. C., "UNREP Ships of the Future," Association of Senior Engineers, Naval Ship Systems Command (Mar 1972).

6. Brown, S. H. and R. Alvestad, "Hybrid Computer Simulation of Maneuvering During Underway Replenishment," International Shipbuilding Progress, Vol. 21, No. 241 (Sep 1974).

7. Alvestad, R. and S. H. Brown, "Hybrid Computer Simulation of Maneuvering During Underway Replenishment in Calm and Regular Seas," International Shipubilding Progress, Vol. 22, No. 250 (June 1975).

8. Alvestad, R., "Automatic Control of Underway Replenishment Maneuvers in Random Seas," Journal of Ship Research, Vol. 22, No. 1 (Mar 1978).

9. Brown, S. H. and R. Alvestad, "Sensitivity Study of Control Parameters During Underway Replenishment Simulations Including Approximate Nonlinear Sea Effects," DTNSRDC Report 77-0003 (Jan 1977).

10. Brown, S. H. and R. Alvestad, "Simulation of Maneuvering Control During Underway Replenishment," Journal of Hydronautics, Vol. 12, No. 3 (1978).

11. Pierson, W. J. and L. Moskowitz, "A Proposed Spectral Form for Fully Developed Wind Seas Based on the Similarity Theory of S. A. Kitaigorodskii," Journal of Geophysical Research, Vol. 69, No. 24 (1964).

12. Dimmick, J. G., R. Alvestad, and S. H. Brown, "Simulation of Ship Steering Control for Underway Replenishment," presented at Vehicular Technology Conference, Denver, CO (Mar 1978).

13. Dimmick, J. G., "A Modular Ship Bridge Control System," Proceedings of the Naval Institute (Sep 1976).

14. Dimmick, J. G., "A Quickened Display for Ship Steering Control," presented at ASNE Symposium, San Diego, CA (8 Oct 1976).

15. Poulton, E. C., "Tracking Skill and Manual Control," Academic Press, New York, NY (1974).

16. Birmingham, H. P. and F. V. Taylor, "A Design Philosophy for Man-Machine Control Systems," Proceedings of the IRE, Vol. 1 (Dec 1954).

17. Dimmick, J. G., et al, "Combination Pursuit and Compensatory Display System," U.S. Patent No. 4,129,087 (Dec 1978).

18. Birmingham, H. P. and F. V. Taylor, "Why Quickening Works," presented at the ASNE-ARS Joint Aviation Conference, Dallas, TX (17-20 Mar 1958).

19. St. Denis, M. and W. J. Pierson, Jr., "On the Motions of Ships in Confused Seas," Society of Naval Architects and Marine Engineers, Vol. 61 (Nov 1953).

20. Calvano, C. N., "An Investigation of the Stability of a System of Two Ships Employing Automatic Control While on Parallel Courses in Close Proximity," M.S. Thesis, Dept. of Naval Architecture and Marine Engineering, Massachusetts Institute of Technology (May 1970).

21. Salvesen, W., E. Tuck, and O. Faltinson, "Ship Motion and Sea Loads," presented at SNAME Annual Meeting (Nov 1970).

22. Volterra, V., "Theory of Functionals and of Integral and Integro Differential Equations," Blackie and Sons, Ltd., London (1930).

23. Wiener, N., "Response of a Nonlinear Device to Noise," Report 129, Radiation Laboratory, Massachusetts Institute of Technology (1942).

24. Smitt, L. W. and M. S. Chislett, "Large Amplitude PMM Tests and Maneuvering Predictions for a Mariner Class Vessel," Tenth Symposium on Naval Hydrodynamics (24-28 June 1974).

25. Neal, E., "Second-Order Hydrodynamic Forces Due to Stochastic Excitation," presented at the Tenth Symposium on Naval Hydrodynamics, Cambridge, MA (24-28 June 1974).

26. Vassilopoulos, L. A., "The Application of Statistical Theory of Nonlinear Systems to Ship Motion Performance in Random Seas," International Shipbuilding Progress, Vol. 14, No. 150 (1967).

27. Tick, L. J., "The Estimation of Transfer Functions of Quadratic Systems," Technometrics, Vol. 3, No. 4 (Nov 1961).

28. Hasselmann, K., "On Nonlinear Ship Motions in Irregular Waves," Journal of Ship Research, Vol. 10, No. 1 (Mar 1966).

29. Newman, J. N., "The Drift Force and Moment on Ships in Waves," Journal of Ship Research (Mar 1967).

30. Dalzell, J. F., "Application of Cross-Bi-Spectral Analysis to Ship Resistance in Waves," Report SIT-DL-72-1606, Davidson Laboratory, Stevens Institute of Technology (May 1972).

31. Dalzell, J. F., "Cross-Bispectral Analysis: Application to Ship Resistance in Waves," Journal of Ship Research, Vol. 18, No. 1 (Mar 1974).

32. Ku, Y. H. and A. A. Wolf, "Volterra-Wiener Functionals for the Analysis of Nonlinear Systems," Journal of the Franklin Institute, Vol. 281, No. 1 (Jan 1966).

33. Lee, C. M., "The Second-Order Theory for Non-Sinusoidal Oscillations of a Cylinder in a Free Surface," Proceedings of the Eighth Symposium on Naval Hydrodynamics, ACR-179, U.S. Office of Naval Research (Aug 1970).

34. Newman, J. N., "Second-Order, Slowly-Varying Forces on Vessels in Irregular Waves," International Symposium on Marine Vehicles and Structures in Waves, London (Apr 1974).

35. Salvesen, N., "Second-Order Steady-State Forces and Moments on Surface Ships in Oblique Regular Waves," published in "The Dynamics of Marine Vehicles and Structures in Waves," edited by R. E. O. Bishop and W. G. Price, Institution of Mechanical Engineers, Mechanical Engineering Publications Limited, London (Apr 1974).

36. Corlett, E. C. B., "Studies on Interaction at Sea," Journal of Navigation, Royal Institute of Navigation, London, Vol. 32, No. 2 (May 1979).

37. Chey, Y., "Experimental Determination of Wave-Excited Forces and Moments Acting on a Ship Model Running in Oblique Regular Waves," Report 1046, Davidson Laboratory, Stevens Institute of Technology (Oct 1964).

38. Lalangas, "Lateral and Vertical Forces and Moment on a Restrained Series 60 Ship Model in Oblique Regular Waves," Report 920, Davidson Laboratory, Stevens Institute of Technology.

39. Verhage, J. H. G. and M. F. Shuljs, "The Low-Frequency Drifting Force on a Floating Body in Waves," Publication No. 320, Netherlands Ship Model Basin, Wageningen.

40. Ashe, G. M., "Trajectory Predictions for Ships Engaged in Close Proximity Operations," M.S. Thesis, Massachusetts Institute of Technology (May 1975).

41. Abkowitz, M. A., G. M. Ashe, and R. M. Fortson, "Interaction Effects of Ships Operating in Proximity in Deep and Shallow Water," 11th Symposium on Hydrodynamics.

42. Cox, G. G. and L. E. Motter, "Prediction of Standard Maneuvering Characteristics for a Naval Auxiliary Oiler (AO 177 Class)," NSRDC Report SPD-624-01 (June 1975).

INITIAL DISTRIBUTION

Copies	
2	ONR 1 Code 436 1 Code 438/R. Cooper
2	Naval Postgraduate School/Dr. Thaler
9	NAVSEA 1 SEA 321/D. McCallum 1 SEA 512/E. Meere 1 SEA 513/L. Nelson 1 SEA 513/R. Stankey 1 SEA 525/J. McIntire 1 SEA 62T1L/G. Mueller 3 SEA 6212/A. Chaikin
1	NAVSSES/J. Banham
12	DTIC

CENTER DISTRIBUTION

Copies	Code	Name
1	152	R. Wermter
1	1524	W. Lin
1	1560	G. Hagen
1	1561	C. Lee
1	1562	M. Martin
1	1568	G. Cox
2	273	W. Blumberg
10	2731	S. Brown
10	2732	J. Dimmick
10	5211.1	Reports Distribution
2	522.1	Library (C)
2	522.2	Library (A)
2	5231	Office Services

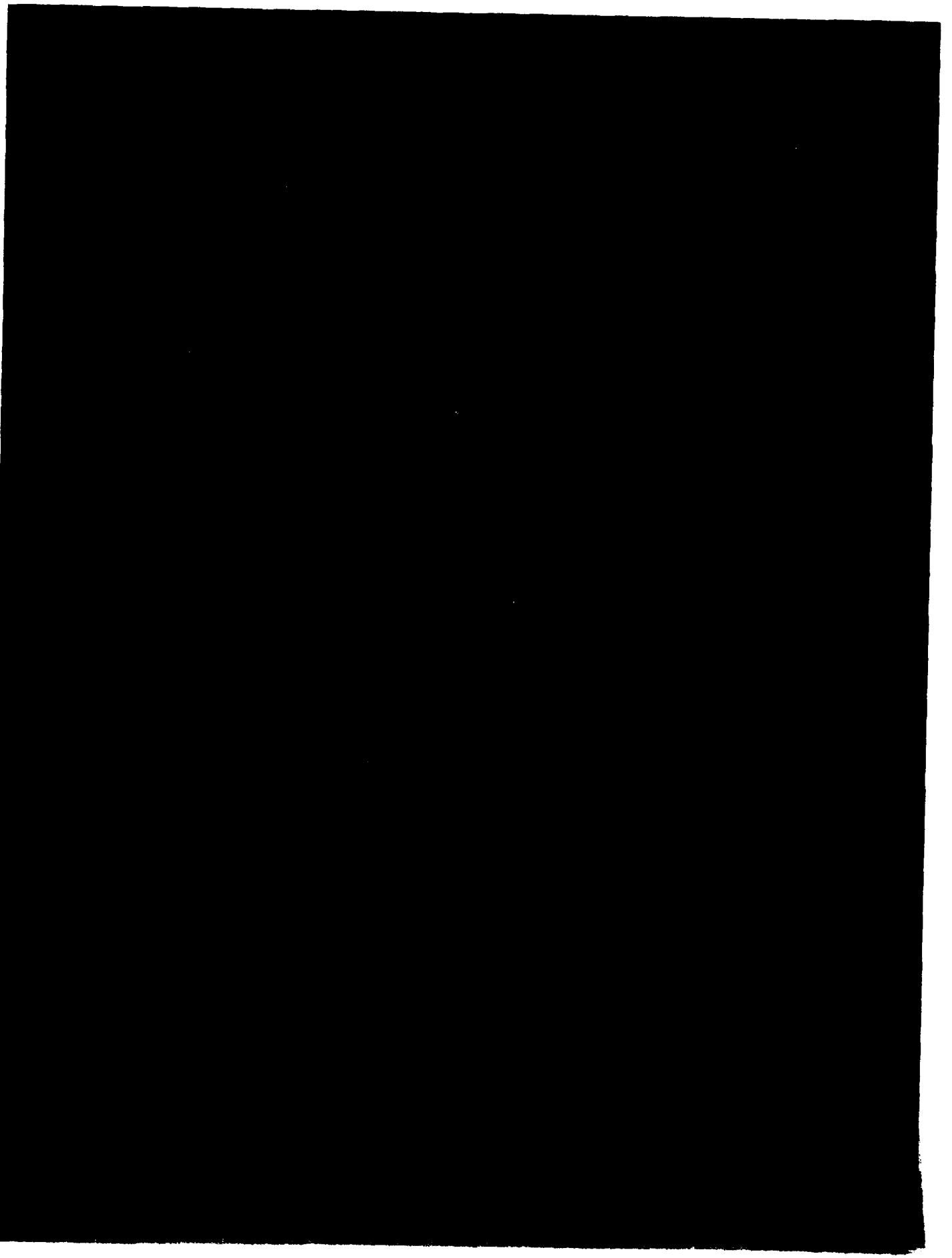


DATE
ILMED
-8